Aus dem Institut für
Sozialmedizin, Epidemiologie und Gesundheitsökonomie
der Medizinischen Fakultät Charité – Universitätsmedizin Berlin

DISSERTATION

Changes of Human Brain Activity after Complex Somatosensory Stimulation with Acupuncture Needles

zur Erlangung des akademischen Grades
Doctor rerum medicinalium (Dr. rer. medic.)

vorgelegt der Medizinischen Fakultät
Charité – Universitätsmedizin Berlin

von

Wenjing Huang

aus Sichuan, China

Datum der Promotion: 08.12.2017

Table of Contents

Summary

Abstract

Introduction: Research on acupuncture mechanism with neural correlates is of great importance and interest. Brain imaging techniques enable the non-invasive exploration of the potential mechanism of acupuncture effects.

Method: In order to summarise the current evidence of brain response to acupuncture stimulation a systematic review and meta-analysis was carried out. On this basis, clinical experiments were designed to evaluate the differences in brain activity after standardised needle stimulation at different point locations in healthy volunteers. EEG, event-related fMRI, and resting-state functional connectivity fMRI were used to assess the instant and sustained neural responses after needling the acupuncture point ST36 and two control points (CP1 same dermatome, CP2 different dermatome). Different analyses were performed to investigate the EEG background rhythm, fMRI BOLD response, seed-based functional connectivity, as well as centrality changes.

Results: The meta-analysis showed, besides notable heterogeneity of acupuncture and fMRI studies, that acupuncture seems to modulate activity within specific brain areas: including sensorimotor cortices, limbic regions, and cerebellum. The EEG study showed an increased mu rhythm power after needling stimulation on ST36 compared to CP1 or CP2, with no relevant differences between the two control points. The fMRI BOLD analysis found more pronounced insula and secondary somatosensory cortex (S2) activation, as well as precuneus deactivation during ST36 stimulation. The S2 seed-based functional connectivity analysis revealed increased connectivity to right precuneus when comparing ST36 to both control points; albeit in different regions. Higher centrality in parahippocampal gyrus and middle temporal gyrus were identified after ST36 stimulation in comparison to the two control points.

Conclusion: These experimental findings indicate that compared to stimulation on non-acupuncture points, stimulation on the acupuncture point may modulate differently within several brain networks, such as somatosensory, saliency processing and default mode network. This might hint to a potential mechanism of pain perception and modulation due to acupuncture stimulation. The experimental results are consistent with the findings of the systematic review and meta-analysis. Brain imaging techniques and analyses seem to be valuable for future studies investigating the neural mechanism of acupuncture.

Abstrakt

Einleitung: Die Erforschung der Akupunktur-Wirkungsweise mit neuronalen Korrelaten ist von großer Bedeutung und Interesse. Brain Imaging-Techniken ermöglichen die nicht-invasive Erforschung der potenziellen Mechanismen der Akupunktur-Wirkung.

Methodik: Um aktuelle Befunde über die Wirkung von Akupunktur-Stimulation auf Hirnaktivitäten zu erfassen, wurde eine systematische Übersichtsarbeit und Meta-Analyse durchgeführt. Auf dieser Basis wurden klinische Experimente entwickelt, um den Unterschied zwischen standardisierter Nadelstimulation in verschiedenen Punkten auf die Hirnaktivität bei gesunden Probanden zu untersuchen. EEG, ereigniskorreliertes fMRT und Resting-State fMRT wurden verwendet, um die kurzfristigen und anhaltenden neuronalen Reaktionen nach dem Nadeln des Akupunkturpunktes ST36 und zweier Kontrollpunkte (CP1-in dem gleichen Dermatom, CP2-in einem anderen Dermatom) zu untersuchen. Unterschiedliche Analysen wurden durchgeführt, um den EEG-Hintergrundrhythmus, die fMRI-BOLD-Reaktion, die Resting-State funktionelle Konnektivität zu untersuchen.

Ergebnisse: Die Meta-Analyse wies, trotz merklicher Heterogenität der Akupunktur-fMRT-Studien, darauf hin, dass Akupunktur die Aktivität innerhalb bestimmter Hirnareale moduliert: darunter sensomotorische Kortexe, limbische Regionen und Zerebellum. Die EEG-Studie zeigte eine erhöhte Aktivität des Hintergrundrhythmuses nach Nadel-Stimulation

von ST36 im Vergleich zu CP1 oder CP2, aber nicht zwischen den beiden Kontrollpunkten. Die fMRT-BOLD-Analyse ergab eine stärkere Aktivierung von Insula und Sekundär-somatosensorischem Kortex (S2) sowie eine Precuneus-Deaktivierung während der ST36-Stimulation. Die Konnektivitätsanalyse ergab eine erhöhte Konnektivität zwischen S2 und dem rechten Precuneus beim Vergleich von ST36 mit beiden Kontrollpunkten; wenn gleich in verschiedenen Arealen des Precuneus. Eine höhere Zentralität im Gyrus parahippocampalis und im mittleren temporalen Gyrus wurde nach ST36-Stimulation im Vergleich zu den beiden Kontrollpunkten identifiziert.

Schlussfolgerung: Diese experimentellen Ergebnisse deuten darauf hin, dass im Vergleich zur Stimulation von non-Akupunkturpunkten, die Stimulation vom Akupunkturpunkt Hirnnetzwerke unterschiedlich moduliert: somatosensorisches Netzwerk, Salienz-Verarbeitung- und Ruhezustandsnetzwerk. Dies könnte auf einen möglichen Mechanismus der Schmerzempfindung und -modulation aufgrund einer Akupunkturstimulation hindeuten. Die experimentellen Ergebnisse stimmen mit den Ergebnissen der systematischen Übersichtsarbeit und Meta-Analyse überein. Brain-Imaging-Techniken und -Analysen scheinen für künftige Studien, die den neuronalen Mechanismus der Akupunktur evaluieren, wertvoll zu sein.

1. Introduction

In the past decade there has been growing interest in determining the neurophysiologic correlates of acupuncture by means of functional neuroimaging methods, such as fMRI or EEG.[1,2] From the neurophysiologic aspect, acupuncture is regarded as a complex somatosensory stimulation.[3] The first part of the doctoral work consisted of a systematic review and meta-analysis. The aim was to provide a systematic overview of acupuncture fMRI research considering the following aspects: 1) differences between verum and sham acupuncture, 2) differences due to various methods of acupuncture manipulation, 3) differences between patients and healthy volunteers, 4) differences between different acupuncture points.

One recent patient level data meta-analyses for chronic pain showed statistically significant superiority of acupuncture to sham acupuncture,[4] though the acupuncture point-specific effect is still controversial. One reason might be that various forms of acupuncture control groups have been used in previous clinical trials. The purpose of the experimental study was to evaluate whether the point locations chosen for a complex somatosensory stimulation with acupuncture needles differently influences brain activity in healthy volunteers measured with EEG and fMRI. We compared manual needle stimulation of the acupuncture point (Stomach 36, ST36) at the lower leg and two control point locations (CP1 same dermatome, CP2 different dermatome). Imaging results were expected to differ 1) when comparing the acupuncture point with the two non-acupuncture control points and 2) when comparing the two different dermatomes (CP2 different from ST36 & CP1).

2. Method

2.1 Acupuncture and fMRI systematic review and meta-analysis (Publication I)

A systematic literature search was done for the English, Chinese, Korean and Japanese databases for research articles published from the earliest available up until September 2009, without any language restrictions. All studies using fMRI to investigate the effect of acupuncture on the human brain (at least one group that received needle-based acupuncture) were included for descriptive evaluation. Studies investigating verum acupuncture or with sham acupuncture using the whole brain acquisition were included in the meta-analysis. The meta-analyses were conducted in Talairach coordinate space, using the activation likelihood estimation technique (ALE) implemented in GingerALE 2.1.1 software.[5]

2.2 Brain response to stimulation of an acupuncture point versus two non-acupuncture points measured with EEG and fMRI (Publication II, III)

2.2.1 Participants

A total of 23 healthy subjects (11 female, mean age 26 years, range 19-31 years) participated in the

EEG experiment and 22 healthy subjects (11 female, mean age 26 years, range 21–32 years) participated in the fMRI experiment. Participants had no medical knowledge about acupuncture and all except one had never been treated with acupuncture before the study. Among all the subjects, eight participated in both EEG and fMRI experiments. All participants were right-handed and gave written informed consent. In the EEG experiment three subjects were excluded from acupuncture because of vegetative side effects; in the fMRI experiment, one was excluded.

2.2.2 Acupuncture point selection

The points chosen for the intervention (Figure 1) were developed after literature screening and a consensus process with experts of the Chengdu University of TCM. ST36: on the anterior aspect of the leg and in the L5 dermatome. Control point 1 (CP1): lateral to the ST36 horizontally, at the middle line between Bladder meridian and Gallbladder meridian, in the same dermatome L5. Control point 2 (CP2): B-2 cun dorsally of an acupuncture point GB31 and in the L2 dermatome.

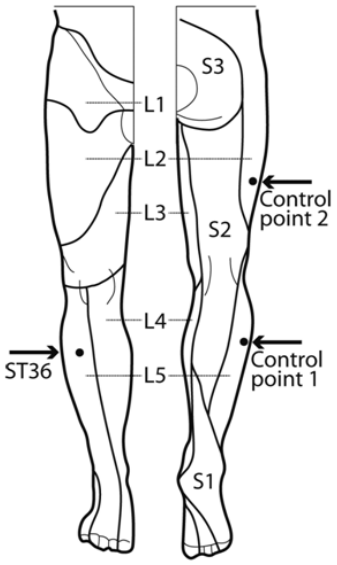

Figure 1: Location of ST36 and Control points on the right leg.[6] View from the front and from the back, figure adapted Drake et al.,2009[7]

2.2.3 Experimental procedure

EEG

All subjects received the needle stimulation of the three different points on three separate days in randomised order. Measurements were taken within two weeks and with at least 24 hours interval

between each measurement. Subjects were told to sit down in a chair in the EEG room and relax with eyes open while concentrating on the point of needling.

The penetrating needle stimulation was performed with sterile, single use, individually wrapped acupuncture needles (0.30×30 mm; asia-med standard, asia-med GmbH & Co. KG, Germany). The needle was vertically inserted 1–2 cm deep depending on the muscle size. The needle stimulation consisted of manually rotating 60–90/rpm and lift-thrusting 0.3–0.5 cm for 15 s, which was identical for the three point locations (Figure 2).

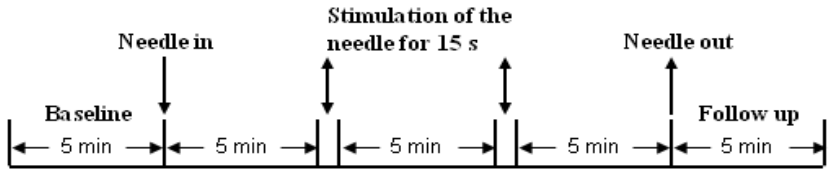

Figure 2: Experiment design of EEG measurement. EEG was recorded for each point stimulation over a 25.5 min period. After the first 5 min baseline, an acupuncture needle was inserted and stimulated manually at a time point 5 and 10 min after insertion. After a further 5 min the needle was removed and the EEG was recorded for a further 5 min without the needle.[6]

A 32-channel EEG was recorded in a noise protected and electrically shielded room using BrainAmp (Brain Product, Germany) with a sampling rate of 1000 Hz. An electrode cap (Electro-Cap International, Eaton, OH) based on the international 10–20 system was placed on the scalp. The electrode FCz was used as reference and the ground electrode was located at the sternum. Electrode impedances were less than 2 kOhm.

fMRI

All the subjects received the needle stimulations in one fMRI session (Figure 3). Each participant was scanned seven runs (6 min each): One resting-state (RS) scan in the very beginning (i.e., baseline, RS_B), then three scans with needle stimulation in an event-related design, each followed by another resting-state scan (i.e., RS_ST36, RS_CP1 and RS_CP2). The three event-related scans were in randomised order over subjects. During needle stimulation, subjects were told to remain in the supine position with eyes open while concentrating on the sensation

caused by the needle stimulation. During the resting-state scans, participants were simply asked to keep calm and stay still with eyes open.

The penetrating needle stimulation was performed with sterile, single use, individually wrapped needles (0.20×30 mm; titanium, DongBang, Acupuncture, Inc., Boryeong, Korea). The needle was first inserted 1–2 cm deep depending on the muscle size vertically. Then auditory cues signalled the timing of the stimulation events to the acupuncturist via headphones. Each event consisted of a 3-s manual rotating 60–90/rpm and lift-thrusting 0.3–0.5 cm (Figure 3). The length of the inter-stimulus interval was randomised from 13 to 21 s. Identical penetrating needle stimulation was performed on the three different point locations.

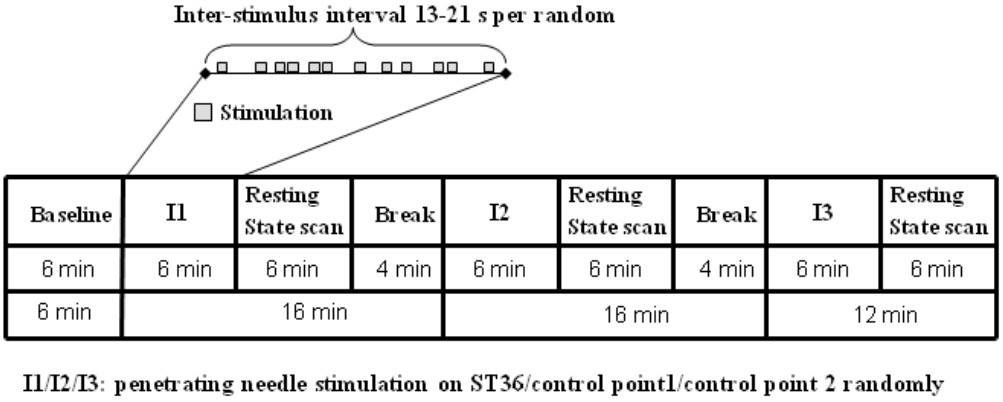

Figure 3: Experiment design of fMRI measurement. After the first resting-state was scanned for 6 min, an acupuncture needle was inserted at one point according to the randomised intervention order and then immediately stimulated manually according to the event-related design. After 6 min intermittent manipulation, the needle was withdrawn and a resting-state scan was continued for 6 min, and then followed by a 4 min break without scanning. The same scan procedure was then applied to the other two interventions on the other two points. But for the third intervention, there was no 4 min break.[6]

fMRI data was acquired using a 3T Siemens Verio MRI System (Siemens Medical, Erlangen, Germany) equipped for echo planer imaging with a 12-channel head coil. fMRI images were acquired using an EPI sequence (30 axial slices, in-plane resolution is 3 mm × 3 mm, slice thickness = 4 mm, flip angle = 90 °, gap = 1 mm, repetition time = 2000 ms, echo time = 30 ms). A structural image was also acquired for each participant, using a T1-weighted MPRAGE sequence (repetition time = 1200ms, echo time = 5.65 ms, and flip angle = 19 °, with elliptical sampling of k space, giving a voxel size of 1 × 1 × 1 mm).

2.2.4 Data analyses

EEG

Data pre-processing

For data analysis custom-built scripts in the software package Matlab (Matlab, MathWorks, Inc.) were used. For each subject the three sessions were merged to perform one ICA calculation (FastICA algorithm in Matlab). The central components cleared from occipital alpha were selected and back projected and the derived dataset was digitally filtered using a standard 3rd order band-pass Butterworth filter (low cut-off 1 Hz, high cut-off 45 Hz) and segmented into 5 epochs each lasting 4 min, based on the markers representing the interventions. The analysis was focused on electrode Cz which is located over the leg representation of primary somatosensory cortex. Frequency analysis was performed using fast Fourier transformation. The power spectral density was computed for each 4 min segment: (1) baseline, (2) after the "needle-insertion", (3) after the first stimulation, (4) after the second stimulation, and (5) follow up. For the statistical analysis of the mu activity, power spectral density was averaged for the frequencies from 10 Hz to 15 Hz.

Statistical analysis

For Cz electrode and each condition, the mu power change compared to baseline was analysed using generalised linear models for within subject comparison with global F-tests and paired t-tests for pair-wise comparisons between stimulation points. For the primary outcome parameter, the mean of both post-stimulation periods, a Bonferroni correction was applied to the pair-wise comparison between the three stimulation points ($p\backslash_{corr}\backslash=0.05/3$).

fMRI

Data pre-processing

fMRI data pre-processing included slice time correction, head motion correction, spatial normalisation to MNI152 space and spatial smoothing with a 6 mm FWHM as implemented in the SPM 8 software package (www.fil.ion.ucl.ac.uk/spm/). Individual structure T1 images were also

normalised to MNI152 space and then segmented into grey matter, white matter and cerebral spinal fluid. We applied the CompCor analysis[8] by DPABI toolbox (toolbox for Data Processing & Analysis of Brain Imaging, http://rfmri.org/dpabi) to generate the nuisance variables. A union grey matter mask (39429 voxels) was created by merging all normalised individual grey matter images and implemented in the following analyses.

General linear model (GLM) analysis

For each subject the first-level GLM analysis was performed on the three different needle stimulations (i.e., ST36, CP1, CP2) in SPM8. The GLM included one stimulation regressor which represented the stimulation sequences and the nuisance regressors. For each of the three point stimulations the individual ß-map (i.e., activity map) was computed. On the second level analyses, the main effect of each of the three point stimulations was visualised by applying these individual ß-maps (age and gender as covariates in all following analysis) to one-sample t-tests to compare them against the null hypothesis. The results were corrected to the alpha-level <0.05 using AlphaSim in AFNI[9] (voxel-wise $p<0.0001$, resulting cluster size>108 mm^3). A within subjects ANOVA (factorial design within SPM8) including the individual ß-maps of all three point stimulations was performed to generate the inter-points comparisons and conjunction maps within one statistical model. The results for the inter-points comparisons as well as for the conjunction maps were corrected to the alpha-level < 0.05 (voxel-wise $p<0.01$, resulting cluster size>783 mm^3).

Seed-based functional connectivity analysis

For each of the four RS scans (RS_B, RS_ST36, RS_CP1, and RS_CP2), temporal band-pass filtering (0.01-0.08Hz) and removal of linear trend were performed by the REST toolbox (www.restfmri.net). The S2 seed (spheres with 6 mm radius, centre: Talairach space, x=-54, y=-21, z=21) was derived from a group-level one-sample t-test across all three point stimulations together. Then, a voxel-wise temporal correlation analysis was performed between the average time course within the ROI and all voxels within the brain mask for each individual's RS scan and transferred

to Fisher's z maps.[10] First, a one-sample t-test against null hypothesis was performed on the spatial correlation maps of each RS scan. The results were corrected to the alpha-level <0.05 using AlphaSim in AFNI (voxel-wise p<0.0001, resulting cluster size>108 mm ^{3}). Then a within subjects ANOVA was performed including the individual spatial correlation maps of all four RS scans. Within this model, the comparisons to baseline, the inter-points comparisons, and the conjunction maps were generated. The results of the different comparisons as well as for the conjunction maps were corrected to the alpha-level < 0.05 (voxel-wise p<0.01, resulting cluster size>783 mm ^{3}).

Centrality analyses

For each individual resting-state scan, the eigenvector centrality map (ECM) and degree centrality map (DCM) was generated by fastECM.[11] Z-standard transform (i.e., for each voxel, subtract the mean value then divide by the standard deviation of the whole brain) and 6 mm FWHM smoothing were performed on the individual DCM and ECM maps.[12,13] A within subjects ANOVA on the ECM/DCM maps of all four RS scans were performed. The comparisons to baseline, the inter-points comparisons and the conjunction maps were generated. All statistical maps were corrected at p < 0.05 by AlphaSim in AFNI (Version 16.2.12).[9] Regions which were detected in the conjunction analysis were selected as ROI. The average and standard error of the mean (SEM) of the z-value within each ROI were calculated.

3. Results

3.1 Acupuncture and fMRI systematic review and meta-analysis (Publication I)

A total of 779 papers were identified, 149 met the inclusion criteria for the descriptive analysis, and 34 were eligible for the meta-analyses. From a descriptive perspective, multiple studies reported that acupuncture modulates activity within specific brain areas, including somatosensory cortices, limbic system, basal ganglia, brain stem, and cerebellum. Meta-analyses for verum acupuncture stimuli confirmed brain activity changes within many of the regions mentioned above. Differences between verum and sham acupuncture were noted in brain response in the middle

cingulate, while some heterogeneity was noted for other regions such as sensorimotor cortices, limbic regions, and cerebellum, depending on how the meta-analyses were performed.

3.2 Brain response to stimulation of an acupuncture point versus two non-acupuncture points measured with EEG and fMRI (Publication II, III)

EEG

Mu rhythm power was significantly enhanced after stimulation of ST36 compared to the stimulation of the two control points. The mean of both post-stimulation periods vs. baseline: 1) ST36 vs. CP1: 21.02 μV^2, 95%CI [4.78;37.27], p=0.012; 2) ST36 vs. CP2: 25.38 μV^2, 95%CI [9.12;41.65], p=0.003; significance level Bonferroni corrected 0.05/3. Comparison of mu rhythm for the two control points found no significant differences (CP2 vs. CP1: -4.36, 95%CI [-20.53;11.81], p=0.598).

fMRI

BOLD response

The results of the intra-point analysis summarising the BOLD response to needle stimulation of ST36 and the two control points are shown in Figure 4A. For all three point stimulations significant activation was found in bilateral insula/S2 and left inferior semi-lunar lobule and deactivation was found in bilateral precuneus, parahippocampal gyrus; right middle temporal gyrus, precentral gyrus, paracentral lobule; left superior frontal gyrus and medial frontal gyrus.

The comparisons of BOLD responses to the different points (ST36 vs. CP1, ST36 vs. CP2, and CP1 vs. CP2) were shown in Figure 4B. The conjunction analysis evaluated shared areas for the comparison of the acupuncture point vs. control points (conjunction of ST36-CP1 and ST36-CP2, shown in Figure 4C) and the comparison of two different dermatomes L2 and L5 (conjunction of ST36-CP2 and CP1-CP2, shown in Figure 4D).

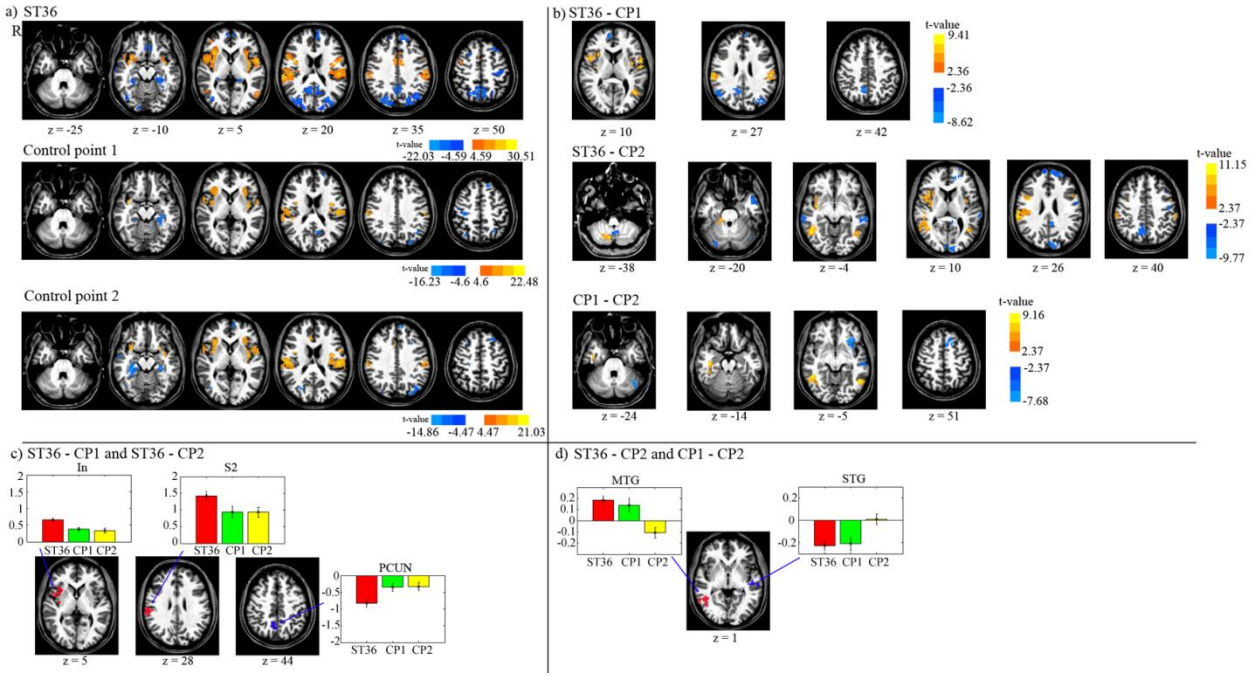

Figure 4: (A) Displayed are the activation and deactivation for the different point stimulations (group-level t-maps, P<0.05, uncorrected). **(B)** The de/activation contrasts between the three different point locations are presented (P<0.05, corrected). **(C)** The conjunction map of the 1st and 2nd row of part (b) (acupuncture vs. control point). **(D)** The conjunction map of the 2nd and 3rd row of part (b) (dermatome L5 vs. L2). The barplots show the beta values across participants (average and standard error) within the respective region. R means right hemisphere. Talairach z coordinates are displayed. Positive values: red, negative: blue. Abbreviation: MTG: middle temporal gyrus; PCUN: precuneus; STG: superior temporal gyrus.[6]

For the comparison between the acupuncture point and control points, the conjunction analysis (Figure 4C) showed higher activation of right insula and S2 and deactivation of right precuneus/posterior cingulate cortex during stimulation of the acupuncture point. For the comparison between the dermatomes, a positive contrast was shown for right middle temporal gyrus due to deactivation during stimulation of CP2 compared to activation when stimulating the other two points (Figure 4D). Left superior temporal gyrus presented pronounced deactivation when stimulating ST36 or CP1 compared to CP2.

Seed-based functional connectivity

The S2 seed-based connectivity analyses were compared between different resting-state scans (Figure 5). ST36 compared to CP1 showed a significantly enhanced S2-connectivity to right precuneus, right middle temporal gyrus, and right parahippocampal gyrus. ST36 compared to CP2 showed a significantly enhanced S2-connectivity to right precuneus/cuneus and right culmen,

whereas the left medial frontal gyrus, left inferior frontal gyrus, and left superior temporal gyrus showed a significantly reduced connectivity to S2.

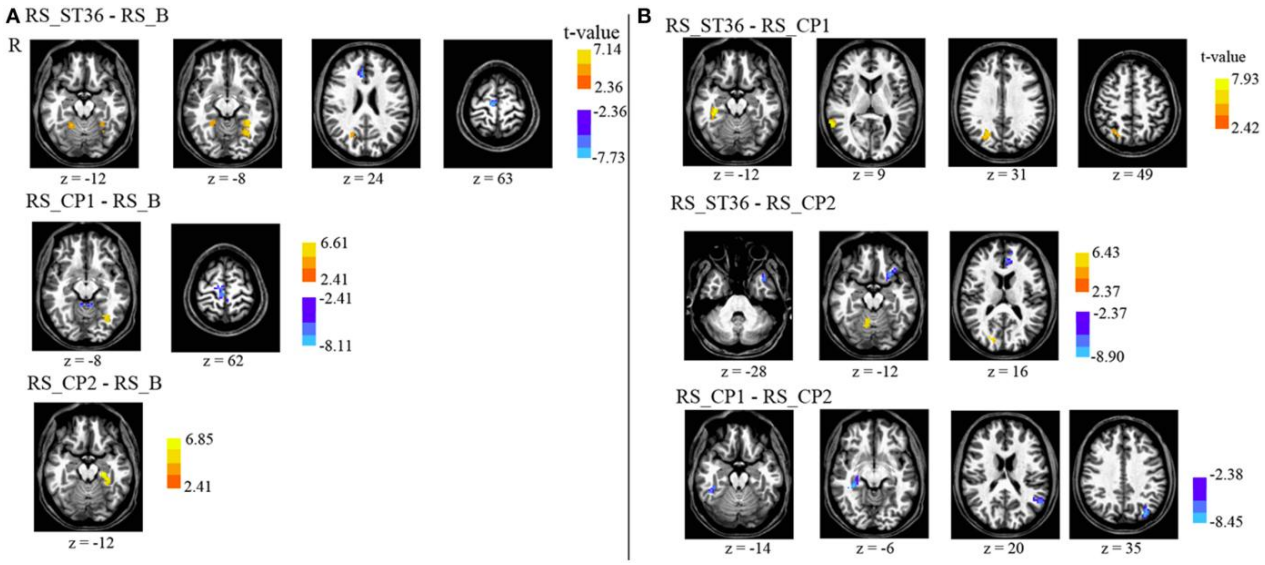

Figure 5: Comparison of the seed-based resting-state connectivity between all resting-state sessions (P<0.05, corrected). (A) The comparison of post-stimulation resting-state scans with the baseline scan. **(B)** The comparison of the post-stimulation resting-state scans with each other. There is no cluster surviving the conjunction analyses across the first and second row (acupuncture vs. control points) as well as across the second and the third row (dermatome L5 vs. L2). R means right hemisphere. Talairach z coordinates are displayed. Positive values: red, negative: blue.[6]

The comparison of the two control points (CP1-CP2) showed a significantly reduced S2-connectivity to right parahippocampal gyrus, left precuneus, and left superior temporal gyrus.

Centrality analyses

The comparison of centrality changes for sustained effects of needle stimulation of all three points against each other and conjunction analyses are displayed in Figure 6. The comparison of the acupuncture point vs. control points (conjunction of RS_ST36-RS_CP1 and RS_ST36-RS_CP2) showed common positive differences (higher centrality for ST36) in parahippocampal gyrus by both ECM and DCM. Another common region with positive differences was found in middle temporal gyrus, but only by ECM. Comparing the effects after stimulation in two different dermatomes L5 and L2 (conjunction of RS_ST36-RS_CP2 and RS_CP1-RS_CP2) revealed no overlapping regions with common differences in centrality.

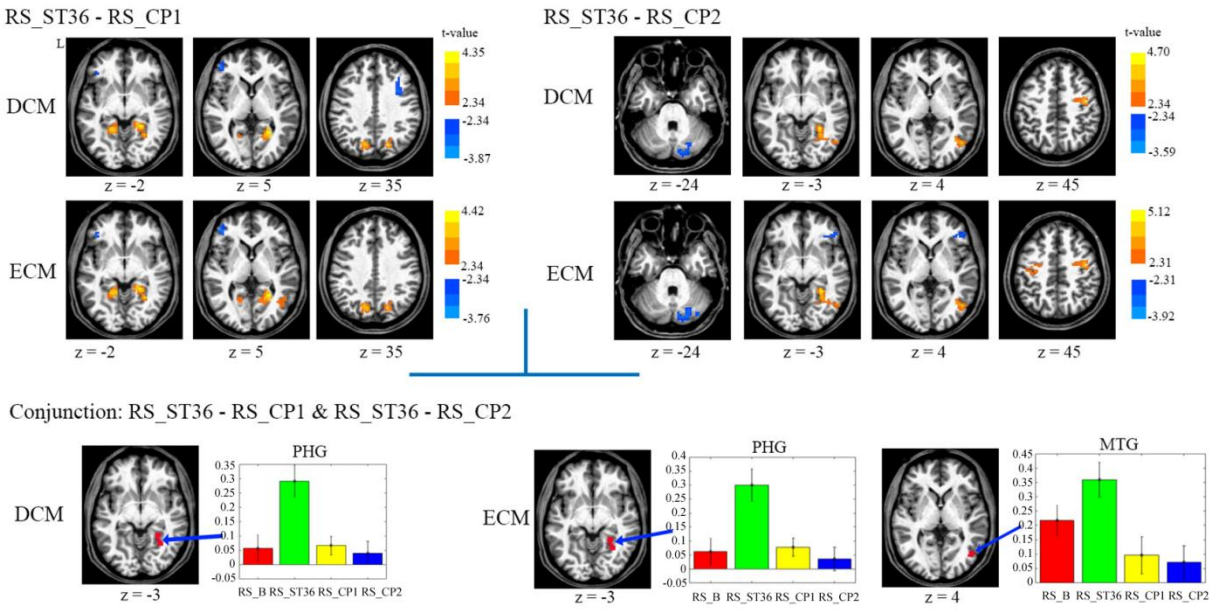

Figure 6: The centrality changes of the post-stimulation of all three points against each other. R means the right hemisphere. The warm colour means increased centrality and the cold colour means decreased centrality. All images were in the Talairach space. P< 0.05, corrected. The average centrality value (mean +/- SEM) of the related centrality measures from each resting-state scan within the selected ROIs which were detected in the conjunction analysis were displayed. Abbreviations: PHG: parahippocampal gyrus; MTG: middle temporal gyrus.[14]

The mean values for the ROIs selected from the conjunction analysis (Figure 6): parahippocampal gyrus showed significantly higher centrality for RS_ST36, in contrast to lower centrality for the other three resting-state scans (baseline and the two control points) in both ECM and DCM. The cluster in middle temporal gyrus (only for ECM) also showed higher centrality for RS_ST36.

4. Discussion

The literature analysis showed that brain response to acupuncture stimuli encompasses a broad network of regions consistent with not just somatosensory, but also affective and cognitive processing. The acupuncture specific effect was mainly found as a greater response in the middle cingulate gyrus of verum compared to sham acupuncture. However, heterogeneity was found for other regions, such as sensorimotor cortices, limbic regions and cerebellum. The heterogeneity might be due to varying acupuncture manipulation techniques, different types of acupuncture controls, different methods of imaging acquisition and data analysis etc. This was the first

meta-analysis of acupuncture and fMRI studies. One later meta-analysis investigating acupuncture and tactile control with more selected publications showed similar results.[15]

The experimental findings are consistent with the evidence of the systematic review and meta-analyses. When comparing the acupuncture point with control points, the instant BOLD response showed pronounced activation in right insula and S2, pronounced deactivation in precuneus/posterior cingulate; the sustained effects during resting-state showed 1) increased connectivity of left S2 to right precuneus, 2) increased centrality in parahippocampal gyrus and middle temporal gyrus, and 3) pronounced increase of mu rhythm.

The instant BOLD changes correspond well with previous findings showing that acupuncture stimulation modulates the pain-related regions, especially insula and S2. Furthermore, deactivation was found in right precuneus during stimulation. In the resting-state scan, both comparisons (RS_ST36-RS_CP1 and RS_ST36-RS_CP2) showed increased connectivity between right precuneus and S2. Whereas S2 and insula are assumed to contribute to the experience of pain,[16] the precuneus seems to be involved in the assessment and integration of pain[17]. Acupuncture related strengthened functional connectivity between S2 and precuneus might represent a possible mechanism that explains the pain relieving effectiveness of acupuncture, especially in chronic pain.

The BOLD signal in parahippocampal gyrus was found mainly deactivated during acupuncture stimulation in previous studies,[18] and also in the current experiment. The level of cerebral blood flow in parahippocampal gyrus was negatively correlated to analgesia after transcutaneous electric stimulation of an acupuncture point, suggesting acupuncture might inhibit pain by inhibiting the pain signal in the parahippocampal gyrus at a later stage.[19] Moreover, recent research found that parahippocampal gyrus is related to the experience of chronic pain and anxiety, and structural changes in parahippocampal gyrus were found in chronic pain patients.[20] Recent studies found significantly reduced grey matter volumes in middle temporal gyrus in chronic pain patients, e.g. lower back pain[21] and cerebral post stroke pain[22]. However, the role of middle temporal gyrus

involved in chronic pain processing is still unclear.[22] These two hubs, parahippocampal gyrus and middle temporal gyrus, which were identified in the centrality analysis, can be linked to the default mode network (DMN).[23,24] The DMN might be the primary network affected by chronic pain.[25] Several studies show that the DMN activity/connectivity is related to memory-based processing,[26] and is modulated in the presence of pain, especially chronic pain[25]. Dhond et al. showed increased DMN connectivity with limbic antinociceptive (anterior cingulate cortex, periaqueductal grey), affective (amygdala, anterior cingulate cortex), and memory (hippocampal formation, middle temporal gyrus) related brain regions following acupuncture, but not sham.[27] The DMN was deactivated during acupuncture stimulation, but not when acupuncture was associated with sharp pain.[28] For chronic pain conditions, such as migraine, the pain relief was correlated with DMN alteration after acupuncture treatments.[29]

The transient desynchronization of mu rhythm was often showed after somatosensory stimulation.[30] However, an after effect of increased mu rhythm following needle stimulation was observed in the experiment. Similar effects of long lasting increased background rhythm have been described for non-invasive brain stimulation protocols such as TDCS/TACS (transcranial direct/alternating current stimulation) or TMS (transcranial magnetic stimulation). [31] The finding of an increased mu rhythm following stimulation of ST36 may represent another potential mechanism of pain modulation, since an increased mu rhythm was previously shown to be associated with a pronounced cortical inhibition[32] and a reduced cortical excitability to painful stimulation[33].

The strengths of this work include a rigorous study design, multimodal data acquisition, combination of hypothesis and data-driven analyses. The subjects were blinded of the different point locations and the researchers were blinded during the pre-processing of the data and during the first steps of data interpretation. To prevent systematic errors, different randomisation procedures were used. The order of point locations was randomised for both experiments, and the inter-stimulus intervals were randomised during the fMRI experiment. Event-related designs can

robustly image brain response to discrete, short duration acupuncture stimuli[34] which correspond well with the clinical application of acupuncture stimulation. For the first time ECM was applied for the analysis of acupuncture fMRI data.

The locations of control point were selected based on the acupuncture meridian theory and dermatome maps. The acupuncture point and nearby CP1 were within L5 and with same peripheral nerve innervations, yet on different muscles. The further CP2 was in a different dermatome L2. However, a lack of consensus on the location and size of individual dermatomes might limit the interpretation of the results. In future studies, different alternative body maps (meridian, dermatome, myotome) might be considered when choosing control point locations.

In summary, the experimental findings indicate that compared to non-acupuncture point locations, somatosensory stimulation at the acupuncture point may modulate the brain activities differently within several brain networks, such as somatosensory, saliency processing and default mode network. These results might hint to a potential mechanism of pain perception and modulation due to acupuncture stimulation. Brain imaging techniques and analyses could be valuable for future studies investigating the neural mechanism of acupuncture effect not only based on healthy subjects, but also diseased ones with evaluation of the correlation between imaging and clinically relevant outcomes.

5. Bibliography

1. Dhond RP, Kettner N, Napadow V. Neuroimaging acupuncture effects in the human brain. *J. Altern. Complement. Med.* 2007;13(6):603-616.

2. Streitberger K, Steppan J, Maier C, Hill H, Backs J, Plaschke K. Effects of verum acupuncture compared to placebo acupuncture on quantitative EEG and heart rate variability in healthy volunteers. *J Altern Complement Med.* 2008;14(5):505-513.

3. Backer M, Hammes M, Sander D, Funke D, Deppe M, Tolle TR, Dobos GJ. Changes of cerebrovascular response to visual stimulation in migraineurs after repetitive sessions of somatosensory stimulation (acupuncture): a pilot study. *Headache.* 2004;44(1):95-101.

4. Vickers AJ, Cronin AM, Maschino AC, Lewith G, Macpherson H, Foster NE, Sherman KJ, Witt CM, Linde K, for the Acupuncture Trialists C. Acupuncture for Chronic Pain: Individual Patient Data Meta-analysis. *Arch. Intern. Med.* 2012:1-10.

5. Eickhoff SB, Laird AR, Grefkes C, Wang LE, Zilles K, Fox PT. Coordinate-based activation likelihood estimation meta-analysis of neuroimaging data: a random-effects approach based on empirical estimates of spatial uncertainty. *Hum Brain Mapp.* 2009;30(9):2907-2926.

6. Nierhaus T, Pach D, Huang W, Long X, Napadow V, Roll S, Liang F, Pleger B, Villringer A, Witt CM. Differential cerebral response to somatosensory stimulation of an acupuncture point vs. two non-acupuncture points measured with EEG and fMRI. *Frontiers in human neuroscience.* 2015;9:74.

7. Drake R, Vogl, A.W., Mitchell, A.W. Gray's anatomy for students. 2nd ed. Philadelphia: Elsevier Health Sciences; 2009:523.

8. Behzadi Y, Restom K, Liau J, Liu TT. A component based noise correction method (CompCor) for BOLD and perfusion based fMRI. *Neuroimage.* 2007;37(1):90-101.

9. Cox RW. AFNI: software for analysis and visualization of functional magnetic resonance neuroimages. *Comput. Biomed. Res.* 1996;29(3):162-173.

10. Greicius MD, Flores BH, Menon V, Glover GH, Solvason HB, Kenna H, Reiss AL, Schatzberg AF. Resting-state functional connectivity in major depression: abnormally increased contributions from subgenual cingulate cortex and thalamus. *Biol. Psychiatry.* 2007;62(5):429-437.

11. Wink AM, de Munck JC, van der Werf YD, van den Heuvel OA, Barkhof F. Fast eigenvector centrality mapping of voxel-wise connectivity in functional magnetic resonance imaging: implementation, validation, and interpretation. *Brain connectivity.* 2012;2(5):265-274.

12. Yan CG, Cheung B, Kelly C, Colcombe S, Craddock RC, Di Martino A, Li Q, Zuo XN, Castellanos FX, Milham MP. A comprehensive assessment of regional variation in the impact of head micromovements on functional connectomics. *Neuroimage.* 2013;76C:183-201.

13. Zuo XN, Ehmke R, Mennes M, Imperati D, Castellanos FX, Sporns O, Milham MP. Network centrality in the human functional connectome. *Cereb. Cortex.* 2012;22(8):1862-1875.

14. Long X, Huang W, Napadow V, Liang F, Pleger B, Villringer A, Witt CM, Nierhaus T, Pach D. Sustained Effects of Acupuncture Stimulation Investigated with Centrality Mapping Analysis. *Frontiers in human neuroscience.* 2016;10:510.

15. Chae Y, Chang DS, Lee SH, Jung WM, Lee IS, Jackson S, Kong J, Lee H, Park HJ, Wallraven C. Inserting needles into the body: a meta-analysis of brain activity associated with acupuncture needle stimulation. *The journal of pain : official journal of the American Pain Society.* 2013;14(3):215-222.

16. Craig AD. How do you feel--now? The anterior insula and human awareness. *Nature reviews. Neuroscience.* 2009;10(1):59-70.

17. Goffaux P, Girard-Tremblay L, Marchand S, Daigle K, Whittingstall K. Individual differences in pain sensitivity vary as a function of precuneus reactivity. *Brain Topogr.* 2014;27(3):366-374.

18. Napadow V, Makris N, Liu J, Kettner NW, Kwong KK, Hui KK. Effects of electroacupuncture versus manual acupuncture on the human brain as measured by fMRI. *Hum Brain Mapp.* 2005;24(3):193-205.

19. Jiang Y, Liu J, Liu J, Han J, Wang X, Cui C. Cerebral blood flow-based evidence for mechanisms of low- versus high-frequency transcutaneous electric acupoint stimulation analgesia: A perfusion fMRI study in humans. *Neuroscience.* 2014;268:180-193.

20. Smallwood RF, Laird AR, Ramage AE, Parkinson AL, Lewis J, Clauw DJ, Williams DA, Schmidt-Wilcke T, Farrell MJ, Eickhoff SB, Robin DA. Structural brain anomalies and chronic

pain: a quantitative meta-analysis of gray matter volume. *The journal of pain : official journal of the American Pain Society.* 2013;14(7):663-675.

21. Luchtmann M, Steinecke Y, Baecke S, Lutzkendorf R, Bernarding J, Kohl J, Jollenbeck B, Tempelmann C, Ragert P, Firsching R. Structural brain alterations in patients with lumbar disc herniation: a preliminary study. *PLoS One.* 2014;9(3):e90816.

22. Krause T, Asseyer S, Taskin B, Floel A, Witte AV, Mueller K, Fiebach JB, Villringer K, Villringer A, Jungehulsing GJ. The Cortical Signature of Central Poststroke Pain: Gray Matter Decreases in Somatosensory, Insular, and Prefrontal Cortices. *Cerebral cortex.* 2016;26(1):80-88.

23. Laird AR, Eickhoff SB, Li K, Robin DA, Glahn DC, Fox PT. Investigating the functional heterogeneity of the default mode network using coordinate-based meta-analytic modeling. *The Journal of neuroscience : the official journal of the Society for Neuroscience.* 2009;29(46):14496-14505.

24. Greicius MD, Krasnow B, Reiss AL, Menon V. Functional connectivity in the resting brain: a network analysis of the default mode hypothesis. *Proc Natl Acad Sci U S A.* 2003;100(1):253-258.

25. Baliki MN, Mansour AR, Baria AT, Apkarian AV. Functional reorganization of the default mode network across chronic pain conditions. *PLoS One.* 2014;9(9):e106133.

26. Vatansever D, Menon DK, Manktelow AE, Sahakian BJ, Stamatakis EA. Default Mode Dynamics for Global Functional Integration. *J. Neurosci.* 2015;35(46):15254-15262.

27. Dhond RP, Yeh C, Park K, Kettner N, Napadow V. Acupuncture modulates resting state connectivity in default and sensorimotor brain networks. *Pain.* 2008;136(3):407-418.

28. Hui KK, Marina O, Claunch JD, Nixon EE, Fang J, Liu J, Li M, Napadow V, Vangel M, Makris N, Chan ST, Kwong KK, Rosen BR. Acupuncture mobilizes the brain's default mode and its anti-correlated network in healthy subjects. *Brain Res.* 2009;1287:84-103.

29. Zhao L, Liu J, Zhang F, Dong X, Peng Y, Qin W, Wu F, Li Y, Yuan K, von Deneen KM, Gong Q, Tang Z, Liang F. Effects of long-term acupuncture treatment on resting-state brain

activity in migraine patients: a randomized controlled trial on active acupoints and inactive acupoints. *PLoS One.* 2014;9(6):e99538.

30. Ploner M, Gross J, Timmermann L, Pollok B, Schnitzler A. Pain suppresses spontaneous brain rhythms. *Cereb. Cortex.* 2006;16(4):537-540.

31. Wagner T, Valero-Cabre A, Pascual-Leone A. Noninvasive human brain stimulation. *Annual review of biomedical engineering.* 2007;9:527-565.

32. Jensen O, Mazaheri A. Shaping functional architecture by oscillatory alpha activity: gating by inhibition. *Frontiers in human neuroscience.* 2010;4:186.

33. Ploner M, Gross J, Timmermann L, Pollok B, Schnitzler A. Oscillatory activity reflects the excitability of the human somatosensory system. *Neuroimage.* 2006;32(3):1231-1236.

34. Napadow V, Lee J, Kim J, Cina S, Maeda Y, Barbieri R, Harris RE, Kettner N, Park K. Brain correlates of phasic autonomic response to acupuncture stimulation: an event-related fMRI study. *Hum Brain Mapp.* 2013;34(10):2592-2606.

Affidavit

I, Wenjing Huang, certify under penalty of perjury by my own signature that I have submitted the thesis on the topic “Changes of Human Brain Activity after Complex Somatosensory Stimulation with Acupuncture Needles”, I wrote this thesis independently and without assistance from third parties, I used no other aids than the listed sources and resources.

All points based literally or in spirit on publications or presentations of other authors are, as such, in proper citations (see "uniform requirements for manuscripts (URM)" the ICMJE www.icmje.org) indicated. The sections on methodology (in particular practical work, laboratory requirements, statistical processing) and results (in particular images, graphics and tables) correspond to the URM (s.o) and are answered by me. My contributions in the selected publications for this dissertation correspond to those that are specified in the following joint declaration with the responsible person and supervisor. All publications resulting from this thesis and which I am author of correspond to the URM (see above) and I am solely responsible.

The importance of this affidavit and the criminal consequences of a false affidavit (section 156,161 of the Criminal Code) are known to me and I understand the rights and responsibilities stated therein.

_____

Date Signature

Declaration of any eventual publications

Wenjing Huang had the following share in the following publications:

Publication 1: Huang W, Pach D, Napadow V, Park K, Long X, Neumann J, Maeda Y, Nierhaus T, Liang F, Witt CM. Characterizing acupuncture stimuli using brain imaging with fMRI--a systematic review and meta-analysis of the literature. *PloS one.* 2012;7(4):e32960.

Contribution in detail (ca. 70%): Contributed to the design of the study, data extraction of the English and Chinese literature, conduction of data analysis, participation of figure preparation, data interpretation, writing the first draft and revision.

Publication 2: Nierhaus T*, Pach D*, Huang W*, Long X, Napadow V, Roll S, Liang F, Pleger B, Villringer A, Witt CM. Differential cerebral response to somatosensory stimulation of an acupuncture point vs. two non-acupuncture points measured with EEG and fMRI. *Frontiers in human neuroscience.* 2015;9:74. (*equal contribution)

Contribution in detail (ca. 40%): Contributed to study conception and experiment design, completion of the study intervention of the experiment, participation of data input, data interpretation, writing the first draft and revision.

Publication 3: Long X*, Huang W*, Napadow V, Liang F, Pleger B, Villringer A, Witt CM, Nierhaus T, Pach D. Sustained effects of acupuncture stimulation investigated with centrality mapping analysis. *Frontiers in human neuroscience.* 2016;10:510. (*equal contribution)

Contribution in detail (ca. 50%): Contributed to study conception and experiment design, completion of the study intervention of the experiment, participation of data input, data interpretation, writing the first draft and revision.

Signature, date and stamp of the supervising University teacher

_____

Signature of the doctoral candidate

_____

Print copies of selected publications

Publication 1: Huang W, Pach D, Napadow V, Park K, Long X, Neumann J, Maeda Y, Nierhaus T, Liang F, Witt CM. Characterizing acupuncture stimuli using brain imaging with fMRI--a systematic review and meta-analysis of the literature. *PloS one.* 2012;7(4):e32960.

OPEN ACCESS Freely available online

PLoS one

Characterizing Acupuncture Stimuli Using Brain Imaging with fMRI - A Systematic Review and Meta-Analysis of the Literature

Wenjing Huang[1,2], Daniel Pach[1], Vitaly Napadow[4,5], Kyungmo Park[6], Xiangyu Long[8], Jane Neumann[8,9], Yumi Maeda[4,5], Till Nierhaus[7,8], Fanrong Liang[2], Claudia M. Witt[1,3]*

1 Institute for Social Medicine, Epidemiology and Health Economics, Charité University Medical Center, Berlin, Germany, **2** Chengdu University of Traditional Chinese Medicine, Chengdu, China, **3** Center for Integrative Medicine, University of Maryland School of Medicine, Baltimore, Maryland, United States of America, **4** Athinoula A. Martinos Center for Biomedical Imaging, Department of Radiology, Massachusetts General Hospital, Charlestown, Massachusetts, United States of America, **5** Department of Radiology, Logan College of Chiropractic, Chesterfield, Missouri, United States of America, **6** Department of Biomedical Engineering, Kyung Hee University, Yongin, Republic of Korea, **7** Berlin NeuroImaging Center and Department Neurology, Charité, Berlin, Germany, **8** Max Planck Institute for Human Cognitive and Brain Sciences, Leipzig, Germany, **9** Leipzig University Medical Center, IFB Adiposity Diseases, Leipzig, Germany

Abstract

Background: The mechanisms of action underlying acupuncture, including acupuncture point specificity, are not well understood. In the previous decade, an increasing number of studies have applied fMRI to investigate brain response to acupuncture stimulation. Our aim was to provide a systematic overview of acupuncture fMRI research considering the following aspects: 1) differences between verum and sham acupuncture, 2) differences due to various methods of acupuncture manipulation, 3) differences between patients and healthy volunteers, 4) differences between different acupuncture points.

Methodology/Principal Findings: We systematically searched English, Chinese, Korean and Japanese databases for literature published from the earliest available up until September 2009, without any language restrictions. We included all studies using fMRI to investigate the effect of acupuncture on the human brain (at least one group that received needle-based acupuncture). 779 papers were identified, 149 met the inclusion criteria for the descriptive analysis, and 34 were eligible for the meta-analyses. From a descriptive perspective, multiple studies reported that acupuncture modulates activity within specific brain areas, including somatosensory cortices, limbic system, basal ganglia, brain stem, and cerebellum. Meta-analyses for verum acupuncture stimuli confirmed brain activity within many of the regions mentioned above. Differences between verum and sham acupuncture were noted in brain response in middle cingulate, while some heterogeneity was noted for other regions depending on how such meta-analyses were performed, such as sensorimotor cortices, limbic regions, and cerebellum.

Conclusions: Brain response to acupuncture stimuli encompasses a broad network of regions consistent with not just somatosensory, but also affective and cognitive processing. While the results were heterogeneous, from a descriptive perspective most studies suggest that acupuncture can modulate the activity within specific brain areas, and the evidence based on meta-analyses confirmed some of these results. More high quality studies with more transparent methodology are needed to improve the consistency amongst different studies.

Citation: Huang W, Pach D, Napadow V, Park K, Long X, et al. (2012) Characterizing Acupuncture Stimuli Using Brain Imaging with fMRI - A Systematic Review and Meta-Analysis of the Literature. PLoS ONE 7(4): e32960. doi:10.1371/journal.pone.0032960

Editor: Ben J. Harrison, The University of Melbourne, Australia

Received June 14, 2011; **Accepted** February 8, 2012; **Published** April 9, 2012

Funding: Funding provided by Carstens Foundation and Chinese Scholarship Council. The funders had no role in study design, data collection and analysis, decision to publish, or preparation of the manuscript.

Competing Interests: The authors have declared that no competing interests exist.

* E-mail: claudia.witt@charite.de

Introduction

Acupuncture is a therapy of inserting and manipulating fine filiform needles into specific body locations (acupuncture points) to treat diseases. Acupuncture is an ancient Chinese treatment that has been systematically used for over 2000 years [1]. Currently, acupuncture is used widely all over the world, but its biological mechanism is not well understood. From a neurophysiological aspect acupuncture can be regarded as a complex somatosensory stimulation [2]. Although the clinical effect of acupuncture is generally accepted for certain diagnoses [3], such as knee pain, low back pain etc., there exists controversy regarding the specific effect of acupuncture, especially for the specificity of acupuncture points and meridians. In clinical studies large effects produced by sham acupuncture were observed [4–6].

Interest in investigating acupuncture mechanisms with imaging techniques has been growing since the mid 1990 s [7,8]. Positron emission tomography (PET), single photon emission computed tomography (SPECT), and magnetic resonance imaging (MRI)

have been used and, there is also interest in electro-encephalography (EEG). Functional MRI (fMRI), investigating the hemodynamic blood oxygenation level dependent (BOLD) effect, has come to dominate the brain mapping field due to its minimal invasiveness, lack of radiation exposure, excellent spatial resolution and relatively wide availability.

In the previous decade, an increasing number of studies applied fMRI to investigate acupuncture stimulation. The aim of this review was to give a systematic overview about the fMRI research on acupuncture regarding the following four aspects: 1) differences between verum and sham acupuncture, 2) differences due to various methods of acupuncture manipulation, 3) differences between patients and healthy volunteers, 4) differences between different acupuncture points.

Methods

The search strategy, research questions, inclusion and exclusion criteria and data extraction and analysis were predefined in our protocol. During the study, the database search was extended for the Japanese and Korean databases.

Searching

We searched the following sources:

1.PubMed (1948–2009.09) 2.EMBASE (1980–2009.09) 3. CNKI (China National Knowledge Infrastructure) (1915–2009.09) 4.Japanese Ichushi-Web (1983–2009.09) 5.Korean NDSL (National Digital Science Links) (1946–2009.09); KTKP (Korean Traditional Knowledge Portal) (1997–2008)

We searched these databases in the appropriate language using the following MeSH terms and search strategies:

English: 1.fMRI; 2.Functional MRI; 3.MRI, Functional; 4. Magnetic Resonance Imaging, Functional; 5.acupuncture; 6.#1 or #2 or #3 or #4; 7.#5 and #6;

Chinese: 1.针刺(acupuncture); 2.磁共振成像(Magnetic Resonance Imaging); 3.#1 and #2

Japanese: 1.1.鍼(acupuncture); 2.機能的磁気共鳴画像法 (Functional Magnetic Resonance Imaging); 3.#1 and #2

Korean: 1.기능적 자기공명영상 (fMRI, functional Magnetic Resonance Imaging); 2.침 (acupuncture); 3.#1 and #2

We screened the bibliographies of identified trials and reviewed articles for further potentially relevant publications.

Selection

In this review we included all studies using fMRI to investigate the effect of acupuncture on the human brain. Each study had to have at least one group, which received an intervention with any type of needle-based acupuncture. We included trials on healthy volunteers as well as patients and all types of needle acupuncture were accepted. There were no language restrictions and no limitations on outcome measures. Reviews, editorials and trials on animals were excluded.

The available abstracts of all identified references were screened and we excluded all citations that clearly did not fit the inclusion criteria. Full copies of all remaining articles and those references without available abstracts were obtained. Subsequently the three researchers (WJH: Pubmed, Embase and CNKI, KP: Korean databases, YM: Japanese databases) screened the full texts and assessed whether these trials met the inclusion criteria.

In the meta-analysis, we included studies investigating only verum acupuncture or both verum and sham acupuncture by fMRI using whole brain acquisition. Studies were excluded if 1) the number of study participants was less than five; 2) results were not reported as 3-dimensional coordinates in standard stereotactic space; 3) only the results from regions of interest (ROI) were reported or 4) only single subject data instead of group data were reported.

Data extraction and analysis

The three researchers (WJH: Pubmed, Embase and CNKI, KP: Korean databases, YM: Japanese databases) extracted the data for all descriptive information from the publications, namely published journals, language, study place, study type, subjects, handedness, objective, interventions, control groups, block-design, fMRI device type, software for fMRI data analysis, sample size, and results. The extracted data were discussed with three supervisors (CW, DP and VN). Any inconsistencies were discussed and reconsidered until consensus was reached.

Results were structured according to the four research questions. Studies that matched multiple research questions were displayed more than once, but only with the part of the study relevant to the respective research question.

Furthermore, one figure for different acupuncture points from publications in Talairach coordinates was generated by one author (XYL) using Analysis of Functional NeuroImages (AFNI, http://afni.nimh.nih.gov) and MRIcron software (http://www.cabiatl.com/mricro). The anatomical image was generated using MRIcron software.

The meta-analyses were conducted (JN, XYL, WJH) in Talairach space, using the activation likelihood estimation technique (ALE) implemented in GingerALE 2.1.1 software [9–11]. This technique assesses the convergence between activation foci from different experiments. Prior to the analysis, coordinates reported in MNI (Montreal Neurological Institute) space were converted to Talairach anatomical space using the Lancaster transform [12]. For each experiment, every reported activation maximum was modeled by a 3-dimensional Gaussian probability distribution centered at the given coordinate. The width of the Gaussian probability distribution was determined individually for each experiment based on empirical estimates of between-subject variability, taking into account the number of subjects in each experiment [9]. Voxel-wise ALE scores were calculated from the union of the Gaussian probability distributions within and across experiments. In a random effects analysis, ALE scores were tested against a null hypothesis of random distribution across the brain, thereby identifying those regions where empirical ALE values were higher than could be expected by chance. Resulting ALE maps were thresholded at $p<0.05$ (corrected for multiple comparisons by False Discovery Rate). The minimum cluster volume was chosen to exceed the number of voxels corresponding to 5% possible false positives. The contrast studies analysis (subtraction analysis which compares two ALE maps) was performed with randomization testing with 10,000 permutations. As there exists no correction for multiple comparison with this approach, the threshold was set at $p<0.05$ (uncorrected) with a min. cluster size = 200 mm^3 [13].

ALE maps were computed for the following statistical comparisons. From all studies included in the meta-analysis: 1a) greater activation of verum acupuncture points compared to baseline (verum>rest), 1b) greater deactivation of verum acupuncture points compared to baseline (rest>verum). From the studies which provided direct contrasts between verum and sham acupuncture: 2a) greater activation from verum than sham acupuncture (or greater deactivation for sham, i.e. verum>sham), 2b) greater deactivation from verum than sham acupuncture (or greater activation for sham, i.e. sham>verum). From the studies which had both verum and sham acupuncture groups: 3a) greater activation of verum acupuncture points than baseline (verum>

rest), 3b) greater deactivation of verum acupuncture points than baseline (rest>verum), 3c) greater activation of sham acupuncture points than baseline (sham>rest), 3d) greater deactivation of sham acupuncture points than baseline (rest>sham), 3e) comparison ALE map of greater activation of verum than sham acupuncture relative to rest ("verum>rest" - "sham>rest"), 3f) comparison ALE map of greater deactivation of verum than sham acupuncture relative to rest ("rest>verum" - "rest>sham").

Results

Study characteristics

The 149 studies were published between 1999 and 2009 (trial flow see Figure 1), Figure 2 shows the number of publications per year in corresponding countries in the last 11 years. Most of the studies were performed in China, US and Korea and predominantly published in Chinese and English (50.3% Chinese, 38.9% English, 9.4% Korean, 0.7% German and 0.7% Japanese). The median number of subjects per study was 17 (min. 1 to max. 67), and the total number of all studies included 2469 subjects. 24 studies reported parallel group randomized trials. 128 studies were on healthy volunteers, 13 studies on patients, 8 studies on the comparison of patients and healthy volunteers. Most of the trials applied a block design for fMRI data acquisition, with a time range for each block of 8 sec to 6 min, and the number of blocks ranged from one to 12 blocks. 105 studies included right-handed subjects while only 3 studies included also left-handed subjects. 34 studies were included in the meta-analyses.

Descriptive findings of differences between verum and sham acupuncture

51 publications explored four kinds of sham acupuncture including a) a placebo needle (Streitberger needle [14]: with a blunt tip, which when it touches the skin causes a pricking sensation for the patient, simulating the puncturing of the skin. The needle moves inside the handle, and appears to be shortened.); b) needling at non-acupuncture points in close proximity to acupuncture points; c) needling at non-acupuncture points distant to acupuncture points; d) cutaneous stimulation at the same acupuncture points or sham point/area (Table S1). Two of the studies [15,16] are referenced more than once in the table because of the different sham acupuncture methods evaluated in these studies. The studies included mainly healthy volunteers, but four publications [17–20] included patients with Parkinson's disease or stroke.

A placebo needle: Streitberger Needle. The four studies which compared verum acupuncture with the Streitberger Needle were all from the US and showed heterogeneous results [16,19,21,22]. Yoo et al. [16] found more activation associated

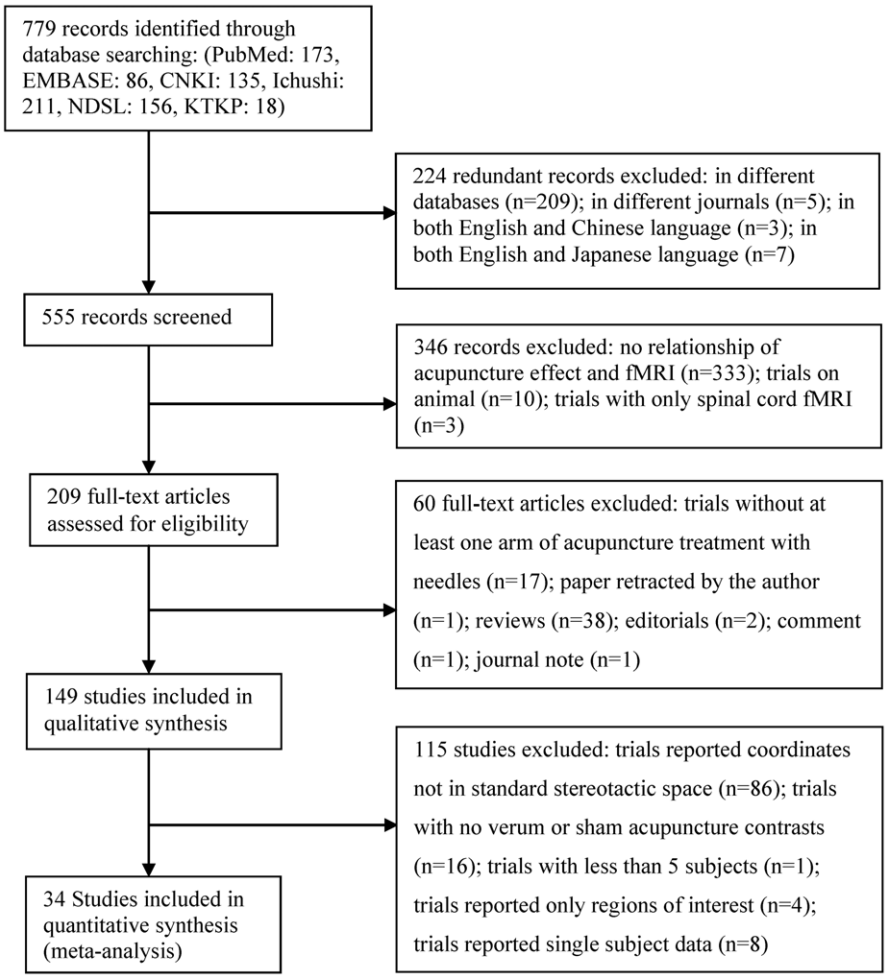

Figure 1. Flow of information through the different phases of the systematic review.
doi:10.1371/journal.pone.0032960.g001

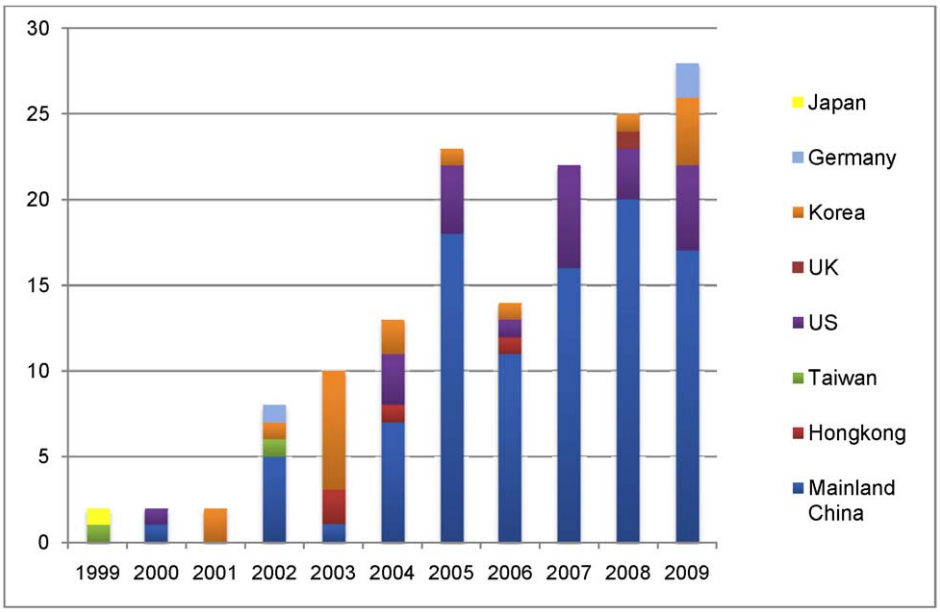

Figure 2. Number of publications on acupuncture and fMRI identified in the last 11 years.
doi:10.1371/journal.pone.0032960.g002

with verum acupuncture in the somatosensory areas and motor areas. Dougherty et al. [21] reported that acupuncture produced more activation in the medial orbitofrontal cortex and more deactivation in brainstem and insula, while the Streitberger needle showed higher activation in the language area (Wernicke), pons, operculum and insula. According to Deng et al. [22] verum acupuncture resulted in more activation in insula and operculum compared to the Streitberger needle placed at a non-acupuncture point. A study with stroke patients [19] (scan during passive finger movement pre and -post 10 weeks treatment of verum acupuncture or the Streitberger placebo needle) showed a trend toward a greater maximum activation change in the motor cortical area for the verum acupuncture group.

Acupuncture at non-acupuncture points in close proximity to acupuncture points. Two third (64%) [15,23–37] of 25 studies showed that acupuncture treatments were associated with more activation, mainly in the somatosensory areas, motor areas, basal ganglia, cerebellum, limbic system and higher cognitive areas (e.g. prefrontal cortex). Three studies [28,37,38] showed also more deactivations in the limbic system in response to acupuncture. In contrast, one study [39] found greater activation in the supplementary motor area in response to sham acupuncture. Five other studies [40–44] found no significant difference between verum and sham acupuncture. One experiment was analyzed twice [45,46] and came to different results.

Acupuncture at non-acupuncture points distant to acupuncture points. Of six studies, two studies [47,48] showed no differences between verum and sham acupuncture. Four studies [49–52] showed more activation associated with acupuncture in the somatosensory areas, brainstem, basal ganglia, higher cognitive areas and part of the limbic system (hypothalamus, nucleus accumbens), and one study [52] showed more activation associated with sham acupuncture in the motor area and operculum. Verum acupuncture showed also more deactivation in part of the limbic system (amygdala, hippocampus, cingulate gyrus/cortex) [47,52]. In addition, Napadow et al. [51] found that both verum and sham acupuncture showed linearly decreasing activation over repeated stimulus blocks in the sensorimotor areas, while verum acupuncture produced bimodal activity in a limbic midbrain region - activation in early blocks, but deactivation in later stimulus blocks.

Cutaneous stimulation at the same acupuncture point or sham point/area. There are 18 studies (15 on healthy volunteers). Only one study [16] on healthy volunteers found greater activation in the somatosensory area during verum acupuncture, whereas in four studies [53–56] somatosensory activation was greater with cutaneous stimulation. For motor areas and higher cognitive areas, five studies [15,16,55,57,58] showed that acupuncture was associated with more activation. For brainstem, basal ganglia, cerebellum and limbic system the results were complex or contradictory: in the basal ganglia, brainstem and cerebellum, two studies [53,59] found that acupuncture was associated with more deactivation while three other studies [15,57,60] found acupuncture associated with more activation; thalamus and insula [15,16,54,58] were activated more while hypothalamus, hippocampus, amygdala and temporal pole [53,54,58,59] were deactivated more by acupuncture. In addition, when eliciting deqi, Hui et al. [53] found extensive deactivation in the cerebrum, brainstem and cerebellum, while eliciting deqi mixed with pain, activation was the predominant pattern. Five Chinese studies [61–65] found almost no significant differences between verum and sham, though two of them found greater activation intensity in the cerebellum or parietal lobe for verum acupuncture [61,62]. Among the three publications on patients, Schockert et al. [20] found more activation in the motor area on stroke patients during acupuncture while Li et al. [17] found more activation in the somatosensory and motor areas with a control, brushing stimulation on stroke patients. In patients with Parkinson's disease Chae et al. [18] showed that acupuncture was associated with more activation than covert cutaneous stimulation in the motor area, basal ganglia, visual and higher cognitive area; and more activation in the motor, visual, higher cognitive areas and limbic system, compared to overt cutaneous stimulation.

Descriptive findings of differences due to various methods of acupuncture manipulation

Manipulation methods can differ in the depth of needling, forms of needle stimulation (e.g. manual versus electrical), intensity of stimulation, and stimulus timing parameters (e.g. duration, frequency, etc.). Here, we summarized the results from those studies comparing different methods of manipulation at acupuncture points in healthy volunteers (see Table 1). Two of the studies [58,66] are displayed more than once in the table as they explored multiple comparisons.

Comparison of different needling depths. Of four studies, two studies [67,68] found no significant difference between deep and superficial needling. Whereas Zhang et al. [25] found more activation in almost all brain areas from deep needling and Wu et al. [52] found more activation from superficial needling in the somatosensory area, motor area and language areas (Broca and Wernicke areas), and from deep needling more deactivation in the limbic system.

Comparison of electro-acupuncture vs. manual acupuncture. Overall, the results of three studies showed that electro-acupuncture tends to produce more activation and less deactivation compared to manual acupuncture. Regarding brain activations, two studies [58,69] found more activation associated with electro-acupuncture in somatosensory areas, motor area, brainstem, cingulate or insula and one study [66] found no significant difference. Regarding brain deactivations, two studies [66,69] showed manual acupuncture was associated with more deactivation in the limbic system [69], cuneus [66], transverse temporal gyrus [66] or middle frontal gyrus [66], yet two studies [58,69] also showed more deactivation from electro-acupuncture in the septal area or precuneus.

Comparison of different frequencies of electro-acupuncture stimulation. Two studies compared different electro-acupuncture frequencies. Napadow et al. [58] found that the brainstem was more activated at 2 Hz than at 100 Hz. But Li et al. [66] found no significant difference between 2 Hz and 20 Hz.

Comparison of different intensities of manual acupuncture stimulation. Of six studies one study [70] observed that a longer duration of manipulation induced more activation in the inferior frontal, temporal, parietal gyrus, occipital lobe, cerebellum or temporal pole and more deactivation in the prefrontal cortex, orbital gyrus or pons than shorter manipulation. Four studies [42,71–73] found more activation in the somatosensory areas, limbic system, visual, language areas or higher cognitive areas in response to stimulation compared to no stimulation. The last study [74] showed that stimulation which induced deqi by maximum manipulation was associated with more activation in the postcentral gyrus and the limbic system than stimulation that didn't induce deqi with minimum manipulation.

Descriptive findings of differences between patients and healthy volunteers

All seven studies comparing healthy volunteers with patients showed that patients responded differently (See Table 2). According to Wang et al. [75] the frontal lobe was activated in stroke patients while motor areas were activated in healthy volunteers. Fu et al. [76] found patients with Alzheimer's disease had more activation in the cingulate gyrus and cerebellum. Liu et al. [77] found more robust activation in the hypothalamus in heroin addicts. Wu et al. [78] found deactivation in primary motor cortex (M1), parahippocampal gyrus, and higher cognitive areas and more activation in the cuneus and the insula in children with spastic cerebral palsy but not in healthy children. Conversely, more activation in caudate nucleus, thalamus and cerebellum was found in healthy children. Napadow et al. [79] compared patients with carpal tunnel syndrome (CTS) before and after five weeks' acupuncture to healthy volunteers receiving no treatment. Following acupuncture, a significant decrease in the activation area was found in contralateral primary somatosensory cortex (SI) and M1 in the CTS patients, as well as, increased separation between digit 3 and digit 2 cortical representations in SI, suggesting acupuncture-induced neuroplasticity. In addition, Napadow et al. compared manual acupuncture to cutaneous stimulation on both CTS patients and healthy volunteers. They found that CTS patients responded to verum acupuncture with less deactivation in the amygdala and greater activation in the lateral hypothalamic area [80], compared to healthy subjects. Moreover, CTS patients responded to sham acupuncture with greater activation in the somatosensory areas, cognitive and affective areas. Li et al. [17] found that stroke patients had more activation in the SI than healthy volunteers when both groups underwent both verum and sham acupuncture.

Descriptive findings of differences between different acupuncture points

The data on acupuncture point specific changes in brain activation and deactivation are shown in Table S2, originating from 76 publications [15,16,22,24,27,31,33,42,45–47,51–53,55,57–59,61,63,64,67,69,81–107] [29,34,37,39,40,43,73,108–126] addressing 37 acupuncture points. Acupuncture points along the 12 regular meridians and one extra meridian (Du meridian) were assessed. The data showed changes in brain activity for each individual acupuncture point from respective publications. The most studied points were LI4, ST36, PC6, LR3 and GB34. These points have a wide clinical applicability and are frequently used in clinical practice. Overall the data showed that acupuncture stimulation mainly influenced the brain activity of the somatosensory areas, motor areas, auditory areas, visual areas, cerebellum, the limbic system and higher cognitive areas.

Furthermore, we generated on a descriptive level map (Figure 3) of 18 acupuncture points from 46 publications, which reported pre-post data on Talairach coordinates. These 18 points were located along 9 meridians. The brain maps of each acupuncture point differ considerably from each other. However, the acupuncture points on the same meridian showed some similarities among the activation/deactivation pattern. For example, the points on the stomach meridian showed activation in the supramarginal gyrus and deactivation in the posterior cingulate, hippocampus, and parahippocampus. In addition, the vision related points GB37 and UB60 showed deactivation in the visual areas such as the cuneus.

Descriptive findings of other comparisons and results

Besides our four main research questions, there are more research findings worth mentioning: comparisons between acupuncture and other stimulations; comparisons of acupuncture under different consciousness states; acupuncture at different time points; acupuncture at group of points; acupuncture effect correlated to expectation. Moreover, resting state functional connectivity was also investigated in several recently published papers.

Acupuncture vs. visual stimulation. Of four studies, Bai et al. [127] compared the stimulation phase and the resting phase of acupuncture stimulation and visual stimulation and found the BOLD signal returned to near-baseline values shortly after the visual stimulus, but for acupuncture stimulation the resting phase activities might be even higher than that of the stimulation phases.

Table 1. Descriptive analysis of differences due to various methods of acupuncture manipulation.

Author (year)	Language	Studyplace	Study design	Case NO.	Group NO.	Intervention	Control	Points	Statistic	Group differences which result in more activation	Group differences which result in more deactivation
a) Comparison of Different Needling Depths											
Li et al. 2000	C	CN	NCT	26	2	MA (muscle layer)	MA (round tip, non-penetrating, stimulating between the epidermis and dermis)	ST36, ST32	NA	NSD	NSD
MacPherson et al. 2008	E	UK	RIO, PB	17	2	MA (8–12 mm)	MA (1–2 mm)	LI4 (R)	Y	NSD	NSD
Zhang et al. 2007	E	CN	NCT,PB	12	2	EA (2–3 cm)	EA (subcutaneous)	GB34, GB39 (L)	Y	*EA (2–3 cm)>EA (subcutaneous): Con. SI, SII, MC, ant. CingC, IN, Th, H, OC, Ce; Bil. PFG, Cau and P*	NSD
Wu et al. 1999	E	CN	Semi-RIO, PB	18	2	MA (2 cm)	MA (1 mm)	ST36 (L)	NA	1) MA (2 cm)>MA (1 mm): Con. Hyp, Nac; 2) MA (1 mm)>MA (2 cm): SI, Th, ant. CingC (BA 32, 34); Con. SMA; Bil. Fop (BA44 and SMA), PO (BA40)	1)MA (2 cm)>MA (1 mm): Bil. Ant. CingC (rostral part, BA 24B), Ipsi. OG, BG, Con. Amyg, H
b) Comparison of Electro-acupuncture vs. Manual Acupuncture											
Kong et al. 2002	E	CN	RIO	11	2	MA (3 Hz, 180 rpm)	EA (3 Hz)	LI4 (L)	Y	*EA>MA: Con. preCG; SII (CO, PO); Ipsi. Put/In*	*1) MA>EA: Con. STG and Put/IN, post. Cing, STG and Ipsi. LN/In; 2) EA> MA: Con. preCun*
Li et al. 2003	E	CN	NCT	20	3	MA	1) EA (2 Hz); 2) EA (20 Hz)	BL60, 65, 66, 67 (R)	Y	NSD	*MA>2 EA groups: Bil. Cun(BA18), TTG (BA41), MFG (BA46)*
Napadow et al. 2005	E	US	NCT, PB	13	3	MA (ERRM, 1 Hz)	1) EA (2 Hz); 2) EA (100 Hz)	ST36 (L)	Y	*1) EA 2 Hz >MA: SI, Con. Cing-am, NRP; 2) EA 100 Hz>MA: SI, Con. Cing-am*	*EA>MA: septal area*
c) Comparison of Different Frequencies of Electro-acupuncture Stimulation											
Li et al. 2003	E	CN	NCT	20	2	EA (2 Hz)	EA (20 Hz)	BL60, 65, 66, 67 (R)	Y	NSD	NSD
Napadow et al. 2005	E	US	NCT, PB	13	2	EA (2 Hz)	EA (100 Hz)	ST36 (L)	Y	*EA 2 Hz>EA 100 Hz: NRP*	NA
d) Comparison of Different Intensities of Manual Acupuncture Stimulation											
Li et al 2006	E	CN	RCT/P	18	3	MA (30 s)	1) MA (60 s); 2) MA (180 s)	LI4 (R)	Y	*1) 60 s>30 s: Ipsi. IFG,ITG; 2) 180 s>60 s: Bil. Tpole, Ce, OL; 3) 180 s>30 s: Bil. Tpole, Ce, IPL*	*1) 60 s>30 s: Bil. OG, Ipsi. TL, P; 2) 180 s> 60 s: Bil. dlPFC, MEFG; 3) 180 s>30 s: Bil. dlPFC, MEFG*
Gareus et al. 2002	E	DE	NCT	21	2	MA (twisting)+ visual stimu (Bil.)	MA (no stimu)+ visual stimu (L)	GB37	NA	1) MA(twisting+visual)> MA(no stimu+visual): IN, PO, PTC, IPL, supCol, Cun, MOG, CingG	NA

Table 1. Cont.

Author (year)	Language	Studyplace	Study design	Case NO.	Group NO.	Intervention	Control	Points	Statistic	Group differences which result in more activation	Group differences which result in more deactivation
Hu et al. 2005	C	CN	RCT	19	3	MA(twirling, 120–200 rpm) (Bil.)	1) MA (no stimu) +visual stimu (L); 2) MA (no stimu)+visual stimu (Bil.)	GB37, LR3	Y	MA>MA (no stimuli)+ visual stimuli (L/Bil.): V1	NA
Fang et al. 2004	E	CN	RIO, PB	15	2	MA (ERRM, rotating, 2 Hz)	MA (no stimu)	LR3, GB40 (L)	Y	*MA(rotaing)>MA(no stimu): Bil. SII; Ipsi. FOP(BA10), Ce; Con. Th*	NA
Cheng et al. 2009	C	CN	NCT	12	2	MA (rotating, 1.5 Hz)	MA (no stimu)	KI3 (R)	Y	*MA(rotaing)>MA(no stimu): Ipsi. STG (BA22); Con. MFG(BA46),IFG(BA45), IPL(BA40); Bil. postCG(BA2,3)*	NA
Gong et al. 2003	C	CN	NCT, PB, OB	64	2	MA (with deqi, 1 cun deep, thrusting and lifting at 0.3–0.5 cun)	MA (no deqi, 0.4 cun deep, thrusting and lifting at 0.1–0.2 cun)	ST36, ST39 (R)	Y	*deqi>no deqi: Bil. CingC, IN, upper wall of latS, Con. postCG*	NA

Words in italics means statistically significant;
Amyg = Amygdala, ant. = anterior, BA = Brodmann area, BG = basal gyrus, Bil. = bilateral, C = Chinese, Cau = caudate nucleus, Ce = cerebellum, Cing = cingulate, Cing-am = anterior middle cingulate, CingC = cingulate cortex, CingG = cingulate gyrus, CN = China, CO = central operculum, Con. = contralateral, Cun = cuneus, DE = Germany, dlPFC = dorsolateral prefrontal cortex, E = English, EA = electro-acupuncture, ERRM = even reinforcing and reducing method, Fop = frontal operculum, H = hippocampus, Hyp = hypothalamus, IFG = inferior frontal gyrus, IN = insula, Ipsi = ipsilateral, IPL = inferior parietal lobule, ITG = inferior temporal gyrus, L = left, latS = lateral sulcus, LN = lenticular nucleus, MA = manual acupuncture, MC = motor cortex, MEFG = medial frontal gyrus, MFG = middle frontal gyrus, MOG = middle occipital gyrus, NA = information unavailable, Nac = nucleus accumbens, NCT = non-randomized controlled trial, NRP = nucleus raphe pontis, NSD = non statistically different, OB = observer blinded, OC = occipital cortex, OG = orbital gyrus, OL = occipital lobe, P = pons, PB = patient blinded, PFG = prefrontal gyrus, PO = parietal operculum, postCG = postcentral gyrus, preCG = precentral gyrus, preCun = precuneus, PTC = parieto-temporal cortex, Put = putamen, R = right, RCT/P = parallel group randomized trial, RIO = randomized intervention order, rpm = rotations per minute, SI = primary somatosensory area, SII = second somatosensory area, SMA = supplementary motor area, stimu = stimulation, STG = superior temporal gyrus, supCol = superior colliculi, Th = thalamus, TL = temporal lobe, Tpole = temporal pole, TTG = transverse temporal gyri, V1 = primary visual cortices, Y = yes.
doi:10.1371/journal.pone.0032960.t001

Table 2. Descriptive analysis of differences between patients and healthy volunteers.

Author (year)	Language	Stduyplace	Studydesign	Pat.NO.	HVNO.	Disease	Intervention	Control	Statistic	Response for both groups	Differences for both groups
Wang et al. 2004	C	CN	NCT	17	20	lesions in left central sulcus	EA (1 Hz, 0.1–03mA) ST36, GB34 (R)	N	Y	NA	Activation:1) Pat:Con. FL (the areas which are near the lesions and 3 cm anterior to central sulcus); 2) HV: SMA, MC
Fu et al. 2005	C	CN	NCT	6	6	Alzheimer's disease	EA (1 Hz) PC6 (R)	N	Y	Activation:Bil. TL, FL	Activation: Pat.>HV: CingG, Ce
Liu et al. 2007	E	CN	NCT	6	6	heroin addicts	MA ST36 (L)	N	Y	Activation:Con. Hyp, Th, paraHG	*Activation:1)Pat.>HV: Con. Hyp; 2)HV>Pat. Con. Th, paraHG*
Napadow et al. 2007*	E	US	NCT	13	12	Carpal tunnel syndrome	Electro-stimuli 100 Hz (Digit2, Digit3, Digit5) (Pat.: affected side; HV: dominant hand side)	N	Y	NA	1) Pat.: stimulating Digit3, decreased extent of activation: BA1, BA4; 2) no significant change in HV
Wu et al. 2008	E	CN	NCT	11	10	spastic cerebral palsy	MA (ERRM, rotating 2 Hz) LR3 (L)	N	Y	*Activation:Con. STG(BA22); Ipsi. H*	*1) Deactivation:Pat.>HV:Bil. MFG (BA10),preCG(BA4); Con. MTG(BA21), paraHG; Ipsi. SFG(BA8), IFG(BA46); 2) Activation:Pat.>HV: Bil. OL(Cun); Ipsi. IN ; HV> Pat.:Bil. Cau, Th, Ce*
Napadow et al. 2007	E	US	NCT	13	12	Carpal tunnel syndrome	MA (1.5 cm 1 Hz) LI4, (Pat.:affected side, HV: dominant hand side)	CS (1 Hz, monofilament) LI4 (Pat.:affected side, HV: dominant hand side)	Y	1)Activation:*Con.LHA*; 2) Deactivation:*Con Amyg;* pgACC, amACC, rspPCC, dlPFC, vmPFC, ant. IN, septal area, SI, SMA, Th	*1) Activation:Pat.>HV: LHA; 2) Deactivation:HV> Pat. :Amyg*
Li et al. 2006	E	CN	NCT	12	12	Stroke	EA (2 Hz) LI4,LI11 (L)	CS (1 Hz rough sponge brushing finger and palm) (L)	Y	Activation:CS> EA:Con. M1, SI	Activation: Pat.>HV: SI (for both CS and EA)

*published in Human Brain Mapping.

Words in italics means statistically significant;

amACC = anterior-middle anterior cingulate cortex, Amyg = Amygdala, BA = Brodmann area, Bil. = bilateral, C = Chinese, Cau = caudate nucleus, Ce = cerebellum, CingG = cingulate gyrus, CN = China, Con. = contralateral, CS = cutaneous stimulation, dlPFC = dorsolateral prefrontal cortex, EA = electro-acupuncture, ERRM = even reinforcing and reducing method, FL = frontal lobe, H = hippocampus, HV = healthy volunteers, Hyp = hypothalamus, IFG = inferior frontal gyrus, IN = insula, Ipsi. = ipsilateral, L = left, LHA = lateral hypothalamic area, M1 = primary motor cortex, MA = manual acupuncture, MC = motor cortex, MFG = middle frontal gyrus, MTG = middle temporal gyrus, N = no, NA = information unavailable, NCT = non-randomized controlled trial, OL = occipital lobe, paraHG = parahippocampal gyrus, Pat. = patient, pgACC = pregenual cingulate cortex, preCG = precentral gyrus, R = right, rspPCC = retrosplenial posterior cingulate cortex, SI = primary somatosensory area, SFG = superior frontal gyrus, SMA = supplementary motor area, STG = superior temporal gyrus, Th = thalamus, TL = temporal lobe, vmPFC = ventromedial prefrontal cortex, Y = yes.

doi:10.1371/journal.pone.0032960.t002

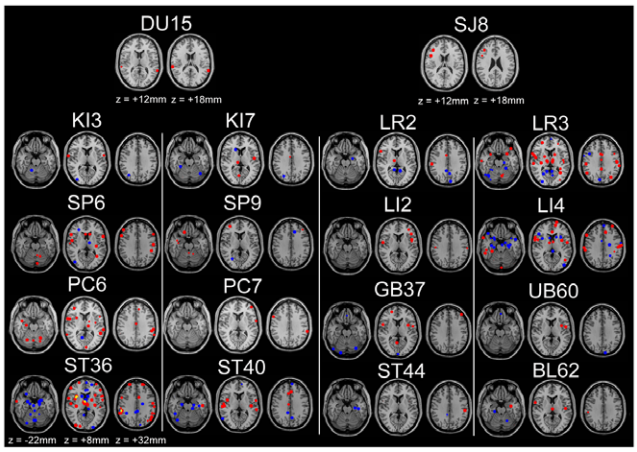

Figure 3. Map of brain response to 18 different acupuncture points. Red: activation; Blue: deactivation; Yellow: overlap.
doi:10.1371/journal.pone.0032960.g003

Hu et al. [71] and Gareus et al. [72] had contradictory results. Surprisingly, Hu et al. [71] reported no significant activation in the visual cortex during visual stimulation but from acupuncture stimulation, whereas Gareus et al. [72] found no activation in the visual cortex during acupuncture stimulation, and activation from visual stimulation. Li et al. [66] found both visual stimulation and acupuncture could activate the visual cortex.

Acupuncture vs. word generation paradigm. One study from Li et al. [29] found acupuncture at language specific acupuncture points SJ8 and Du15 did not activate the typical language areas in the left inferior frontal cortex which were activated during a word-generation task.

Acupuncture vs. finger tapping. Of three studies, both Kong et al. [39] and Hu et al. [81] found finger-tapping task can produce more reliable fMRI signal changes than that evoked by electro-acupuncture stimulation. However, Wang et al. [128] found no significant difference between electro-acupuncture at ST36, GB34 and a finger-tapping task.

Acupuncture in different states of consciousness (awake or anesthetized). One study from Wang et al. [129] compared healthy subjects who underwent acupuncture at ST36 in two different consciousness states. The result showed activation in the awake state was greater than under anesthetic in the somatosensory area, the limbic system and basal ganglia.

Acupuncture at different time points. One study from Zeng et al. [130] compared acupuncture at KI3 and KI7 at two different time points – "open point time" and "closed point time" (the open or closed time point is determined by the Chinese medicine theory "Zi-Wu-Liu-Zhu"—the body's Qi and blood circulation schedule; acupuncture at the open point time results in maximum clinical effect and vice versa) [1]. The result showed acupuncture at "open point time" was associated with more deactivation in the frontal lobe, temporal lobe, cingulate cortex and cerebellum than acupuncture at the "closed point time".

Acupuncture of group of points. In 29 papers [25,35,38,44,49,62,65,68,71,74,75,93,100,109,130–144] more than one acupuncture point was stimulated simultaneously. Of these groups of points, some were functional related, some were on the same meridian, some had close locations for electric stimulation, few were real acupuncture clinical formula. 15 of these 29 papers were included among our first four main questions. Overall the results of these studies were very heterogeneous and only three studies [93,109,136] reported an interaction effect between acupuncture points.

Acupuncture effect correlated to expectations. Three studies by Kong et al. [145–147] applied an expectancy model, and found positive expectation can increase acupuncture analgesia based on the objective fMRI signal changes in response to noxious stimuli. The study indicated that different mechanisms exist between acupuncture analgesia and expectancy evoked placebo analgesia. For the verum acupuncture group, there were only a few small differences (in primary motor cortex and middle frontal gyrus) between the high expectancy side and low expectancy side. However, for the sham acupuncture group, more differences were observed in contralateral operculum, ipsilateral insula, inferior frontal gyrus, medial frontal gyrus and superior frontal gyrus. So this result suggested expectancy might involve distinct mechanisms between verum acupuncture and sham acupuncture.

Functional connectivity modulated by acupuncture. Eight studies investigated functional connectivity of resting state. One of the first such studies (Dhond et al. study [57]) found that verum acupuncture, but not monofilament tapping increased resting state connectivity of the default mode network (DMN) to pain, affective and memory related regions of the brain. Verum acupuncture also increased sensorimotor network (SMN) connectivity to pain-related brain regions. Zhang et al. [148] and Bai et al. [149] found that acupuncture stimulation may induce the modulation of the "acupuncture-related" network, represented by significant changes of functional connectivity in several regions of the brain, such as the bilateral frontal gyrus, bilateral temporal gyrus, inferior parietal lobe, middle occipital gyrus, pre- and postcentral gyrus, anterior cingulate cortex (ACC), parahippocampus, insula, tonsil, pyramis, culmen, precuneus and cuneus. Qin et al. [150,151] identified an amygdala-related network during the resting state both after verum and penetrating sham acupuncture at a nearby point. Compared to sham, verum acupuncture increased the connectivity between the amygdala, the PAG (periaqueductal gray) and the insula, and decreased the connectivity between the amygdala with the middle frontal cortex, the postcentral gyrus and the posterior cingulate cortex (PCC). Zhang et al. [119] compared the visual related functional networks between pre- and post- electro-acupuncture on the visual-related point GB37 and the non-visual related point KI8 and described a positive correlation between the pre-post resting states in visual networks for the GB37 group while an anti-correlation for the KI8 group. Liu et al. [152] found a similar result when comparing electro-acupuncture at GB37 and KI8. In addition, in a later study Liu et al. [153] reported that the DMN could be modulated after electro-acupuncture at the three acupuncture points (GB37, BL60 and KI8) and at a nearby sham point. As for intrinsic connectivity, the PCC and precuneus strongly interacted with other nodes during the pre- and post-stimulation states. The correlation was interrupted between the PCC/precuneus and the ACC. The orbital prefrontal cortex negatively interacted with the left medial temporal cortex only at the acupuncture points.

Results from the ALE meta-analysis

A total of 34 studies were eligible for the inclusion criteria for the ALE meta-analyses (Table 3). A total of 10 meta-analyses were performed.

The meta-analysis for verum acupuncture stimuli on greater activation of verum acupuncture points compared to baseline (1a, verum>rest) included 36 experiments, 377 subjects and 470 foci. The result showed significant convergence in the supramarginal gyrus, secondary somatosensory cortex (SII), pre-supplementary

Table 3. Studies included in the ALE meta-analyses.

Author (year)	Intervention (verum)	Control (sham)	Subjects		Contrast		Included in following meta-analyses
			Intervention	Control	Pre-post	Between group	
Wang et al. 2007	EA(5 Hz random wave, 1–3mA) LI4 (R)	sham EA (5 Hz random wave, 1–3mA), NAP (1 cm apart from the right corner of the mouth) (R)	5	5	verum>rest; rest>verum; sham>rest; rest>sham		1a/b; 3a/b/c/d/e/f
Wang et al. 2006	MA (2.54 cm, ERRM, 1 Hz) LR3 (R)	sham MA, NAP (near LR3) (R)	10	10	verum>rest; sham>rest		1 a; 3a/c/e
Zhang et al. 2005	EA (3 cm, 2 Hz, 10 V), GB34, GB39 (L)	sham EA (3 cm, 2 Hz, 10 V), NAPs (3–4 cm lateral to GB34, GB39 respectively) (L)	16	18	verum>rest; rest>verum; sham>rest; rest>sham		1a/b; 3a/b/c/d/e/f
Hui et al. 2005	MA (2–3 cm, rotating 60 rpm) ST36 (R)	CS (tapping, monofilament), ST36 (R)	11	11	verum>rest; rest>verum; sham>rest; rest>sham		1a/b; 3a/b/c/d/e/f
Yoo et al. 2004	MA (1 cm, rotating, 2 Hz) PC6 (R)	1) sham MA (1 cm, rotating, 2 Hz), NAP (1.5–2 cm interior to PC6) (R); 2) CS (brushing, 2 Hz, monofilament) area unclear	12	12	verum>rest; sham>rest	verum>sham	1a; 2a; 3a/c/e
Wu et al. 1999	MA (1 cm, ERRM, 1–2 Hz) LI4 (L)	sham MA (5 mm, manipulation lightly), NAP (2–3 cm lateral fromST36) (L)	9	9	verum>rest; rest>verum; sham>rest		1a/b; 3a/b/c/e/f
Wu et al. 2002	EA (2–3 cm, 4 Hz) GB34 (L)	1) sham EA (2–3 cm, 4 Hz) NAP (4–5 cm lateral from GB34) (L); 2) mini EA (0.3–0.5 cm, 4 Hz, mini CUR), NAP (4–5 cm from sham point)	15	15	verum>rest; sham>rest	verum>sham	1a; 2a; 3a/c/e
Wang et al. 2009	EA (2 Hz, 0.8–1.8mA, continuous wave) ST42, ST36 (R)	sham EA (2 Hz, 0.8–1.8mA, continuous wave), NAP (at the depression inferior and posterior to the Capitula fibula), NAP (1 cun below GB 40)	30	10	verum>rest; rest>verum; sham>rest;		1a/b; 3a/b/c/e/f
Fang et al. 2008	MA (2–4 mm, rotating 160 rpm) LR3, LR2, ST44 (L)	sham MA(2–4 mm, rotating 160 rpm), NAP (metatarsal III and IV on the dorsum of the left foot) (L)	10	10	verum>rest; rest>verum; sham>rest; rest>sham		1a/b; 3a/b/c/d/e/f
Guan et al. 2008	EA (2 Hz, 10–20mA) GB37 (Bil)	sham EA (2 Hz, 10–20mA), NAP (Bil)	8	8	verum>rest; sham>rest		1a; 3a/c/e
Kong et al. 2007	EA (2 Hz) UB60, GB37 (R)	sham EA (2 Hz), NAP(1.5 cm post. and inf. to the small head of the fibula) (R)	6	6	verum>rest; rest>verum; sham>rest; rest>sham		1a/b; 3a/b/c/d/e/f
Fukunaga et al. 1999	EA (10–15 mm, 4 Hz) LI4 (R)	CS (brushing, cosmetic brush 4 Hz) LI4 (R)	17	17	verum>rest; sham>rest		1a; 3a/c/e
Napadow et al. 2005	MA (ERRM, 1 Hz/ 2 Hz/100 Hz) ST36 (L)	CS (tapping, 1 Hz, monofilament) ST36 (L)	13	13	verum>rest; rest>verum; sham>rest;		1a/b; 3a/b/c/e/f
Chae et al. 2009	MA (0.8 cm, rotating 1 Hz) LR2 (L)	CS (unclear) LR2 (L)	10	10		verum>sham	2a
Chae et al. 2009	MA (0.8 cm, rotating 1 Hz) LR2 (L)	1) CS: covert (rotating 1 Hz) LR2 (L); 2) CS: overt (rotating 1 Hz) LR2 (L)	10	10		verum>sham	2a

Table 3. Cont.

Author (year)	Intervention (verum)	Control (sham)	Subjects		Contrast		Included in following meta-analyses
			Intervention	Control	Pre-post	Between group	
Li et al. 2008	1) MA ST36 (R); 2) MA ST43 (R); 3) MA LR3 (R) 4) MA LR6 (R)	1) sham MA, NAP (dorsum between the first and second metatarsals, approximately 10 mm from the 2 real acupoints: ST43, LR3) (R); 2) sham MA, NAP (near ST36 and LR6) (R), same manipulation	1)9; 2) 9; 3)10; 4)8	1)7; 2)8		verum>sham	2a
Li et al. 2008	1) MA (15 mm, rotating,1 Hz) ST43 (R); 2) MA (15 mm, rotating,1 Hz) ST44 (R)	sham MA (15 mm, rotating,1 Hz) NAP (10 mm beside the two points)	1)9; 2)9	7		verum>sham	2a
Yan et al. 2005	1) MA (15 mm, ERRM, 1 Hz) LI4 (R); 2)) MA (15 mm, ERRM, 1 Hz) LR3 (R)	1)sham MA (15 mm, ERRM, 1 Hz), NAP1 (10 mm anterior to LR3) (R); 2) sham MA (15 mm, ERRM, 1 Hz), NAP2(10 mm anterior to LI4) (R)	1)8; 2)10	1)7; 2)9		verum>sham; sham>verum	2a/b
Lu et al. 2008	MA (15 mm, ERRM, 1 Hz) LR6 (R)	sham MA (15 mm, ERRM, 1 Hz), NAP (lateral to LR6) (R)	8	8		verum>sham	2a
Dougherty et al. 2008	MA (ERRM, 180 rpm) LI4 (R)	Streitberger needle LI4 (R), manipulation gentlely	6	6		verum>sham; sham>verum	2a/b
Napadow et al. 2009	MA (1.5 cm, rotating, 0.5 Hz) PC6 (L)	CS (tapping, 0.5 Hz, monofilament) PC6 (L)	15	15		verum>sham	2a
Wang et al. 2005	MA (rotating, 2 Hz) BL62 (R)		6		verum>rest; rest>verum;		1a/b
Hou et al. 2002	MA (rotating, 2 Hz) LI4 (R)		6		verum>rest		1a
Kong et al. 2002	1)MA (rotating, 3 Hz) LI4 (L); 2) EA (3 Hz) LI4 (L)		11		verum>rest; rest>verum;		1a/b
Zhang et al. 2007	MA (25 mm) LI4, PC6, SP6, ST36 (R)		11		verum>rest; rest>verum;		1a/b
Li et al. 2005	MA (15 mm, ERRM, 1 Hz) LI4 (R)		6		verum>rest; rest>verum;		1a/b
MacPherson et al. 2008	MA (8–12 mm) LI4 (R)		17		verum>rest; rest>verum;		1a/b
Wu et al. 2007	MA (1.2cun) ST36 (R)		11		verum>rest; rest>verum;		1a/b
Chen et al. 2008	MA (0.3–0.5 cm, ERRM, 1–2 Hz) PC7 (R)		8		verum>rest		1a
Wang et al. 2007	EA (5 Hz, 1–3mA) LI4 (R)		6		verum>rest; rest>verum;		1a/b
Wu et al. 2008	MA (1.2cun) ST36, ST40 (R)		12		verum>rest		1a
Li et al. 2003	1) EA (2 Hz) SJ8 2) EA (2 Hz) DU15		18		verum>rest		1a

Table 3. Cont.

Author (year)	Intervention (verum)	Control (sham)	Subjects		Contrast		Included in following meta-analyses
			Intervention	Control	Pre-post	Between group	
Deng et al. 2008	MA LI2 (non-dominant hand side)		13		verum>rest		1a
Li et al. 2006	MA (15 mm, ERRM, 1 Hz, 30 s/60 s/180 s) LI4 (R)		18		verum>rest; rest>verum;		1a/b

CS = cutaneous stimulation, CUR = current, EA = electro-acupuncture, ERRM = even reinforcing and reducing method, L = left, MA = manual acupuncture, NAP = non-acupuncture point, R = right.

doi:10.1371/journal.pone.0032960.t003

motor area (pre-SMA), middle cigulate gyrus, insula, thalamus and precentral gyrus. The meta-analysis for greater deactivation of verum acupuncture points compared to baseline (1b, rest>verum) included 22 experiments, 219 subjects and 265 foci and the result revealed significant convergence in the subgenual anterior cingulate, subgenual cortex, amygdala/hippocampal formation, ventromedial prefrontal cortex (vmPFC), nucleus accumbens, and PCC (Table 4, Figure 4A).

For the direct contrast of verum and sham acupuncture on greater activation from verum than sham acupuncture or greater deactivation for sham acupuncture (2a, verum>sham) we included in the meta-analysis 17 experiments, 156 subjects and 171 foci, resulting in significant convergence in fusiform gyrus, cerebellum, SI and middle cingulate gyrus. Whereas, on greater deactivation from verum than sham acupuncture or greater activation for sham (2b, sham>verum, 21 subjects, 3 experiments and 27 foci) the result showed significant convergence in supramarginal gyrus, superior temporal gyrus and cuneus (Table 5, Figure 4B).

The Subtraction analysis for verum versus sham acupuncture included in the first step analyses 3a–d for the pre-post contrast on verum or sham acupuncture compared to baseline (Table 5, Figure 4C). The analysis of greater activation of verum acupuncture than baseline (3a, verum>rest) included 234 subjects, 20 experiments and 305 foci and revealed significant convergence in middle cingulate gyrus, pre-SMA, superior temporal gyrus, supramarginal gyrus, SII, thalamus and insula. The analysis of greater deactivation of verum acupuncture compared to baseline (3b, rest>verum, 172 subjects, 15 experiments and 222 foci) came to the following significant convergence: subgenual anterior cingulate, amygdala/hippocampal formation, vmPFC and PCC. Comparing results on greater activation of sham acupuncture points than baseline (3c, sham>rest) from 164 subjects, 15 experiments and 200 foci, showed significant convergence in cerebellum, supramarginal gyrus, superior temporal gyrus and thalamus. Including data on greater deactivation of sham acupuncture points compared to baseline (3d, rest>sham) from 50 subjects, 5 experiments and 52 foci, resulted in significant convergence in pregenual anterior cingulate, subgenual cortex and parahippocampal gyrus.

Finally, in the contrast (subtraction) comparing the between-group differences for verum and sham acupuncture, significant differences between "verum>rest" and "sham>rest" (3e) as well as between "rest>verum" and "rest>sham" (3f) were identified. The subtraction analysis for "verum>rest" - "sham>rest" showed convergent activations in pre-SMA, middle cingulate gyrus, claustrum, insula, supramarginal gyrus, SII and dorsolateral prefrontal cortex (dlPFC). The subtraction analysis for "rest> verum" - "rest>sham" revealed convergence in amygdala/ hippocampal formation (Table 5, Figure 4D).

Discussion

Overall the results indicate that studies on acupuncture neuroimaging are very heterogeneous in terms of the study question, methodology and quality, this is the case in the descriptive analysis as well as in the meta-analysis.

From the descriptive view on the data it seems that compared to sham, verum acupuncture tended to be associated with more activation in the basal ganglia, brain stem, cerebellum, and insula and more deactivation was seen in the so-called "default mode network" and limbic brain areas, such as the amygdala and the hippocampus. In addition, a trend for more robust brain activation with greater intensity of acupuncture stimulation seems to be there. However, electro-acupuncture at low frequency also

Table 4. Clusters showing significant convergence for verum acupuncture points (FDR pN corrected at the cluster level, $p<0.05$) from ALE meta-analyses.

Brain region	BA	Talairach coordinates			ALE value	Volume (mm^3)
		X	y	z		
Verum>rest (1a)						
Supramaginal gyrus/insula/SII	40	54	−26	24	0.0460	15440
	40	−54	−24	20	0.0565	8072
Pre-supplementary motor area/middle cingulate	6	−2	6	48	0.0318	9576
Thalamus		08	−16	8	0.0323	3776
Precentral gyrus	44	−46	−2	8	0.0259	3696
Rest>verum (1b)						
Anterior cingulate	32	0	34	−8	0.0406	6032
Subgenual cortex	25	2	8	−4	0.0202	1304
Amygdala/hippocampal formation		−28	−8	−24	0.0253	3240
Ventromedial prefrontal cortex	10	−2	60	10	0.0261	1728
Posterior cingulate	31	−6	−56	22	0.0188	1120

doi:10.1371/journal.pone.0032960.t004

tended to activate a broader range of brain areas than electro-acupuncture at high frequencies. Furthermore, it looks like that patients responded to acupuncture stimulation with a more robust fMRI response compared to healthy volunteers. Acupuncture at different acupuncture points showed in the studies both similarities and differences between points. Finally, studies also suggested that acupuncture modulated the resting state connectivity within several noted networks including the default mode network, sensorimotor network, and amygdala-related network etc.

From the meta-analyses focusing only on brain response to verum acupuncture stimuli, activation was noted in supramarginal gyrus, SII, pre-SMA, middle cigulate gyrus, insula, thalamus and precentral gyrus, while deactivation was noted in pregenual anterior cingulate, subgenual cortex, amygdala/hippocampal formation, vmPFC, nucleus accumbens and PCC. Acupuncture specific effects were noted by meta-analyses of differences between verum and sham, which showed greater response in middle cingulate for verum compared to sham acupuncture. However, the results were variant within the different meta-analyses. The meta-analyses of direct contrast between verum and sham showed significant convergence for ''verum>sham'' in fusiform gyrus, cerebellum and SI, while for ''sham>verum'' in superior temporal gyrus, supramarginal gyrus and cuneus. Whereas, the subtraction meta-analyses of group-derived contrast showed greater activation from verum in pre-SMA, claustrum, insula, supramarginal gyrus, SII, dlPFC, greater deactivation from verum in amygdala/hippocampal formation. This heterogeneity suggests that group-derived contrast for verum and sham acupuncture tended to be above threshold in consistently specific brain areas, but were not significantly different in those areas, when assessed at the single study level.

Strengths and limitations

To our knowledge this is the first systematic and extensive review on fMRI and acupuncture without any language restrictions. Besides the internationally well known databases such as Pubmed and EMBASE, less well known international databases such as the Chinese CNKI, the Japanese Ichushi WEB, and the Korean NDSL and KTKP were searched and the publications found were included in this review. Therefore, this very extensive review provides a transparent and detailed overview of the current literature available. In addition we structured the publications according to the research questions, such as the differences in brain activity associated with acupuncture stimuli between patients and healthy volunteers, to provide a good overview and a strong basis for future study designs, interventions, measurement methods, and possible diagnoses. Moreover, we complemented the systematic and comprehensive literature review with several ALE meta-analyses, providing analytic results for stronger evidence that are supported statistically. However, some studies reported direct contrast between verum and sham acupuncture groups, while some others reported pre-post contrast for each group, resulting in the fact that several meta-analyses had to be performed. The studies included in the descriptive review and the meta-analyses were highly heterogeneous regarding their study design, their aims and their quality of reporting. The reasons for these heterogeneous results are numerous, such as the varying acupuncture manipulation methods, different types of control arms, different methods of acquisition and analyzing the imaging data, the mainly investigated brain regions (region of interest) and the statistical analysis. The large variability between subjects and sessions with respect to the imaging data also needs to be taken into consideration [39,154]. The imprecise nomenclature [155] is sometimes misleading, such as activation, deactivation, changes, baseline. We did not formally assess the quality of the publications, because no valid checklist for this type of research is available, though reporting guidelines are available and should be consulted by future research publications [156]. A narrative review including only studies that are considered to be of high quality would have overcome this problem. However the aim of this paper was to provide a systematic and broad overview for the first time using the publications currently available. We believe that many trials included in this review have limitations regarding their study design, analysis and reporting of their results. Hence, our results have to be interpreted with care. This is underlined by the multitude of contradictory results. Lastly, the field of research on brain imaging for acupuncture is evolving rapidly which may indeed lessen the relevance of older results using sub-optimal methodologies and analysis techniques.

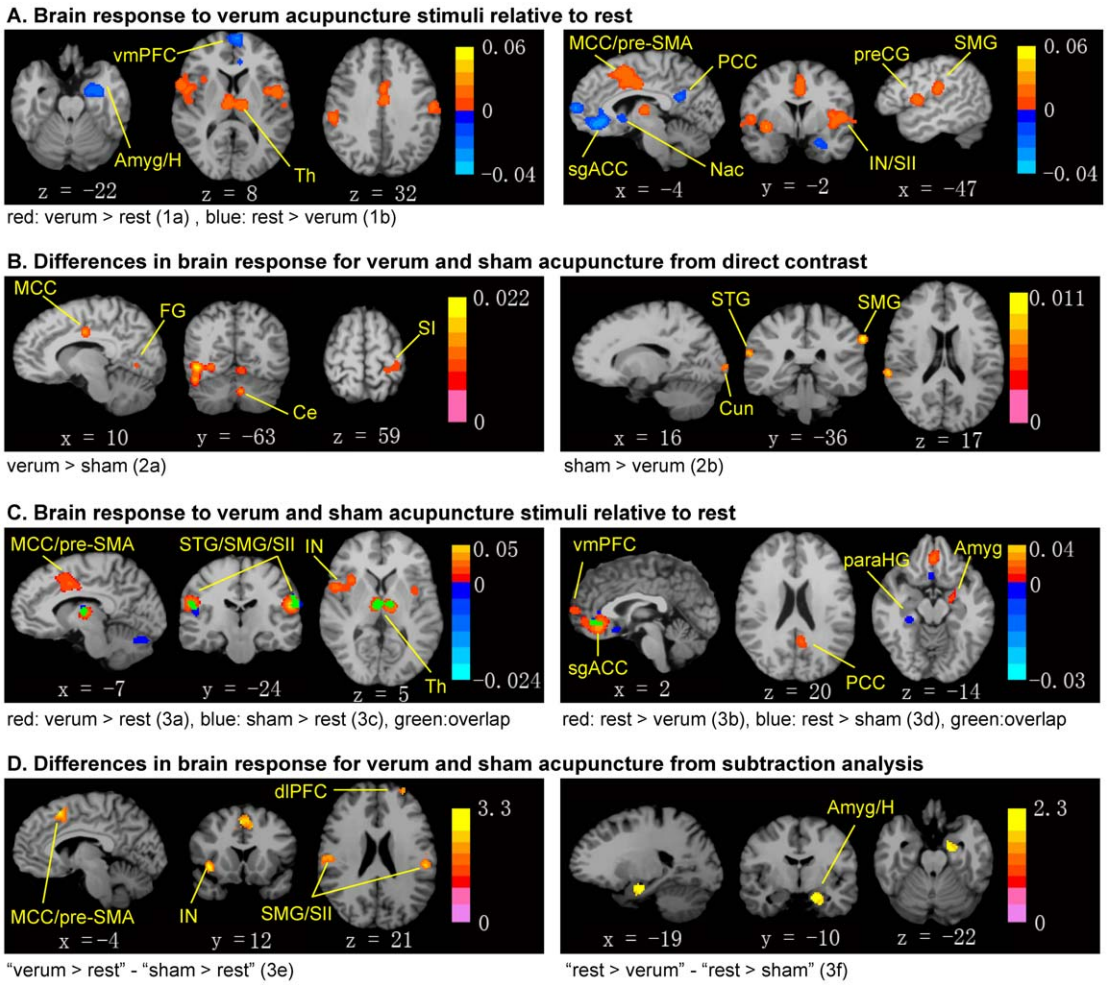

Figure 4. Results from the ALE meta-analyses. Meta-analyses were performed to evaluate brain response to acupuncture across studies, and contrast verum and sham acupuncture. (A) Brain response to verum acupuncture demonstrated activation in sensorimotor and affective/salience processing brain regions and deactivation in the amygdala and DMN brain regions. (B) Differences in brain response for verum and sham acupuncture from direct contrast showed significance in somatosensory areas, limbic regions, visual processing regions and cerebellum. (C) Brain response to verum and sham acupuncture individually demonstrated activation in sensorimotor and affective/salience processing brain regions and deactivation in the amygdala and DMN brain regions associated with verum acupuncture; while sham acupuncture produced activation in somatosensory regions, affective/salience processing regions, cerebellum and deactivation in limbic regions. (D) Differences in brain response between verum and sham acupuncture from subtraction analysis showed more activation in the sensorimotor affective/cognitive processing brain regions and more deactivation in the amygdala/hippocampal formation for verum acupuncture. For subfigures A–C, $p<0.05$, cluster level FDR corrected, color bar showed ALE value; for subfigure D, $p<0.05$, cluster level uncorrected, color bar showed Z value. Amyg: amygdala; Ce: cerebellum; dlPFC: dorsolateral prefrontal cortex; FG: fusiform gyrus; H: hippocampal formation; IN: insula; MCC: middle cingulate cortex; Nac: nucleus accumbens; paraHG: parahippocampal gyrus; PCC: posterior cingulate cortex; preCG: precentral gyrus; pre-SMA: pre-supplementary motor area; SI: primary somatosensory cortex; SII: secondary somatosensory cortex; sgACC: subgenual anterior cingulate cortex; SMG: supramarginal gyrus; Th: thalamus; vmPFC: ventromedial prefrontal cortex.
doi:10.1371/journal.pone.0032960.g004

Discussion of results

The studies on BOLD activation and deactivation from a single point or a group of points came mainly from China and Korea. The controlled studies, including sham acupuncture as a control, were mainly from China and the US: the Chinese studies mainly used penetrating sham at a nearby non-acupuncture point as a control while the US studies mainly applied the non-penetrating Streitberger needle or monofilament tapping at the same acupuncture points. Studies on patients were mainly from China. Although we did not evaluate the quality of the publications, the papers published in English used a clearer reporting style than those published in other languages. The most innovative studies came from the US. These studies had clear study questions and explored acupuncture neurocorrelates with a pain matrix, expectation, autonomic regulation, somatosensory perception and deqi related brain response.

While in the descriptive analysis similarities were observed in the brain response to stimulation at different acupuncture points, some differences across points were also noted. For example, brain deactivation observed in the visual areas (precuneus, cuneus) appeared not only when the vision related points (GB37, UB60) were needled, but also when several non-vision related points (LR2, LR3, ST36) were needled, but not with the other points. One could argue, based on TCM theory, that for the two points on liver meridian (LR2, LR3), the liver opens into the eyes, reflecting its physiological and pathological conditions [157]. The

Table 5. Clusters showing significant convergence for verum versus sham acupuncture (FDR pN corrected at the cluster level, $p<0.05$) from ALE meta-analyses.

Brain region	BA	Talairach coordinates			ALE value	Z value	Volume (mm^3)
		x	y	z			
Direct comparision verum>sham (2a)							
Fusiform gyrus	37	44	−64	−6	0.0197		3720
Culmen of Vermis		−2	−66	−10	0.0160		1520
Cerebellar tonsil		−4	−58	−32	0.0224		1240
Postcentral gyrus	3	−20	−36	64	0.0116		992
Middle cingulate	24	10	−12	34	0.0165		904
Direct comparision sham>verum (2b)							
Supramarginal gyrus	40	−62	−34	34	0.0108		1120
Superior temporal gyrus	42	64	−34	20	0.0088		552
Cuneus	18	18	−98	0	0.0069		400
Verum>rest (3a)							
Middle cingulate/Pre-supplementary motor area	24	−2	2	38	0.0353		7392
Superior temporal gyrus	22	50	6	2	0.0262		6232
Supramarginal gyrus/SII	40	−54	−22	18	0.0484		6040
	40	56	−26	22	0.0402		4080
Thalamus		−8	−16	6	0.0326		4504
Insula	13	−38	−4	0	0.0177		2056
Sham>rest (3c)							
Tuber of vermis		0	−70	−24	0.0239		2664
Supramarginal gyrus/SII	40	−60	−22	22	0.0159		2424
Superior temporal gyrus	41	50	−32	16	0.0168		2320
	22	−52	10	−2	0.0180		808
Thalamus		6	−14	8	0.0206		1848
Rest>verum (3b)							
Anterior cingulate	32	0	32	−8	0.0413		5400
Amygdala/hippocampal formation	34	−18	−8	−20	0.0262		2632
Ventromedial prefrontal cortex	10	−2	60	10	0.0260		1784
Posterior cingulate	31	−6	−56	22	0.0193		1288
Rest>sham (3d)							
Anterior cingulate	32	−4	40	−2	0.0128		1720
Parahippocampal gyrus	36	28	−32	−14	0.0110		392
Subcallosal gyrus	25	4	14	−12	0.0108		360
''Verum>rest'' – ''sham>rest'' (3e)*							
Pre-supplementary motor area/middle cingulate	6	4	12	46		2.7822	2120
Claustrum/insula		32	5	−1		3.2905	1848
Supramarginal gyrus/SII	40	−52	−26	22		2.4181	1728
	40	54	−18	24		2.2904	1168
Dorsolateral prefontral cortex	10	−28	57	23		2.2383	568
''Rest>verum'' – ''rest>sham'' (3f)*							
Amygdala/hippocampal formation	34	−14	−9	−20		2.2768	1104

*uncorrected $p<0.05$.

doi:10.1371/journal.pone.0032960.t005

stimulation of different acupoints in the same spinal segment could induce different fMRI activation patterns in the brain [142] while acupoints on the same meridian show some similarities in the activation/deactivation pattern [23].

The meta-analyses could only be done for publications that provided Talairach data, which was not the case for all of our study questions. The meta-analyses on the specific effect of acupuncture that compared verum and sham acupuncture came up with heterogeneous results. The subtraction analyses reflected descriptive results more than the direct contrast analyses. For example, subtraction meta-analyses confirmed more activation from verum in basal ganglia and insula, more deactivation in the

limbic region of amygdala/hippocampal formation associated with verum, while meta-analyses of direct contrast for verum and sham confirmed more activation in cerebellum associated with verum. The convergence of brain regions shown for these meta-analyses comparing verum and sham acupuncture overlapped for middle cingulate gyrus. The first reason for the heterogeneous results might be the literature heterogeneity. Only two publications had both pre-post and between-group comparison results [15,37]. Also, the different methods of acupuncture stimuli may have a strong impact of the result. Moreover, the direct contrast "verum>sham" included either more activation from verum or more deactivation from the sham. Thus, the results of direct contrast "verum>sham" and subtraction analysis "verum>rest" – "sham>rest" are not directly comparable. The ALE subtraction analysis for the comparison of verum versus sham acupuncture should be interpreted with caution because the groups are disparate in total number of foci. However, we refrained from randomly extracting experiments from the larger foci set [10], as this might have biased our results substantially. In particular, for the "rest>verum" – "rest>sham", extracting 5 experiments out of 15 from "rest>verum" could most probably influence the result by chance. The meta-analysis of direct contrast for "sham> verum" included only three experiments and 27 foci. Hence this analysis might be with not enough power and doesn't represent the general. Nevertheless, we could see that brain regions such as SII, insula, cingulate gyrus, amygdala/hippocampal formation and prefrontal cortices might be important when differentiating the acupuncture specific effect from sham acupuncture. Acupuncture analgesia is considered as one of the most important indications for clinical acupuncture treatment [158], and those brain regions mentioned above are associated with the pain neuromatrix and might contribute in explaining the mechanism of acupuncture specific analgesia.

Comparisons with other reviews

Some of the previous reviews [7,8,159–161] focused on a broader topic of neuroimaging techniques including EEG, PET, SPECT or MEG. Those reviews summarized research questions underlying certain acupuncture mechanisms, such as acupuncture analgesia, acupuncture placebo effect, specificity of meridian and acupuncture points, and acupuncture modulation on brain networks. They displayed the evidence for each research question and cited the relevant literature accordingly. However, in most cases the literature search was not transparently displayed. The other reviews [162–168] focusing on acupuncture and fMRI, had other emphases: Beissner et al. [162] focused on methodological problems, Cho et al. [163] explored neural substrates for hypothalamus-pituitary-adrenal axis and Chae et al. [164] reviewed traditional Korean acupuncture. The four Chinese narrative reviews on fMRI and acupuncture [165–168] discussed several research questions on the specific effects of acupuncture, such as different acupuncture points, manipulation methods, deqi or not deqi, and sham acupuncture. Our systematic literature review aimed to display the available studies as broad as possible and should offer a better and deeper overview on this topic, thus supporting future studies.

Methodological consideration regarding future studies

One of the advantages for fMRI is that there are multiple possibilities by which experiments can be designed and data analyzed, providing information on different aspects of brain physiology. However, the inherent heterogeneity can complicate subsequent reviews and meta-analyses. Certain basic guidelines on proper statistical analyses of fMRI data should be followed, such as calculating difference maps if two conditions, such as brain response to stimulation at different acupoints, are to be contrasted. Furthermore, as suggested by Poldrack et al., publications relating to fMRI investigations of acupuncture should report all pertinent information relating to both imaging and acupuncture procedures [156]. Important topics include design and task specification, planned group comparisons, behavioral performance metrics, imaging details, data pre-processing, intersubject registration, statistical modeling details for both the individual and group level, and statistical inference including approach to multiple comparisons correction. Adoption of these guidelines will improve manuscript reviews and shorten the time to acceptance (or rejection), as well as facilitate the inclusion of publications in future reviews and meta-analyses.

Conclusion

Brain response to acupuncture stimuli encompasses a broad network of regions consistent with not just somatosensory, but also affective and cognitive processing. While published results on acupuncture and fMRI were heterogeneous, from a descriptive perspective most studies suggest that acupuncture can modulate the brain activity within specific brain areas, and the evidence based on meta-analyses confirmed part of these results. Future studies should further improve methodological aspects and reporting related to both fMRI and acupuncture, and strictly control experimental conditions for more robust inference. Specifically, direct contrast analyses should be used to contrast different stimulus conditions (e.g. verum versus sham acupuncture) when evaluating research questions concerning acupuncture specificity.

Supporting Information

Table S1 Descriptive analysis of differences between verum and sham acupuncture.
(DOCX)

Table S2 Descriptive analysis of changes related to cortical and sub-cortical activation and deactivation at verum acupuncture points.
(DOCX)

Acknowledgments

We would like to thank the authors who provided us further details about their trial for our meta-analyses.

Author Contributions

Conceived and designed the experiments: WJH CW DP. Analyzed the data: WJH DP VN KP XYL JN YM CW. Wrote the paper: WJH DP VN KP XYL JN YM TN FRL CW. Data extraction: WJH DP KP YM.

References

1. Liang F (2006) Acupuncture and Moxibustion. Shanghai: Shanghai Scientific and Technical Publishers.
2. Backer M, Hammes M, Sander D, Funke D, Deppe M, et al. (2004) Changes of cerebrovascular response to visual stimulation in migraineurs after repetitive sessions of somatosensory stimulation (acupuncture): a pilot study. Headache 44: 95–101.
3. WHO (2002) Acupuncture: Review and Analysis of Reports on Controlled Clinical Trials: World Health Organization. . 87 p.
4. Linde KSA, Jürgens S, Hoppe A, Brinkhaus B, Witt C, et al. (2005) Acupuncture for Patients with Migraine - A Randomized Trial (ART Migraine). JAMA 293: 2118–2125.

5. Brinkhaus BWC, Jena S, Linde K, Streng A, Wagenpfeil S, et al. (2006) Acupuncture in Patients with Chronic Low Back Pain - A Randomised Controlled Trial. Arch Intern Med 166: 450–457.
6. Melchart D, Streng A, Hoppe A, Brinkhaus B, Witt C, et al. (2005) Acupuncture in patients with tension-type headache: randomised controlled trial. BMJ 331: 376–382.
7. Dhond RP, Kettner N, Napadow V (2007) Neuroimaging acupuncture effects in the human brain. J Altern Complement Med 13: 603–616.
8. Lewith GT, White PJ, Pariente J (2005) Investigating acupuncture using brain imaging techniques: the current state of play. Evid Based Complement Alternat Med 2: 315–319.
9. Eickhoff SB, Laird AR, Grefkes C, Wang LE, Zilles K, et al. (2009) Coordinate-based activation likelihood estimation meta-analysis of neuroimaging data: a random-effects approach based on empirical estimates of spatial uncertainty. Hum Brain Mapp 30: 2907–2926.
10. Laird AR, Fox PM, Price CJ, Glahn DC, Uecker AM, et al. (2005) ALE meta-analysis: controlling the false discovery rate and performing statistical contrasts. Hum Brain Mapp 25: 155–164.
11. Turkeltaub PE, Eden GF, Jones KM, Zeffiro TA (2002) Meta-analysis of the functional neuroanatomy of single-word reading: method and validation. Neuroimage 16: 765–780.
12. Lancaster JL, Tordesillas-Gutierrez D, Martinez M, Salinas F, Evans A, et al. (2007) Bias between MNI and Talairach coordinates analyzed using the ICBM-152 brain template. Hum Brain Mapp 28: 1194–1205.
13. Eickhoff SB, Bzdok D, Laird AR, Roski C, Caspers S, et al. (2011) Co-activation patterns distinguish cortical modules, their connectivity and functional differentiation. Neuroimage 57: 938–949.
14. Streitberger K, Kleinhenz J (1998) Introducing a placebo needle into acupuncture research. Lancet 352: 364–365.
15. Yoo SS, Teh EK, Blinder RA, Jolesz FA (2004) Modulation of cerebellar activities by acupuncture stimulation: evidence from fMRI study. Neuroimage 22: 932–940.
16. Yoo SS, Kerr CE, Park M, Im DM, Blinder RA, et al. (2007) Neural activities in human somatosensory cortical areas evoked by acupuncture stimulation. Complement Ther Med 15: 247–254.
17. Li G, Jack CR, Jr., Yang ES (2006) An fMRI study of somatosensory-implicated acupuncture points in stable somatosensory stroke patients. J Magn Reson Imaging 24: 1018–1024.
18. Chae Y, Lee H, Kim H, Kim CH, Chang DI, et al. (2009) Parsing brain activity associated with acupuncture treatment in Parkinson's diseases. Mov Disord 24: 1794–1802.
19. Schaechter JD, Connell BD, Stason WB, Kaptchuk TJ, Krebs DE, et al. (2007) Correlated change in upper limb function and motor cortex activation after verum and sham acupuncture in patients with chronic stroke. J Altern Complement Med 13: 527–532.
20. Schockert T, Schnitker R, Boroojerdi B, Vietzke K, Qua Smith I, et al. (2009) Kortikale Aktivierungen durch Yamamoto Neue Schädelakupunktur (YNSA) in der Behandlung von Schlaganfallpatienten: Eine Sham-kontrollierte Studie mit Hilfe der funktionellen Kernspintomographie (fMRI). Deutsche Zeitschrift für Akupunktur 52: 21–29.
21. Dougherty DD, Kong J, Webb M, Bonab AA, Fischman AJ, et al. (2008) A combined [11C]diprenorphine PET study and fMRI study of acupuncture analgesia. Behav Brain Res 193: 63–68.
22. Deng G, Hou BL, Holodny AI, Cassileth BR (2008) Functional magnetic resonance imaging (fMRI) changes and saliva production associated with acupuncture at LI-2 acupuncture point: a randomized controlled study. BMC Complement Altern Med 8: 37.
23. Li L, Liu H, Li YZ, Xu JY, Shan BC, et al. (2008) The human brain response to acupuncture on same-meridian acupoints: evidence from an fMRI study. J Altern Complement Med 14: 673–678.
24. Xiao YY, Du L, Hong BK, et al. (2008) Study on fMRI brain map in patients undergoing needling at Zusanli (ST36) by reinforcing method. Zhongguo Zhong Xi Yi Jie He Za Zhi 28: 122–125.
25. Zhang JH, Cao XD, Lie J, Tang WJ, Liu HQ, et al. (2007) Neuronal specificity of needling acupoints at same meridian: a control functional magnetic resonance imaging study with electroacupuncture. Acupunct Electrother Res 32: 179–193.
26. Hu KM, Wang CP, Xie HJ, Henning J (2006) Observation on activating effectiveness of acupuncture at acupoints and non-acupoints on different brain regions. Zhongguo Zhen Jiu 26: 205–207.
27. Wang W, Li KC, Shan BC, Xu JY, Yan B, et al. (2006) Study of acupuncture point Liv 3 with funcitonal MRI. Chin J Radiol 40: 29–35.
28. Yan B, Li K, Xu J, Wang W, Liu H, et al. (2005) Acupoint-specific fMRI patterns in human brain. Neurosci Lett 383: 236–240.
29. Li G, Liu HL, Cheung RT, Hung YC, Wong KK, et al. (2003) An fMRI study comparing brain activation between word generation and electrical stimulation of language-implicated acupoints. Hum Brain Mapp 18: 233–238.
30. Lu N, Zhao JG, Shan BC, Li KC (2008) Study of acupuncture point Liv6 with functional MRI. Chin J Med Imaging Technol 24: 46–48.
31. Huang Y, Li GL, Lai XS, Tang CZ, Yang JJ (2009) An fMRI cerebral functional imaging comparison on needling in Zhigou (SJ6) vs a sham point. Journal of Chengdu University of TCM 32: 3–6.
32. Li L, Xu JY, Li YZ, Liu H, Yuan XL, et al. (2008) fMRI study of acupuncture at adjacent acupoints located on the stomach meridian of Foot-Yanming. Chin J Med Imaging Technol 24: 1001–1003.
33. Lai XS, Su PZ, Huang Y, Zou YQ, Wu JX, et al. (2009) Comparison of fMRI cerebral functional imaging between needling Waiguan (SJ5) and combined SJ5 and sham point. Tianjin Journal of Traditional Chinese Medicine 26: 113–115.
34. Jeun SS, Kim JS, Kim BS, Park SD, Lim EC, et al. (2005) Acupuncture stimulation for motor cortex activities: a 3T fMRI study. Am J Chin Med 33: 573–578.
35. Choi N-g, Han J-b, Jang S-j (2009) Comparaison of brain activation iamges associated with sexual arousal induced by visual stimulation and SP6 acupucnture : fMRI at 3 tesla. JOURNAL OF RADIOLOGICAL SCIENCE AND TECHNOLOGY 32: 183–194.
36. Choe B-y (2002) Clinical Application of Functional MRI : Motor Cortex Activities by Acupuncture. Journal of the Korean Magnetic Resonance Society 6: 89–93.
37. Wu MT, Sheen JM, Chuang KH, Yang P, Chin SL, et al. (2002) Neuronal specificity of acupuncture response: a fMRI study with electroacupuncture. Neuroimage 16: 1028–1037.
38. Zhang JH, Feng XY, Li J, Tang WJ, Li Y (2005) Functional MRI studies of acupoints and non-acupoints electroacupuncture analgesia modulating within human brain. Chinese computed medical imaging 11: 10–16.
39. Kong J, Gollub RL, Webb JM, Kong JT, Vangel MG, et al. (2007) Test-retest study of fMRI signal change evoked by electroacupuncture stimulation. Neuroimage 34: 1171–1181.
40. Kong J, Kaptchuk TJ, Webb JM, Kong JT, Sasaki Y, et al. (2007) Functional neuroanatomical investigation of vision-related acupuncture point specificity-A multisession fMRI study. Hum Brain Mapp.
41. Cho Z-H, Hwang S-c, Son Y-d, Kang C-k, Wong EK, et al. (2004) Acupuncture Analgesia : A Sensory Stimulus Induced Analgesia Observed by functional Magnetic resonance Imaging. The Journal of Korean Acupuncture & Moxibustion Society 21: 57–71.
42. Fang JL, Krings T, Weidemann J, Meister IG, Thron A (2004) Functional MRI in healthy subjects during acupuncture: different effects of needle rotation in real and false acupoints. Neuroradiology 46: 359–362.
43. Wesolowski T, Lotze M, Domin M, Langner S, Lehmann C, et al. (2009) Acupuncture reveals no specific effect on primary auditory cortex: a functional magnetic resonance imaging study. Neuroreport 20: 116–120.
44. Wang GB, Liu C, Wu LB, Yan B, Gao SZ, et al. (2009) Functional magnetic resonance imaging on acupuncturing Yuan-Source and He-Sea acupoints of stomach meridian of foot Yangming. ACTA ACADEMIAE MEDICINAE SINICAE 31: 171–176.
45. Fang JL, Jin Z, Wang Y, Li K, Zeng YW, et al. (2005) Comparison of central effects of acupuncturing Taichong and nearby two acupoints by functional MRI. Chin J Med Imaging Technol 21: 1332–1336.
46. Fang J, Jin Z, Wang Y, Li K, Kong J, et al. (2008) The salient characteristics of the central effects of acupuncture needling: Limbic-paralimbic-neocortical network modulation. Hum Brain Mapp.
47. Wang W, Liu L, Zhi X, Huang JB, Liu DX, et al. (2007) Study on the regulatory effect of electro-acupuncture on hegu point (LI4) in cerebral response with functional magnetic resonance imaging. Chin J Integr Med 13: 10–16.
48. Ai L, Dai JP, Zhao BX, Tian J, Fan YP, et al. (2004) Investigation of analgesic mechanism of acupuncture : a fMRI study. Chin J Med Imaging Technol 20: 1197–1200.
49. Li G, Huang L, Cheung RT, Liu SR, Ma QY, et al. (2004) Cortical activations upon stimulation of the sensorimotor-implicated acupoints. Magn Reson Imaging 22: 639–644.
50. Liu WC, Feldman SC, Cook DB, Hung DL, Xu T, et al. (2004) fMRI study of acupuncture-induced periaqueductal gray activity in humans. Neuroreport 15: 1937–1940.
51. Napadow V, Dhond R, Park K, Kim J, Makris N, et al. (2009) Time-variant fMRI activity in the brainstem and higher structures in response to acupuncture. Neuroimage 47: 289–301.
52. Wu MT, Hsieh JC, Xiong J, Yang CF, Pan HB, et al. (1999) Central nervous pathway for acupuncture stimulation: localization of processing with functional MR imaging of the brain–preliminary experience. Radiology 212: 133–141.
53. Hui KK, Liu J, Marina O, Napadow V, Haselgrove C, et al. (2005) The integrated response of the human cerebro-cerebellar and limbic systems to acupuncture stimulation at ST 36 as evidenced by fMRI. Neuroimage 27: 479–496.
54. Hui KK, Marina O, Claunch JD, Nixon EE, Fang J, et al. (2009) Acupuncture mobilizes the brain's default mode and its anti-correlated network in healthy subjects. Brain Res 1287: 84–103.
55. Napadow V, Dhond RP, Kim J, LaCount L, Vangel M, et al. (2009) Brain encoding of acupuncture sensation–coupling on-line rating with fMRI. Neuroimage 47: 1055–1065.
56. Fukunaga M (1999) Brain activation under electro-acupuncture stimulation using functional magnetic resonance imaging. The bulletin of Meiji University of oriental medicine 25: 7–19.
57. Dhond RP, Yeh C, Park K, Kettner N, Napadow V (2008) Acupuncture modulates resting state connectivity in default and sensorimotor brain networks. Pain 136: 407–418.

58. Napadow V, Makris N, Liu J, Kettner NW, Kwong KK, et al. (2005) Effects of electroacupuncture versus manual acupuncture on the human brain as measured by fMRI. Hum Brain Mapp 24: 193–205.
59. Hui KK, Liu J, Makris N, Gollub RL, Chen AJ, et al. (2000) Acupuncture modulates the limbic system and subcortical gray structures of the human brain: evidence from fMRI studies in normal subjects. Hum Brain Mapp 9: 13–25.
60. Chae Y, Lee H, Kim H, Sohn H, Park JH, et al. (2009) The neural substrates of verum acupuncture compared to non-penetrating placebo needle: an fMRI study. Neurosci Lett 450: 80–84.
61. Huang Y, Zeng TJ, Wang YJ, Lai XS, Zhang YZ, et al. (2009) A comparison of functional magnetic resonance imaging of cerebral regions activated by cutaneous needling and regular needling at Waiguan (SJ5) acupoint. Journal of Anhui TCM college 28: 25–28.
62. Wu JX, Huang Y, Lai XS, Zou YQ, Tang CZ, et al. (2009) The fMRI comparative study on cutaneous or routine needling in acupoints Waiguan (SJ5) and Neiguan (PC6). Chinese archives of traditional Chinese medicine 27: 1625–1627.
63. Huang Y, Song YB, Lai XS, Tang CZ, Yang JJ (2009) Comparison study between shallowly skin needling and routine needling in Neiguan (PC6) by fMRI. Journal of Shandong University of TCM 33: 243–245.
64. Huang Y, LI XX, Lai XS, Zou YQ, Wu JX (2009) Study of fMRI of cerebral functional regions induced by cutaneous and routine needling in Zhigou (SJ6). Hebei J TCM 31: 254–256.
65. Zou YQ, Huang Y, Lai XS, Tang CZ, Yang JJ (2008) The fMRI comparative study on cutaneous or routine needling in acupoints Waiguan (SJ5) and Zhigou (SJ6). Journal of Yunnan University of traditional Chinese medicine 31: 44–47.
66. Li G, Cheung RT, Ma QY, Yang ES (2003) Visual cortical activations on fMRI upon stimulation of the vision-implicated acupoints. Neuroreport 14: 669–673.
67. MacPherson H, Green G, Nevado A, Lythgoe MF, Lewith G, et al. (2008) Brain imaging of acupuncture: comparing superficial with deep needling. Neurosci Lett 434: 144–149.
68. Li DZ, Li XZ (2000) Comparative study of pricking the cutaneous region of acupoint and needling its depth by means of fMRI. Zhongguo Zhen Jiu. pp 491–492.
69. Kong J, Ma L, Gollub RL, Wei J, Yang X, et al. (2002) A pilot study of functional magnetic resonance imaging of the brain during manual and electroacupuncture stimulation of acupuncture point (LI-4 Hegu) in normal subjects reveals differential brain activation between methods. J Altern Complement Med 8: 411–419.
70. Li K, Shan B, Xu J, Liu H, Wang W, et al. (2006) Changes in FMRI in the human brain related to different durations of manual acupuncture needling. J Altern Complement Med 12: 615–623.
71. Hu KM, Wang CP, Henning J (2005) Observation on relation of acupuncture at Guangming (GB 37) and Taichong (LR 3) with central nervous reaction. Zhongguo Zhen Jiu 25: 860–862.
72. Gareus IK, Lacour M, Schulte AC, Hennig J (2002) Is there a BOLD response of the visual cortex on stimulation of the vision-related acupoint GB 37? J Magn Reson Imaging 15: 227–232.
73. Cheng HJ, Chen SJ, Zhu F (2009) Magnetic resonance imaging study of twisting or untwisting Taixi acupoint (KI3) on brain function. Journal of clinical rehabilitative tissue engineering research 13: 5020–5022.
74. Gong HH, Wang YZ, Xiao XZ, Qiu CM, Wang LY, et al. (2003) Investigation of cerebral cortical functional areas of the acupoints in zu-san-li and xia-ju-xu by fMRI. Journal of diagnostic imaging & interventional radiology 12: 133–136.
75. Wang W, Qi JP, Xia YL, Huang XL, Li WX, et al. (2004) The response of human motor cortex to acupuncture of S36 and G34 as revealed by functional MRI. Chin J Phys Med Rehabil 26: 472–475.
76. Fu P, Jia JP, Zhu J, Huang JJ (2005) [Effects of acupuncture at Neiguan (PC 6) on human brain functional imaging in different functional states]. Zhongguo Zhen Jiu 25: 784–786.
77. Liu S, Zhou W, Ruan X, Li R, Lee T, et al. (2007) Activation of the hypothalamus characterizes the response to acupuncture stimulation in heroin addicts. Neurosci Lett 421: 203–208.
78. Wu Y, Jin Z, Li K, Lu ZL, Wong V, et al. (2008) Effect of acupuncture on the brain in children with spastic cerebral palsy using functional neuroimaging (FMRI). J Child Neurol 23: 1267–1274.
79. Napadow V, Liu J, Li M, Kettner N, Ryan A, et al. (2007) Somatosensory cortical plasticity in carpal tunnel syndrome treated by acupuncture. Hum Brain Mapp 28: 159–171.
80. Napadow V, Kettner N, Liu J, Li M, Kwong KK, et al. (2007) Hypothalamus and amygdala response to acupuncture stimuli in Carpal Tunnel Syndrome. Pain 130: 254–266.
81. Hu JP, Li YG, Cao DR, Gong SB (2008) Reproducibility of functional MR imaging during electroacupuncture stimulation at PC6 (Neiguan). ACTA ACADEMIAE MEDICINAE MILITARIS TERTIAE 30: 1878–1882.
82. Fu P, Jia JP, Min BQ (2005) Acupuncture at Neiguan acupoint for brain functional MRI of patients with Alzheimer disease. Chin J Neurol. pp 118–119.
83. Ha C-h, Lee H, Lim Y-k, Hong K-e, Lee B-r, et al. (2003) A fMRI study on the cerebral activity induced by Electro-acupuncture on Taichong(Liv3). The Journal of Korean Acupuncture & Moxibustion Society 20: 187–207.
84. Xu FM, Xie P, Lv FJ, Mou J, Li YM, et al. (2007) The fMRI study of acupuncture at the five transport points of liver meridian. Journal of Nanjing TCM University 23: 224–227.
85. Yan LP, Sun ZR, Xie B, Ma X (2005) Brain functional response after electroacupuncture at Quchi point with fMRI method. JCAM 21: 61–63.
86. Hong K-e, Lee B-r, Lee H, Yim Y-k, Kim Y-j (2003) A fMRI study on the cerebral activity induced by Electro-acupuncture on Sanyinjiao(Sp6). The Journal of Korean Acupuncture & Moxibustion Society 20: 86–103.
87. Parrish TB, Schaeffer A, Catanese M, Rogel MJ (2005) Functional magnetic resonance imaging of real and sham acupuncture. Noninvasively measuring cortical activation from acupuncture. IEEE Eng Med Biol Mag 24: 35–40.
88. Kim J-h, Lee H, Lim Y-k, Hong K-e, Lee B-r, et al. (2003) A fMRI study on the cerebral activity induced by Electro-acupuncture on Sp9(Yinlingquan). The Journal of Korean Acupuncture & Moxibustion Society 20: 114–133.
89. Zhu MJ, Hu KM (2004) A fMRI study of the TCM theory "the liver connects eye links". Journal of Hainan medical college 10: 169–170.
90. Bae E-j, Hong K-e, Lee H, Lee B-r, Yim Y-k, et al. (2003) A fMRI study on the cerebral activity induced by Electro-acupuncture on Fenglon(St40). The Journal of Korean Acupuncture & Moxibustion Society 20: 208–226.
91. Chi X (2009) A fMRI study of acupuncture on Zhongzhu (SJ3) point. Acta Chinese medicine and pharmacology 37: 37–38.
92. Chi X, Ju YL, Sun ST (2007) Study of acupuncture Zhongzhu (SJ3) Houxi (SI3) by functional MRI (fMRI). Chinese archives of traditional Chinese medicine 25: 843–844.
93. Huang Y, Li TL, Lai XS, Zou YQ, Wu JX, et al. (2009) Functional brain magnetic resonance imaging in healthy people receiving acupuncture at Waiguan versus Waiguan plus Yanglingquan points: a randomized controlled trail. Journal of Chinese integrative medicine 7: 527–531.
94. Zhang R, Zou YQ, Huang SQ, Chen ZG, Liang BL, et al. (2007) MRI cerebral function imaging following acupuncture at Hegu, Zusanli, Neiguan and Sanyinjiao points. Journal of clinical rehabilitative tissue engineering research 11: 4271–4274.
95. Hou JW, Huang WH, Wang Q, Feng JW, Pu YL, et al. (2002) Functional MRI studies of acupuncture analgesia modulating within the human brain. Chin J Radiol 36: 206–210.
96. Wang W, Xu HB, Kong XQ, Huang JB, Zhi X, et al. (2009) Experimental study on fMRI in human brain with electroacupuncture. J Pract Radiol 25: 305–308.
97. Li K, Shan BC, Liu H, Wang W, Xu JY, et al. (2005) fMRI study of acupuncture at large intestine 4. Chin J Med Imaging Technol 21: 1329–1331.
98. Liu H, Shan BC, Gao DS, Xu JY, Wang W, et al. (2006) Different cerebellar responding to acupuncture at Liv3 and LI4: an fMRI study. Chin J Med Imaging Technol 22: 1165–1167.
99. Yin L, Jin XL, Shi X, TIan JH, Ma L, et al. (2002) Imaging with PET and fMRI on brain function in acupuncturing the ST36 (Zusanli). Chin J Rehabil Theory Practice 8: 523–524.
100. Xu JY, Wang FQ, Wang H, Shan BC, Lv J, et al. (2004) Control study on effects of acupuncture at Hegu (LI4) and Taichong (LR3) points on fMRI cerebral function imaging. Zhongguo Zhen Jiu 24: 263–265.
101. Long Y, Liu B, Liu X, Yan CG, Chen ZG, et al. (2009) Resting-state functional MRI evaluation of after-effect of acupuncture at Zusanli point. Chin J Med Imaging Technol 25: 373–376.
102. Xiao YY, Wu RH, Pei RQ, Lin R, Rao HB (2004) Functional MR imaging (fMRI) of acupuncture: observation of stimulating the acu-point ST36 (zusanli). J Pract Radiol 20: 106–108.
103. Fu P, Jia JP, Xu M, Wang M (2005) Changes of brain function in different areas of cerebral cotices due to electroacupuncture at the point ST36 through MRI. Chinese journal of clinical rehabilitation 9: 92–93.
104. Wu ZY, Miao F, Xiang QY, Hao J, Cao Y, et al. (2007) The MRI research of brain function on acupuncture at Zusanli (ST36) point. Chinese journal of traditional medical science and technology 14: 305–307.
105. Fang SH, Zhang SZ, Liu H (2006) Study on brain response to acupuncture by functional magnetic resonance imaging–observation on 14 healthy subjects. Zhongguo Zhong Xi Yi Jie He Za Zhi 26: 965–968.
106. Tian LF, Zhou C, Chen M, Zhou TG, Cai K, et al. (2006) Using functional magnetic resonance imaging to study the correlation between the acupoint and cerebral region. Zhen Ci Yan Jiu 31: 113–115.
107. Kim Y-i, Kim Y-h, Lim Y-k, Lee H, Lee B-r, et al. (2003) A fMRI study on the cerebral activity induced by Electro-acupuncture on Zusanli(St36). The Journal of Korean Acupuncture & Moxibustion Society 20: 133–150.
108. Chi X, Sun ST (2007) Cerebral functional magnetic resonance imaging study of point Waiguan acupuncture. Shanghai J Acu-mox 26: 30–31.
109. Park T-g, Kim Y-I, Hong K-e, Yim Y-k, Lee H, et al. (2004) A study on Brain activity induced by electro-acupuncture on Taechung(LR3) and Hapkok(LI4) using functional Magnetic Resonance Imaging. The Korean Journal of Meridian & Acupoint 21: 29–46.
110. Chen WJ, Shou YQ, Li JH, Xu ZS, Liu H (2007) The effect of acupuncture at the acupoint Sanyinjiao on brain function as revealed by the functional magnetic resonance imaging. Chin J Phys Med Rehabil 29: 774–779.
111. Wu ZY, Miao F, Xiang QY, Hao J, Ge LB, et al. (2008) Comparative study on acupuncturing the different acupoints of the same meridian with functional magnetic resonance imaging. Chinese J Med Imaging 16: 101–105.
112. Cai K, Chen M, Wang WC, Zhou C, Zhou TG, et al. (2007) fMRI of cortical activation by acupuncture. Information of medical equipment 22: 84–86.

113. Guan YQ, Yang XZ (2008) Brain BOLD-fMRI study of electroacupuncture stimulating the acupoint related visual. Hebei J TCM 30: 1065–1068.
114. Chen P, Zhao BX, Qin W, Chen HY, Tian J, et al. (2008) Study on the mechanism of acupuncture at Daling (PC 7) for mental diseases by fMRI. Zhongguo Zhen Jiu 28: 429–432.
115. Park K-y, Lee B-r, Lee H, Yim Y-k, Hong K-e, et al. (2003) A fMRI study on the cerebral activity induced by Electro-acupuncture on Taixi(K3). The Journal of Korean Acupuncture & Moxibustion Society 20: 194–208.
116. Yoon J-h, Hwang M-s, Bae G-t, Lee S-h, Lee S-d, et al. (2001) The new finding on BOLD response of motor acupoint KI6 by fMRI. The Journal of Korean Acupuncture & Moxibustion Society 18: 60–69.
117. Kwon C-h, Lee J-b, Hwang M-s, Yoon J-h (2004) The New Finding on BOLD Response of Moter Acupoint KI6 by fMRI. The Journal of Korean Acupuncture & Moxibustion Society 21: 177–186.
118. Kang J-h, Lee H, Lee B-r, Hong K-e, Yim Y-k, et al. (2003) A fMRI study on the cerebral activity induced by Electro-acupuncture on K7(Fuliu). The Journal of Korean Acupuncture & Moxibustion Society 20: 66–84.
119. Zhang Y, Liang J, Qin W, Liu P, von Deneen KM, et al. (2009) Comparison of visual cortical activations induced by electro-acupuncture at vision and nonvision-related acupoints. Neurosci Lett 458: 6–10.
120. Chi X, Sun ST, Bao DP (2006) fMRI study of acupuncture at Houxi (SI3) point. JCAM 22: 37–38.
121. Chen SJ, Liu B, Fu WB, Wu SS, Chen J, et al. (2008) A fMRI observation on different cererbral regions activated by acupuncture of Shenmen (HT 7) and Yanglao (SI 6). Zhen Ci Yan Jiu 33: 267–271.
122. Chen HD, Ying GL, Jiang B, He WL (2006) Studding effect of acupuncturing Baihui point for brain function with fMRI method. Journal of Zhejiang University of traditional Chinese medicine 30: 656–659.
123. Wang AC, Wang YL, Jiang T, Ma B, Chen JF, et al. (2005) Observation on changes of cerebral images after acupuncture of Shenmai (BL62) by using fMRI. Zhen Ci Yan Jiu 30: 43–47.
124. Deng ZS, Qiu ML, C. F-S SL (2005) A study on response of the specific functional areas of the human brain to acupuncture stimulating visual-ralated acupoints using BOLD fMRI. J Pract Radiol 21: 1240–1242.
125. Rheu K-h, Choi I-h, Park H-j, Lim S (2006) fMRI Study on the Brain Activity Induced by Manual Acupuncture at BL62. The Korean Journal of Meridian & Acupoint 23: 89–103.
126. Fu P, Jia JP, Wang M (2005) Acupuncture at Shenmen acupoint for brain functional MRI of patients with Alzheimer disease. Chinese journal of clinical rehabilitation. pp 120–121.
127. Bai L, Qin W, Tian J, Liu P, Li L, et al. (2009) Time-varied characteristics of acupuncture effects in fMRI studies. Hum Brain Mapp 30: 3445–3460.
128. Wang W, Zhu F, Qi JP, Xia YL, Xia LM, et al. (2002) Comparison study of human brain response to acupuncture stimulation vs finger tapping task by using real time fMRI. Chin J Radiol 36: 211–214.
129. Wang SM, Constable RT, Tokoglu FS, Weiss DA, Freyle D, et al. (2007) Acupuncture-induced blood oxygenation level-dependent signals in awake and anesthetized volunteers: a pilot study. Anesth Analg 105: 499–506.
130. Zhen JP, Liu C, He JZ, Wang BG, Yang DH, et al. (2008) The research of brain fMRI in acupuncture of KI in different time. Chinese imaging journal of integrated traditional and western medicine 6: 325–331.
131. Park J-m, Gwak J-y, Cho S-y, Park S-u, Jung W-a, et al. (2008) Effects of Head Acupuncture Versus Upper and Lower Lims Acupuncture on Signal Activation of Blood Oxygen Level Dependent (BOLD) fMRI on the Brain and Somatosensory Cortex. The Journal of Korean Acupuncture & Moxibustion Society 25: 151–165.
132. Teng J, Wang YL, Wang AC, Zhao JN, Liu M (2008) Study on cerebral images with frontal-three-needle penetration by functional magnetic resonance imaging. Journal of Shandong University of TCM 32: 104–106.
133. Zhou Y, Jin J (2008) Effect of acupuncture given at the HT 7, ST 36, ST 40 and KI 3 acupoints on various parts of the brains of Alzheimer' s disease patients. Acupunct Electrother Res 33: 9–17.
134. Li J, Zhang JH, Dong JC (2007) Influence of acupuncture analgesia on cerebral function imaging in sciatica patients. Shanghai J Acu-mox 26: 3–6.
135. Chang JL, Gao Y, Zhang H, Tan ZJ, Jiang GD (2007) A preliminary discussion of the effect of electroacupuncture at acupoints HT5 and GB39 on lingual function and fMRI changes in a case of subcortical aphasia. Chinese journal of rehabilitation medicine 22: 13–17.
136. Wang W, Li KC, Shan BC, Yan B, Hao J, et al. (2006) fMRI study of acupuncture at "four gate points" on normal aging people. Chin J Med Imaging Technol 22: 829–832.
137. Zhou C, Wang JZ, Chen M, Zhou TG, Cai K, et al. (2005) The correlative study between acupoint stimulations and corresponding brain cortices on functional MRI. Chin J Radiol 39: 252–255.
138. He YZ, Wang LN, Huang L, Wang XH, Liu SR, et al. (2006) Effects of acupuncture on the cortical functional areas activated by index finger motion in the patient with ischemic stroke. Zhongguo Zhen Jiu 26: 357–361.
139. Xu FM, Xie P, Lu FJ, Mou J, Li YM, et al. (2007) Study on corresponding areas the liver and lung channels in brain with fMRI. Zhongguo Zhen Jiu 27: 749–752.
140. Qiu MG, Wang J, Xie B, Wu BH, Zhang SX, et al. (2005) Establishment of analyzing methods for functional MR images when electroacupuncture stimulation on Guangming and Waiguan acupoints. ACTA ACADEMIAE MEDICINAE MILITARIS TERTIAE 27: 1970–1972.
141. Xu JY, Wang FQ, Shan BC, Chen Y, Wang H, et al. (2004) PET and fMRI to evaluate the results of acupuncture treatment of the cognition of alzheimer's disease. Chinese imaging journal of integrated traditional and western medicine 2: 85–87.
142. Zhang WT, Jin Z, Luo F, Zhang L, Zeng YW, et al. (2004) Evidence from brain imaging with fMRI supporting functional specificity of acupoints in humans. Neurosci Lett 354: 50–53.
143. Cho Z-h, Kim K-y, Kim H-k, Lee B-r, Wong EK, et al. (2001) Correlation between acupuncture stimulation and cortical activation - further evidence. The Journal of Korean Acupuncture & Moxibustion Society 18: 105–113.
144. Chang SX, Feng GS, Kong XQ, Li G, Liu DX, et al. (2002) Functional MRI study of cortical function area activation with electronic acupuncture stimulation of multiple acupoints. Lin Chuang Fang She Xue Za Zhi 21: 99–102.
145. Kong J, Kaptchuk TJ, Polich G, Kirsch I, Vangel M, et al. (2009) An fMRI study on the interaction and dissociation between expectation of pain relief and acupuncture treatment. Neuroimage 47: 1066–1076.
146. Kong J, Kaptchuk TJ, Polich G, Kirsch I, Vangel M, et al. (2009) Expectancy and treatment interactions: a dissociation between acupuncture analgesia and expectancy evoked placebo analgesia. Neuroimage 45: 940–949.
147. Kong J, Gollub RL, Rosman IS, Webb JM, Vangel MG, et al. (2006) Brain activity associated with expectancy-enhanced placebo analgesia as measured by functional magnetic resonance imaging. J Neurosci 26: 381–388.
148. Zhang Y, Qin W, Liu P, Tian J, Liang J, et al. (2008) An fMRI study of acupuncture using independent component analysis. Neurosci Lett.
149. Bai L, Tian J, Qin W, Pan X, Yang L, et al. (2007) Exploratory analysis of functional connectivity network in acupuncture study by a graph theory mode. Conf Proc IEEE Eng Med Biol Soc 2007: 2023–2026.
150. Qin W, Tian J, Bai L, Pan X, Yang L, et al. (2008) FMRI Connectivity Analysis of Acupuncture Effects on an Amygdala-Associated Brain Network. Mol Pain 4: 55.
151. Qin W, Tian J, Pan X, Yang L, Zhen Z (2006) The correlated network of acupuncture effect: a functional connectivity study. Conf Proc IEEE Eng Med Biol Soc 1: 480–483.
152. Liu P, Qin W, Zhang Y, Tian J, Bai L, et al. (2009) Combining spatial and temporal information to explore function-guide action of acupuncture using fMRI. J Magn Reson Imaging 30: 41–46.
153. Liu P, Zhang Y, Zhou G, Yuan K, Qin W, et al. (2009) Partial correlation investigation on the default mode network involved in acupuncture: an fMRI study. Neurosci Lett 462: 183–187.
154. Yeo S, Kim Y, Choe I-h, Rheu C-h, Choi Y-g, et al. (2009) Reproducibility Between two physicians of fMRI study on the Brain Activity Induced by Acupuncture. Journal of Meridian & Acupoint 26: 39–51.
155. Raichle ME, Mintun MA (2006) Brain work and brain imaging. Annu Rev Neurosci 29: 449–476.
156. Poldrack RA, Fletcher PC, Henson RN, Worsley KJ, Brett M, et al. (2008) Guidelines for reporting an fMRI study. Neuroimage 40: 409–414.
157. Sun G (2008) Basic Theroy of Traditional Chinese Medicine. Beijing: China Press of Traditional Chinese Medicine. 315 p.
158. Han JS (2011) Acupuncture analgesia: areas of consensus and controversy. Pain 152: S41–48.
159. Dhond RP, Kettner N, Napadow V (2007) Do the neural correlates of acupuncture and placebo effects differ? Pain 128: 8–12.
160. Li X, Liu X, Liang F (2008) Functional brain imaging studies on specificity of meridian and acupoints. Neural Regen Res 3: 777–781.
161. Campbell A (2006) Point specificity of acupuncture in the light of recent clinical and imaging studies. Acupunct Med 24: 118–122.
162. Beissner F, Henke C (2009) Methodological Problems in fMRI Studies on Acupuncture: A Critical Review With Special Emphasis on Visual and Auditory Cortex Activations. Evid Based Complement Alternat Med.
163. Cho ZH, Hwang SC, Wong EK, Son YD, Kang CK, et al. (2006) Neural substrates, experimental evidences and functional hypothesis of acupuncture mechanisms. Acta Neurol Scand 113: 370–377.
164. Chae Y, Park HJ, Hahm DH, Hong M, Ha E, et al. (2007) fMRI review on brain responses to acupuncture: the limitations and possibilities in traditional Korean acupuncture. Neurol Res 29 Suppl 1: S42–48.
165. Zhao L, You ZL, Tang Y, Liang FR (2009) Observation of brain response to acupuncture stimuli using fMRI. Lishizhen medicine and materia medica research 20: 1343–1345.
166. Li XT, Song XG (2009) An overview of the application of functional MRI technique on clinical acupuncture. Journal of Anhui TCM College 4: 78–80.
167. Jiang C, Zhou SY, Zhao L, Li Y (2010) To evaluate the application of fMRI technique in acupuncture research. Journal of practical traditional Chinese medicine 26: 275–277.
168. Hu T, Hu KM (2009) The application progress on brain response to acupuncture using functional MRI. Med J West China 21: 1987–1988.

Publication 2: Nierhaus T*, Pach D*, Huang W*, Long X, Napadow V, Roll S, Liang F, Pleger B, Villringer A, Witt CM. Differential cerebral response to somatosensory stimulation of an acupuncture point vs. two non-acupuncture points measured with EEG and fMRI. *Frontiers in human neuroscience.* 2015;9:74. (*equal contribution)

frontiers in
HUMAN NEUROSCIENCE

ORIGINAL RESEARCH ARTICLE
published: 13 February 2015
doi: 10.3389/fnhum.2015.00074

Differential cerebral response to somatosensory stimulation of an acupuncture point vs. two non-acupuncture points measured with EEG and fMRI

Till Nierhaus[1,2]*†, Daniel Pach[3]*†, Wenjing Huang[3,4†], Xiangyu Long[2], Vitaly Napadow[5,6], Stephanie Roll[3], Fanrong Liang[4], Burkhard Pleger[2], Arno Villringer[1,2†] and Claudia M. Witt[3,7†]

[1] Mind-Brain Institute at Berlin School of Mind and Brain, Charité – Universitätsmedizin Berlin and Humboldt-University, Berlin, Germany
[2] Department of Neurology, Max Planck Institute for Human Cognitive and Brain Sciences, Leipzig, Germany
[3] Institute for Social Medicine, Epidemiology, and Health Economics, Charité – Universitätsmedizin Berlin, Berlin, Germany
[4] Acupuncture and Tuina School, Chengdu University of Traditional Chinese Medicine, Chengdu, China
[5] Department of Radiology, Athinoula A. Martinos Center for Biomedical Imaging, Massachusetts General Hospital, Charlestown, MA, USA
[6] Department of Radiology, Logan University, Chesterfield, MO, USA
[7] Institute for Complementary and Integrative Medicine, University Hospital Zurich, Zurich, Switzerland

Edited by:
Leonhard Schilbach, University Hospital Cologne, Germany

Reviewed by:
Matthew R. Longo, Birkbeck, University of London, UK
Philipp Georg Sämann, Max Planck Institute of Psychiatry, Germany

***Correspondence:**
Till Nierhaus, Mind-Brain Institute and Berlin School of Mind and Brain, Humboldt-University, Luisenstraße 56, 10117 Berlin, Germany
e-mail: till.nierhaus@charite.de;
Daniel Pach, Institute for Social Medicine, Epidemiology, and Health Economics, Charité – Universitätsmedizin Berlin, 10098 Berlin, Germany
e-mail: daniel.pach@charite.de

† *These authors have contributed equally to this work.*

Acupuncture can be regarded as a complex somatosensory stimulation. Here, we evaluate whether the point locations chosen for a somatosensory stimulation with acupuncture needles differently change the brain activity in healthy volunteers. We used EEG, event-related fMRI, and resting-state functional connectivity fMRI to assess neural responses to standardized needle stimulation of the acupuncture point ST36 (lower leg) and two control point locations (CP1 same dermatome, CP2 different dermatome). Cerebral responses were expected to differ for stimulation in two different dermatomes (CP2 different from ST36 and CP1), or stimulation at the acupuncture point vs. the control points. For EEG, mu rhythm power increased for ST36 compared to CP1 or CP2, but not when comparing the two control points. The fMRI analysis found more pronounced insula and S2 (secondary somatosensory cortex) activation, as well as precuneus deactivation during ST36 stimulation. The S2 seed-based functional connectivity analysis revealed increased connectivity to right precuneus for both comparisons, ST36 vs. CP1 and ST36 vs. CP2, however in different regions. Our results suggest that stimulation at acupuncture points may modulate somatosensory and saliency processing regions more readily than stimulation at non-acupuncture point locations. Also, our findings suggest potential modulation of pain perception due to acupuncture stimulation.

Keywords: somatosensory stimulation, functional magnetic resonance imaging (fMRI), electroencephalography (EEG), acupuncture, background rhythm, functional connectivity

INTRODUCTION

In a recent patient level data meta-analyses for chronic pain that included 29 randomized controlled trials, acupuncture was shown to be statistically significant superior to sham acupuncture (Vickers et al., 2012). Nevertheless, as the difference in effect size between real and sham acupuncture was small (standard mean difference of 0.15–0.23), the acupuncture point-specific effect is still controversial. One reason might be that various forms of sham acupuncture have been used in previous clinical trials. Often a penetrating sham acupuncture has been applied where either the control point location is different (Ma et al., 2012) (not a specific acupuncture point), the method of the stimulation is changed (Kleinhenz et al., 1999) (e.g., only superficial needling, no manually rotating and lift-thrusting), or both (Diener et al., 2006). Sanchez-Araujo (1998) showed in his review that studies where the control points were chosen to be near the real acupuncture points failed more frequently to show statistically significant differences between real acupuncture and sham acupuncture compared to using control acupuncture points located in different dermatomes (Sanchez-Araujo, 1998). In the past decade there has been growing interest in determining the neurophysiologic correlates of acupuncture by means of functional neuroimaging methods such as fMRI or EEG (Hui et al., 2000; Dhond et al., 2007; Hori et al., 2010; Huang et al., 2012). From a neurophysiological viewpoint, acupuncture is regarded as a complex somatosensory stimulation (Bäcker et al., 2004) and therefore is also interesting for experiments using conventional somatosensory stimulation protocols.

The purpose of this study was to evaluate whether the point locations chosen for a complex somatosensory stimulation with acupuncture needles differentially impact brain activity in healthy volunteers. We used electroencephalogram (EEG) and functional magnetic resonance imaging (fMRI) to compare standardized needle stimulation on three different point locations on the right leg: one acupuncture point (Stomach 36, ST36) and two control points that are widely accepted to not co-localize with points in

any acupuncture system. One of these control points was chosen to be near the real acupuncture point in the same dermatome L5 (CP1), while the other was chosen to be in a different dermatome L2 (CP2). Imaging results are expected to differ either when comparing the two different dermatomes (CP2 different from ST36 and CP1), or when comparing the acupuncture point with the two non-acupuncture control points.

Using fMRI, the blood oxygenation level dependent (BOLD) signal can localize brain regions modulated by sensory stimulation (Bandettini et al., 1992; Frahm et al., 1992; Kwong et al., 1992; Ogawa et al., 1992; Kurth et al., 2000; Ruben et al., 2001). Several studies have demonstrated acupuncture-related brain activity changes in somatosensory and pain-related areas such as primary somatosensory cortex (S1), secondary somatosensory cortex (S2), and thalamus (Napadow et al., 2009; Huang et al., 2012). Also, functional connectivity MRI (fcMRI) revealed acupuncture-related changes in network connectivity between areas related to sensorimotor and pain processing (Dhond et al., 2008). Therefore, stimulation of the acupuncture point might specifically activate brain regions associated with pain and modulate their connectivity. Using EEG, stimulation effects can be shown by investigation of background rhythmic activity, in the somatosensory system the "mu rhythm," respectively (Gastaut, 1952; Kuhlman, 1978). While the precise function of the mu rhythm is not clear, it is frequently referred to as an "idle rhythm" reflecting a resting-state of the somatosensory system (Ritter et al., 2009). Recent studies assume that EEG background activity is produced by inhibitory inter-neuronal activity and might reflect inhibitory top-down control (Klimesch et al., 2007; Jensen and Mazaheri, 2010). With respect to the clinical effectiveness shown for pain conditions, the stimulation of the acupuncture point might inhibit somatosensory areas and therefore increase mu-rhythmic activity.

We designed a blinded study including two series of experiments (one with EEG, one with fMRI) focusing on brain activity changes associated with complex somatosensory stimulation at one acupuncture point and two control points either close or distant to the acupuncture point. Our study was not aimed at evaluating clinical effects of acupuncture. We believe that our data provide new insights regarding cerebral processing of complex somatosensory stimulations and clarify the role of stimulus location for brain responses to complex somatosensory stimulation.

MATERIALS AND METHODS

SUBJECTS

Twenty-three healthy subjects (11 female, 12 male, mean age 26 years, range 19–31 years) participated in the EEG experiment, and 22 healthy subjects (11 female, 11 male, mean age 26 years, range 21–32 years) participated in the fMRI experiment. Participants had no medical knowledge about acupuncture and all except one had never been treated with acupuncture before the study. Participants were informed about the needle stimulation in both experiments as follows: "…one acupuncture needle will be inserted into the muscle at three different points of the upper and lower leg…." Among all the subjects, eight participated in both EEG and fMRI experiments. All participants were right-handed (laterally score: 88.2 ± 13.4 [S.D.] over a range of −100 [fully left-handed] to 100 [fully right-handed]) according to the Edinburgh inventory (Oldfield, 1971) and gave written informed consent to participate in the experiment according to the declaration of Helsinki. The study was approved by the ethics committee of the University of Leipzig. Prior to participation all subjects underwent a comprehensive neurological examination and confirmed they were not taking any acute or chronic medication. In the EEG experiment three subjects were excluded from acupuncture because of vegetative side effects (1 sweating/male, 2 dizziness/female); in the fMRI experiment one was excluded (sweating/female).

DETAILED DESCRIPTION OF POINT LOCATIONS

The points chosen for the intervention were developed after literature screening and a consensus process between the authors and experts of the Chengdu University of TCM, Prof Liang and Prof Li (**Figure 1A**).

1. Acupuncture point ST36 (Zusanli 足三里):
   To locate ST36, which is placed on the anterior lower leg, the acupuncture points ST35 and ST41 are used as anatomical landmarks. ST36 is located on the line connecting ST35 with ST41, 3 B-cun inferior to ST35 (ST35 is located on the anterior aspect of the knee, in the depression lateral to the patellar ligament. ST41 is located on the anterior aspect of the ankle, in the depression at the center of the front surface of the ankle joint, between the tendons of extensor hallucis longus and extensor digitorum longus) (Who Regional Office for the Western Pacific, 2008). According to Chinese medicine theory, for healthy subjects, ST36 is a commonly used acupuncture point to strengthen Qi and blood as a health preservation application. ST36 is located on the stomach meridian within the stomach meridian area. The skin area of ST36 belongs to L5 dermatome (Yan, 2006).
2. Control point 1 (located in the same dermatome and not in the same meridian skin area):
   The point is located lateral to the ST36 horizontally, at the middle line between Bladder meridian and Gallbladder meridian. Control point 1 is selected according to the principle of selecting non-acupuncture points from the middle line between two meridians which is commonly used in Chinese studies (Yang et al., 2009). Control point 1 is located in L5 dermatome and between Gallbladder and Bladder meridian skin area.
3. Control point 2 (located in another dermatome and not in the same meridian skin area):
   The point is located 2 B-cun dorsally of GB31 (avoidance of bladder meridian: GB31 is located on the lateral aspect of the thigh, in the depression posterior to the iliotibial band where the tip of the middle finger rests when standing up with the arms hanging alongside the thigh). Control point 2 is already a validated non-acupuncture point used in other acupuncture studies (Brinkhaus et al., 2003; Melchart et al., 2005; Linde et al., 2006) and it is located in L2 dermatome and Gallbladder meridian skin area.

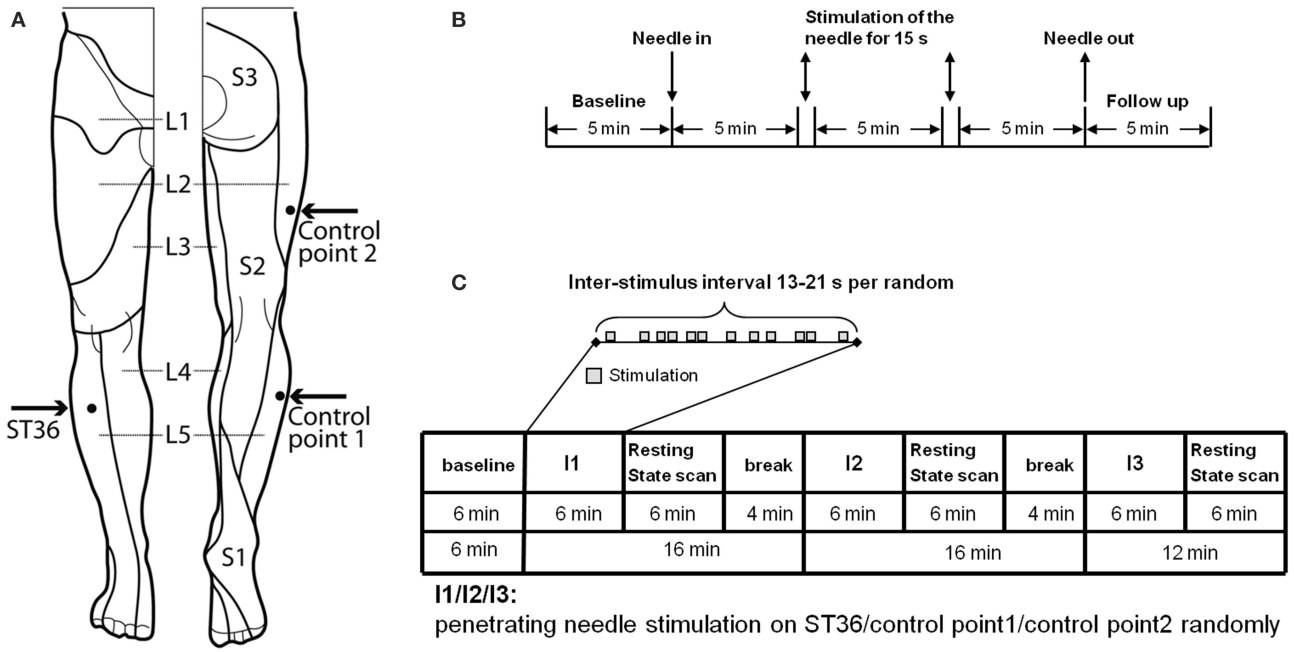

FIGURE 1 | Experimental design. (A) Location of ST36 and Control points on the right leg (view from the front and from the back, figure adapted Drake et al., 2009). **(B)** Experiment design of EEG measurement. On each of the 3 randomized measurement days EEG was recorded for every subject in a sitting position, with open eyes over a 25.5-min period. After the first 5-min baseline, an acupuncture needle was inserted and was stimulated manually at a time point 5 and 10 min after insertion. After a further 5 min the needle was removed and the EEG was recorded for a further 5 min without the needle. After the measurement, individual needle sensation was measured with a questionnaire. **(C)** Experiment design of fMRI measurement. In the fMRI scanner each subject was told to lie relaxed, in a supine position, with open eyes and to concentrate on the sensation caused by the needle stimulation. After the first resting-state was scanned for 6 min, an acupuncture needle was inserted into one point according to the randomized intervention order. The needle was then immediately stimulated manually according to the event-related design. After 6 min intermittent manipulation, the needle was withdrawn and a resting-state scan was continued for 6 min, and then followed by a 4-min break for the subject without scanning. The same scan procedure was then applied for the other two interventions on the other two points. But for the third intervention, there was no 4-min break. After each post-intervention resting-state scan individual needle sensation was measured with questionnaires.

EEG

Experimental Procedure

All subjects received the needle stimulation of the three different points (**Figure 1**)—the acupuncture point ST36 in dermatome L5, the control point in the same dermatome (CP1 in L5), the control point in a different dermatome (CP2 in L2)—on 3 separate days in consecutive order. The order was randomized. Measurements were taken within 2 weeks and with at least 24 h interval between each measurement. Subjects were told to sit down in a chair in the EEG room and relax with eyes open while concentrating on the point of needling.

The penetrating needle stimulation was performed by a Chinese acupuncture physician with sterile, single use, individually wrapped acupuncture needles (0.30 × 30 mm; asia-med standard, asia-med GmbH & Co. KG, Germany). The needle was vertically inserted 1–2 cm deep into the skin depending on the size of the respective muscle on the right leg. After 5 min the needle was stimulated (manually rotating 60–90/rpm and lift-thrusting 0.3–0.5 cm for 15 s). The 15 s stimulation was repeated after 5 min without stimulation. Penetrating needle stimulation was identical for each of the three point locations (**Figure 1**).

Data acquisition

A 32-channel EEG was recorded in a noise protected and electrically shielded room using BrainAmp (Brain Product, Germany) with a sampling rate of 1000 Hz. An electrode cap (Electro-Cap International, Eaton, OH) based on the international 10–20 system was placed on the scalp. The electrode FCz was used as reference and the ground electrode was located at the sternum. Electrode impedances were less than 2 kOhm. Including the 5-min baseline, the intervention, and the follow-up measurements the EEG was recorded for 25.5 min.

After each measurement the subjects were asked to fill in the MGH Acupuncture Sensation Scale (MASS questionnaire Kong et al., 2007) to measure the subjective needle sensation.

Data preprocessing

For data analysis custom-built scripts in the software package Matlab (Matlab, MathWorks, Inc.) were used. Since somatosensory alpha activity (Rolandic activity) can be covered by strong occipital alpha activity, an independent component analysis (ICA) was performed to allow for a preselection of "central" ICA components. For each subject the three sessions were merged to perform one ICA calculation (FastICA algorithm in Matlab). Rolandic rhythmic activity is characterized by a central

localization and a peak in the frequency spectrum in the alpha (8–15 Hz) and beta (16–30 Hz) range. Thus, ICA components were investigated for each subject and selected only if both a central topography and two peaks in the frequency spectrum were identifiable. Using this procedure, 2–10 (mean 5 ± 2 S.D.) central components were selected per subject. The selected central components were back projected and the derived dataset (now cleared from occipital alpha) was digitally filtered using a standard 3rd order band-pass Butterworth filter (low cut-off 1 Hz, high cut-off 45 Hz) and segmented into 5 epochs each lasting 4 min, based on the markers representing the interventions. Since we performed needle stimulation on the leg further data analysis was focused on electrode Cz which is located over the leg representation of S1. Frequency analysis was performed using fast Fourier transformation. The power spectral density was computed for each 4-min segment: (1) for baseline, (2) after the "needle-insertion," (3) after the first stimulation, (4) after the second stimulation, and (5) for follow up. For the statistical analysis of the mu activity, power spectral density was averaged for the frequencies from 10 Hz to 15 Hz.

Statistical analysis

For Cz electrode and each condition, the mu power change and percentage change compared to baseline was analyzed using generalized linear models for our within subject design with global *F*-tests and paired *t*-tests for pair-wise comparisons between stimulation points. For our primary outcome parameter, the mean of both post-stimulation periods, a Bonferroni correction was applied to the pair-wise comparison between the three stimulation points ($pR_{corr} = 0.05/3$).

To evaluate the correlation between alpha percentage change from baseline and needle sensation (MASS Index), Spearman correlation coefficients based on the ranks of the variables were used for Cz electrode, each condition, and each needle stimulation.

The needle sensation expressed by the MASS Index was compared descriptively for the three needle stimulations at different points by presenting means and 95% confidence intervals. To test a global stimulation point effect (within-subject effect) on the MASS Index, generalized linear models (GLM) were fitted using a multivariate approach (Wilks' lambda) because sphericity was often not met. To test pair-wise differences between the three points, paired *t*-tests were used.

fMRI

Experimental Procedure

As shown in **Figure 1C**, each participant was scanned seven times (each scan 6 min): One resting-state scan in the very beginning (i.e., baseline, RS_B), then three scans with needle stimulation of one point in an event-related design, each followed by another resting-state scan (i.e., RS_ST36, RS_CP1 and RS_CP2). The three event-related scans were in randomized order over subjects. During scanning, subjects were told to remain in the supine position with eyes open while concentrating on the sensation caused by the needle stimulation. During the resting-state, participants were simply asked to keep calm and stay still with eyes open.

The penetrating needle stimulation was performed by an acupuncture physician with sterile, single use, individually wrapped needles (0.20×30 mm; titanium, DongBang, Acupuncture, Inc., Boryeong, Korea). The needle was first inserted 1–2 cm deep into the skin depending on the size of the muscle vertically on the right leg. The needle was manually manipulated according to the event-related design starting immediately after insertion. Auditory cues signaled the timing of the stimulation events to the acupuncturist via headphones. Each event consisted of a 3-s needle stimulation rotating 60–90/rpm and lift-thrusting 0.3–0.5 cm. The length of the inter-stimulus interval was randomized from 13 to 21 s (**Figure 1B**). After the event-related scan the needle was removed. Identical penetrating needle stimulation was performed on the three different point locations (**Figure 1**).

Data acquisition

fMRI Data was acquired using a 3T Siemens Verio MRI System (Siemens Medical, Erlangen, Germany) equipped for echo planer imaging with a 12-channel head coil. fMRI images were acquired using an EPI sequence (30 axial slices, in-plane resolution is $3 \times 3 \times 5$ mm, slice thickness = 4 mm, flip angle = 90°, gap = 5 mm, repetition time = 2000 ms, echo time = 30 ms). A structural image was also acquired for each participant, using a T1-weighted MPRAGE sequence (repetition time = 12 ms, echo time = 5.65 ms, and flip angle = 19°, with elliptical sampling of k space, giving a voxel size of $1 \times 1 \times 1$ mm). Subjects' heads were immobilized by cushioned supports, and they wore earplugs to attenuate MRI gradient noise throughout the experiment.

Within the break following resting-state scans, subjects were asked to rate the items of the MGH Acupuncture Sensation Scale (MASS questionnaire Kong et al., 2007) to measure the subjective needle sensation.

Data pre-processing

FMRI data pre-processing included slice time correction, head motion correction, spatial normalization to MNI152 space and spatial smoothing with a 6 mm FWHM as implemented in the SPM 8 software package (www.fil.ion.ucl.ac.uk/spm/). Individual structure T1 images were also normalized to MNI152 space and then segmented into gray matter, white matter and cerebral spinal fluid (CSF). A threshold of 0.99 was used to cut off each segmented image. For each participant, 3 mm erosion was implemented on the white matter image and 1 mm erosion on the CSF image, and these two images were then combined into one anatomical mask. We applied principal component analysis (PCA) within this CSF/white matter mask to disentangle the variance related to each fMRI dataset (3 task scans and 4 resting-state scans) using the CompCor analysis (Behzadi et al., 2007) by DPABI toolbox (toolbox for Data Processing & Analysis of Brain Imaging, http://rfmri.org/dpabi). The first five principal components together with the six head motion parameters were later applied to each individual's first level GLM as nuisance variables to regress out associated variance. A union gray matter mask (Supplemental Figure 1) was created by merging all normalized individual gray matter images. The following analyses were conducted within this average gray matter mask.

GLM analysis

For each subject the first-level GLM contained the three different needle stimulation conditions (i.e., ST36, CP1, CP2; 6 min

stimulation for each point). For each condition, one stimulation regressor, together with the first five principal components from the CompCor analysis and six head motion parameters as nuisance regressors were included in the GLM. For the stimulation regressor, each stimulation onset was modeled with the boxcar function covering the following 3s stimulation duration. These box-car functions were convolved with the standard hemodynamic response function (HRF) as implemented in SPM 8. The long inter-stimulus intervals of 13–21 s were not explicitly modeled with the first level GLMs and hence represented an implicit baseline measure. For each of the three stimulation points we computed the individual ß-map.

On the second level (group) analyses, the main effect of each of the three stimulation points (i.e., ST36, CP1, CP2) was visualized by applying these individual ß-maps (together with age and gender as covariates) to one-sample *t*-tests to compare them against the null hypothesis. The results were corrected to the alpha-level <0.05 using AlphaSim in AFNI (Cox, 1996) (i.e., 39429 voxels within the gray matter mask, voxel-wise $p < 0.0001$, resulting cluster size >108 mm^3). We performed a within subjects ANOVA (factorial design within SPM8) including the individual ß-maps of all three conditions (ST36, CP1, CP2) as well as age and gender as covariates to generate the inter-points comparisons (i.e., ST36—CP1, ST36—CP2 and CP1—CP2) and conjunction maps within one statistical model. Conjunction of "ST36-CP1 and ST36-CP2" was calculated to compare the activation between acupuncture and control points, conjunction of "ST36-CP2 and CP1-CP2" was calculated to compare activations of the different dermatomes (L5 vs. L2). Using AlphaSim in AFNI, the results for the interpoint-comparisons as well as for the conjunction-maps were corrected to the alpha-level < 0.05 (i.e., 39429 voxels within the gray matter mask, voxel-wise $p < 0.01$, resulting cluster size >783 mm^3). We used "3dclust" in AFNI to detect clusters from the corrected statistical maps. All clusters that were reported in the tables are spatially separated and bigger than the volume criterion from the AlphaSim simulation analysis.

Functional connectivity analyses

For each of the four resting-state scans (RS_B, RS_ST36, RS_CP1, and RS_CP2) the first 10 volumes were discarded to account for the saturation of the BOLD response. Temporal band-pass filtering (0.01–0.08 Hz) and removal of linear trend was performed by the REST toolbox (www.restfmri.net). Seed-based voxel-wise functional connectivity analysis was performed for each resting-state scan using region of interest (ROI) spheres with 6 mm radius as seeds. As a proof of concept, one seed was placed on posterior cingulate cortex (PCC, Talairach space, $x = -2, y = -36, z = 37$ from a previous study Fox et al., 2005) that, as hypothesized, revealed the default mode network (Supplemental Figure 1). The other seed was derived from a group-level one-sample *t*-test across all three stimulation points together, with the maximum found at the parietal operculum as the anatomical site of S2 (Talairach space, $x = -54, y = -21, z = 21$).

Then, the average time course within the ROI was extracted as the seed signal, and a voxel-wise temporal correlation analysis was performed across all voxels within the averaged gray matter mask for each individual resting-state scan. The correlation maps were transferred to Fisher's z maps for further statistical analysis (Greicius et al., 2007). First, a one-sample *t*-test against null hypothesis was performed on the spatial correlation maps of each resting-state scan (together with age and gender as covariates) for the PCC-seed and the S2-seed, respectively. The results were corrected to the alpha-level <0.05 using AlphaSim in AFNI (i.e., 39429 voxels within the gray matter mask, voxel-wise $p < 0.0001$, resulting cluster size >108 mm^3). Again, we performed a within subjects ANOVA including the individual spatial correlation maps of all four resting-state scans as well as age and gender as covariates. Within this model, we generated the comparisons to baseline (RS_ST36-RS_B, RS_CP1-RS_B, and RS_CP2-RS_B), the inter-points comparisons (RS_ST36-RS_CP1, RS_ST36-RS_CP2, and RS_CP1-RS_CP2), and the conjunction maps. Conjunction of "RS_ST36-RS_CP1 and RS_ST36-RS_CP2" was calculated to compare functional connectivity between acupuncture and control points, conjunction of "RS_ST36-RS_CP2 and RS_CP1-RS_CP2" was calculated to compare connectivity between the different dermatomes (L5 vs. L2). Using AlphaSim in AFNI, the results for the different comparisons as well as for the conjunction-maps were corrected to the alpha-level <0.05 (i.e., 39429 voxels within the gray matter mask, voxel-wise $p < 0.01$, resulting cluster size >783 mm^3). As described above, we used "3dclust" in AFNI to detect clusters from the corrected statistical maps.

Needle sensation analyses

The needle sensation expressed by the MASS Index was compared descriptively for the three needle stimulations at different points by presenting means and 95% confidence intervals. To test a global stimulation point effect (within-subject effect) on MASS Index, generalized linear models (GLM) were fitted using a multivariate approach (Wilks' lambda) because sphericity was often not met. To test pair-wise differences between the three points, paired *t*-tests were used.

For each region that was detected in the conjunction analyses (**Figures 3C,D**), Pearson correlation coefficients were calculated across participants between the mean beta value across voxels within the respective region and the MASS index of each stimulation point.

RESULTS

EEG

Mu rhythm

The mu rhythm is one of the important human brain background rhythms and is associated with the primary somatosensory area, thus having a central topography (Salmelin and Hari, 1994). In healthy volunteers we stimulated the three different points mentioned above in the same manner and compared their respective influences on mu rhythm. Data is shown for electrode Cz which is closest to the lower limb representation in S1. Mu rhythm power was significantly enhanced after stimulation of ST36 compared to the stimulation of the two control points (mean of stimulation phase 1 and phase 2 vs. baseline: ST36 vs. CP1 21.02 μV^2 95%CI [4.78;37.27], $p = 0.012$, ST36 vs. CP2 25.38 [9.12;41.65], $p = 0.003$, significance level Bonferroni corrected 0.05/3). Comparison of mu rhythm for the two control

points found no significant differences (CP2 vs. CP1 −4.36 [−20.53;11.81], $p = 0.598$, **Figure 2**).

Needle sensation

As our results for the mu rhythm may have been influenced by differences in needle sensation, the evoked sensation was measured using the MGH Acupuncture Sensation Scale (MASS Kong et al., 2007).

The MASS Index was used as a measure of needle sensation for ST36, CP1, and CP2 (3.15 [2.00;4.30], 3.37 [2.47;4.28], and 1.81 [1.13;2.50], respectively). Comparisons of ST36 vs. CP2 and CP1 vs. CP2 were statistically different (pairwise t-test, $p = 0.034$ and $p < 0.001$, respectively). However, a significant difference was not found between ST36 and CP1 ($p = 0.674$).

No correlations were found when exploring the relationship between the MASS index and the percentage change of mu rhythm power (all r-values between −0.16 and 0.40 with $p > 0.080$).

FMRI

Stimulation scans

The results of the intra-point analysis summarizing the BOLD response to needle stimulation of ST36 and the two control points are shown in **Figure 3A** and **Table 1**. For all three point stimulations we found significant activation in bilateral insula/S2 and left inferior semi-lunar lobule and deactivation in bilateral precuneus, right middle temporal gyrus, left superior frontal gyrus, right precentral gyrus, left medial frontal gyrus, right paracentral lobule, and bilateral parahippocampal gyrus.

We compared BOLD responses of the different points (ST36 vs. CP1, ST36 vs. CP2, and CP1 vs. CP2, shown in **Figure 3B** and **Table 2**) and with a conjunction analysis we evaluated shared areas for the comparison of acupuncture point vs. control points (conjunction of ST36-CP1 and ST36-CP2) and the comparison of two different dermatomes L5 and L2 (conjunction of ST36-CP2 and CP1-CP2).

For the comparison between acupuncture point and control points (ST36-CP1 and ST36-CP2), the conjunction analysis (**Figure 3C**, **Table 2**) revealed that right insula and right S2 presented higher activation during stimulation of ST36. The right precuneus/posterior cingulate cortex (PCC) presented pronounced deactivation during stimulation of the acupuncture point.

For the comparison between the dermatomes (ST36-CP2 and CP1-CP2), a common positive contrast was shown for right middle temporal gyrus (MTG) due to deactivation during stimulation of CP2 compared to activation when stimulating the other two points (**Figure 3D**, **Table 2**). Left superior temporal gyrus (STG) presented pronounced deactivation when stimulating ST36 or CP1 compared to stimulation of CP2.

Resting-state scans

At the first stage, the default mode network and somatosensory network were detected via the seed-based correlation analysis within the resting-state scans. By visual inspection, PCC, mPFC and bilateral angular gyrus (prominent marker of the default mode network) were all found in the PCC-seed-based correlation analysis (Supplemental Figure 1). For the S2-seed-based correlation analysis, we found bilateral S2, supplementary motor area (SMA), and bilateral S1/M1 as prominent areas corresponding to the somatosensory network (Supplemental Figure 1, **Table 3**). The results of the S2-seed-based correlation analysis were further compared between the different resting-state scans.

The different brain areas that showed changes in functional connectivity after stimulation of the three different points

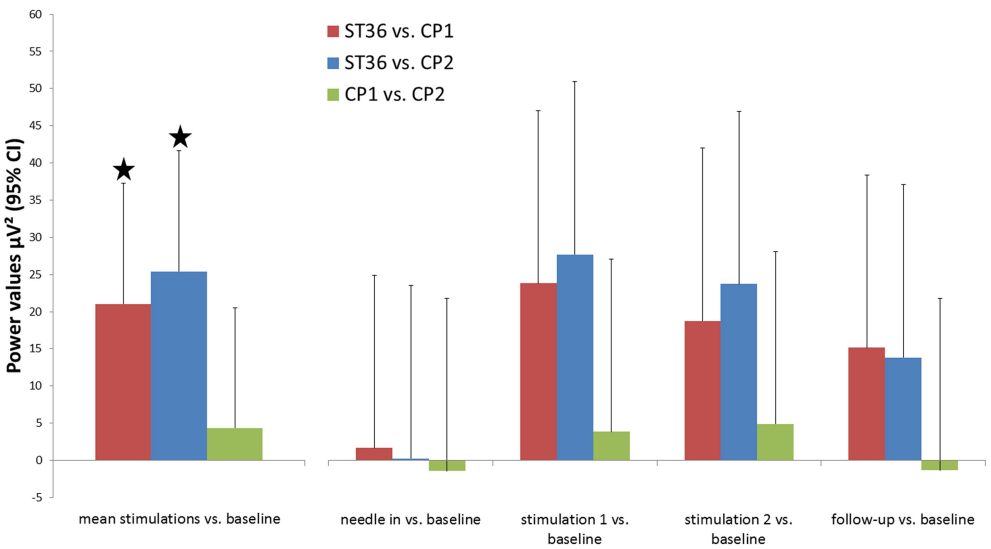

FIGURE 2 | Changes in background rhythm strength in the comparison of the three point locations. Power spectral density was calculated for segments of 4 min in the middle of each measurement block (baseline, needle-in, stimulation 1, stimulation 2, follow-up) and power values for frequencies 10–15 Hz (μ-rhythm) were averaged. The primary outcome parameter, the mean of both post-stimulation blocks, is highlighted on the left. Results are shown for electrode Cz (located over the leg representation of the somatosensory cortex). * Indicate significant differences after Bonferroni correction.

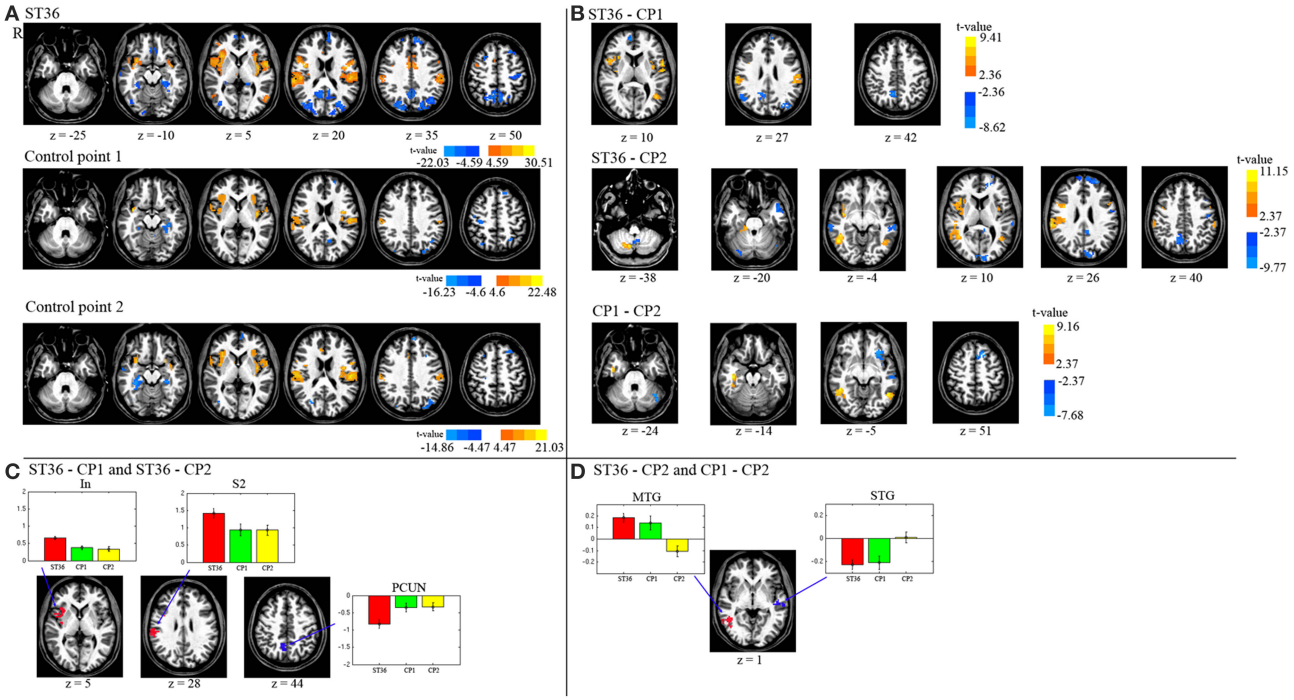

FIGURE 3 | (A) Displayed are the activation and deactivation for the different point stimulations (group-level t-maps, $P < 0.05$, corrected). **(B)** The de/activation contrasts between the three different point locations are presented ($P < 0.05$, corrected). **(C)** The conjunction map of the 1st and 2nd row of part **(B)** (acupuncture vs. control points). **(D)** The conjunction map of the 2nd and 3rd row of part **(B)** (dermatome L5 vs. L2). The barplots show the beta values across participants (average and standard error) within the respective region. R means right hemisphere. Talairach z coordinates are displayed. positive values: red, negative: blue.

compared to the baseline resting-state session are depicted in **Table 4** and **Figure 4A**.

ST36 as compared to CP1 revealed a significantly enhanced S2-connectivity to right precuneus, right MTG, and right parahippocampal gyrus (**Figure 4B**, **Table 4**).

ST36 as compared to CP2 showed a significantly enhanced S2-connectivity to right precuneus/cuneus and right culmen, whereas the left medial frontal gyrus, left inferior frontal gyrus, and left superior temporal gyrus showed a significantly reduced connectivity to S2 (**Figure 4B**, **Table 4**).

Comparing the two control points (CP1-CP2) revealed a significantly reduced S2-connectivity to right parahippocampal gyrus, left precuneus, and left superior temporal gyrus (**Figure 4B**, **Table 4**).

The conjunction analyses of the seed-based resting state connectivity for the comparison of acupuncture point vs. control points (conjunction of RS_ST36-RS_CP1 and RS_ST36-RS_CP2), as well as the comparison of two different dermatomes L5 and L2 (conjunction of RS_ST36-RS_CP2 and RS_CP1-RS_CP2) revealed no commonly change in connectivity.

Needle sensation

Similar to the EEG experiment the needle sensation was also assessed with the MASS (Kong et al., 2007). The MASS Index for ST36, CP1 and CP2 were 4.71 [3.53;5.89], 3.59 [2.51;4.68], and 3.32 [2.34;4.29], respectively. Differences between ST36 vs. CP1 and ST36 vs. CP2 were statistically significant (pairwise *t*-test, $p = 0.009$ and $p = 0.005$, respectively). There was no significant difference between CP1 and CP2 ($p = 0.587$).

No correlation was found when exploring the relationship between the MASS index and the mean beta values within the ROIs detected in the conjunction analysis (all r-values between −0.48 and 0.51 with $p > 0.05$, corrected for multiple comparison).

DISCUSSION

We compared the stimulation of the acupuncture point ST36 with two control points that were non-acupuncture points: one near the real acupuncture point in the same dermatome (CP1 in L5) and one in a different dermatome (CP2 in L2). We expected the EEG and fMRI imaging results to be different either when comparing the points in the two different dermatomes (CP2 different from ST36 & CP1), or when comparing the acupuncture point with the two non-acupuncture control points. Comparisons between points in the two different dermatomes (ST36 vs. CP2 and CP1 vs. CP2) showed more pronounced activation at right middle temporal gyrus and deactivation at left superior temporal gyrus when stimulating dermatome L5 (ST36 or CP1). When comparing the acupuncture point with the control points (ST36 vs. CP1 and ST36 vs. CP2) we found (i) pronounced BOLD activation in right insula and right S2, pronounced deactivation in precuneus/PCC, and (ii) a pronounced increase of mu rhythm power in the EEG data following stimulation of ST36. Moreover, increased connectivity of left S2 to the right precuneus was

Table 1 | Foci with significant BOLD response from the three points ($P < 0.05$, corrected).

Task	Area	Left/Right hemisphere	Brodmann areas	Talairach space, x,y,z	*T*–value	*p*–value	Volume (mm^3)
ST36	Insula/SII	L	13	−36, −3, 17	30.51	1.72E-17	28431
	Insula	R	13	36, −5, −2	28.78	5.12E-17	21708
	Precuneus	L	31	−20, −73, 25	−21.57	1.05E-14	12555
	Middle temporal gyrus	R	19	30, −76, 22	−20.61	2.41E-14	11016
	SII	R	40	55, −24, 22	26.74	2.00E-16	10908
	Precuneus	R	7	11, −56, 46	−17.50	4.63E-13	9045
	Precuneus	R	7	−3, −62, 52	−20.18	3.54E-14	7668
	Superior frontal gyrus	L	9	−8, 56, 25	−15.54	3.87E-12	5211
	Parahippocampal gyrus	L	37	−28, −47, −7	−13.85	2.89E-11	2835
	SMA	L	24	−8, −3, 38	17.73	3.67E-13	2835
	SMA	R	24	6, 6, 30	18.36	1.96E-13	2673
	Precentral gyrus	L	4	−36, −16, 49	−12.48	1.74E-10	1971
	Inferior temporal gyrus	R	19	39, −70, 1	−12.92	9.60E-11	1917
	Parahippocampal gyrus	R	36	30, −36, −7	−13.34	5.59E-11	1485
	Medial frontal gyrus	L	11	−6, 25, −15	−12.88	1.02E-10	1242
	Inferior semi-lunar lobule	L	/	−17, −67, −36	14.25	1.78E-11	1215
	Middle temporal gyrus	L	37	−53, −62, 6	14.47	1.36E-11	1188
	Inferior semi-lunar lobule	R	/	11, −67, −41	16.03	2.22E-12	1134
	Middle frontal gyrus	R	9	25, 22, 41	−12.63	1.42E-10	1107
	Paracentral Lobule	R	6	6, −30, 68	−18.25	2.19E-13	1026
	Superior temporal gyrus	R	21	61, −21, 1	−14.97	7.46E-12	864
	Precentral gyrus	R	4	25, −21, 60	−15.75	3.03E-12	837
	Medial frontal gyrus	R	25	11, 31, −15	−12.41	1.92E-10	567
	Medial frontal gyrus	R	10	6, 53, 6	−12.86	1.05E-10	513
	Middle temporal gyrus	L	21	−53, 3, -18	−13.52	4.39E-11	486
	Lingual gyrus	L	19	−22, −67, 1	−11.45	7.47E-10	486
	Thalamus	L	/	−11, −36, 9	−12.22	2.48E-10	486
	Supramarginal gyrus	R	39	50, −53, 25	−11.33	8.85E-10	432
	Middle frontal gyrus	R	6	39, 0, 46	11.88	4.00E-10	432
	Superior frontal gyrus	L	8	−25, 28, 49	−12.64	1.39E-10	405
	Precentral gyrus	R	6	17, −19, 68	−13.95	2.58E-11	405
	Postcentral gyrus	L	5	−17, −44, 68	12.27	2.31E-10	378
	Inferior frontal gyrus	R	46	41, 42, 4	12.34	2.10E-10	351
	Cerebellar Tonsil	L	/	−31, −59, −41	13.77	3.21E-11	324
	Cerebellar Tonsil	R	/	3, −53, −38	−11.22	1.05E-09	297
	Pyramis	R	/	44, −64, −31	−10.85	1.81E-09	297
	Middle temporal gyrus	R	37	44, −56, 4	10.72	2.21E-09	297
	Precuneus	R	7	25, −53, 54	−14.91	7.95E-12	270
	Middle temporal gyrus	R	21	58, −5, −12	−11.66	5.48E-10	243
	Superior temporal gyrus	L	21	−59, −24, 1	−11.00	1.46E-09	243
	Lingual gyrus	R	18	14, −88, −10	−10.40	3.62E-09	216
	Middle temporal gyrus	R	21	61, −11, −12	−10.39	3.72E-09	189
	Thalamus	R	/	6, −16, 9	11.49	6.99E-10	189
	Superior temporal gyrus	R	38	44, 8, −10	11.23	1.03E-09	162
	Middle occipital gyrus	L	19	−34, −70, 1	−10.70	2.30E-09	162
	Superior frontal gyrus	R	8	17, 48, 38	−12.31	2.19E-10	162
	Superior frontal gyrus	R	6	8, 3, 65	10.72	2.22E-09	162
	Caudate	R	/	0, 14, 1	−12.13	2.81E-10	108
	Postcentral gyrus	R	40	61, −19, 20	14.42	1.43E-11	108
	Anterior cingulate	R	24	6, 25, 22	10.15	5.43E-09	108
	Precuneus	L	7	−17, −70, 46	−10.86	1.79E-09	108
	Precuneus	L	7	−22, −56, 49	−10.01	6.72E-09	108

(Continued)

Table 1 | Continued

Task	Area	Left/Right hemisphere	Brodmann areas	Talairach space, x,y,z	*T*–value	*p*–value	Volume (mm^3)
CP1	Insula	R	38	36, 0, −7	22.48	4.91E-15	8613
	Insula	L	38	−34, −8, 4	16.14	1.96E-12	7020
	SII	R	2	55, −19, 25	17.84	3.28E-13	6264
	SII	L	13	−48, −19, 20	15.99	2.33E-12	4428
	Parahippocampal gyrus	L	30	−25, −38, −2	−15.45	4.28E-12	2160
	Postcentral gyrus	R	30	33, −21, 46	−13.00	8.65E-11	1323
	Inferior semi-lunar lobule	L	/	−11, −67, −41	14.62	1.12E-11	1134
	Precuneus	L	7	−22, −76, 38	−11.76	4.74E-10	729
	Precentral gyrus	R	6	19, −16, 68	−12.98	8.93E-11	540
	Parahippocampal gyrus	L	35	−28, −19, −15	−10.91	1.67E-09	432
	Middle temporal gyrus	L	21	−56, −21, −4	−11.23	1.03E-09	432
	Angular gyrus	L	40	−39, −56, 36	−11.06	1.33E-09	405
	Paracentral Lobule	R	6	6, −33, 62	−11.85	4.21E-10	405
	Parahippocampal gyrus	R	19	33, −38, −2	−16.07	2.13E-12	378
	Superior frontal gyrus	L	10	−20, 53, 20	−10.36	3.86E-09	324
	Posterior cingulate	L	31	−8, −56, 20	−10.44	3.43E-09	270
	Superior frontal gyrus	L	8	−14, 31, 49	−10.93	1.61E-09	243
	Medial frontal gyrus	L	8	−6, 48, 41	−10.97	1.52E-09	216
	Precuneus	L	7	−25, −53, 49	−10.66	2.44E-09	216
	Superior Parietal Lobule	R	7	28, −62, 52	−11.23	1.02E-09	189
	Posterior Cingulate	R	30	8, −53, 14	−9.83	9.08E-09	162
	Cingulate gyrus	R	24	3, 3, 30	10.79	2.00E-09	162
	Parahippocampal gyrus	R	36	25, −36, −12	−10.19	5.05E-09	135
	Middle occipital gyrus	R	19	36, −70, 9	−9.99	6.93E-09	135
	Precuneus	R	19	30, −73, 33	−10.66	2.44E-09	135
	Culmen	L	/	−6, −47, −10	−10.97	1.52E-09	108
	Middle temporal gyrus	R	7	30, −64, 28	−10.02	6.69E-09	108
	Precentral gyrus	R	4	44, −11, 49	−11.41	7.95E-10	108
CP2	SII/Insula	L	13	−50, −19, 22	20.91	1.84E-14	22491
	Insula/SII	R	13	33, 20, −2	21.03	1.66E-14	8559
	Middle occipital gyrus	R	37	36, −67, 1	−14.44	1.40E-11	8019
	Postcentral gyrus	R	3	58, −21, 38	17.67	3.89E-13	7182
	Precuneus	L	19	−28, −79, 36	−11.90	3.92E-10	1998
	Inferior semi-lunar lobule	L	/	−14, −67, −38	16.18	1.88E-12	972
	Superior frontal gyrus	L	9	−8, 50, 33	−12.76	1.19E-10	810
	Middle temporal gyrus	R	39	41, −56, 25	−12.81	1.12E-10	756
	Superior frontal gyrus	L	8	−25, 28, 49	−11.26	9.88E-10	729
	Parahippocampal gyrus	L	27	−25, -30, -7	−12.50	1.69E-10	594
	Cingulate gyrus	L	23	−6, −16, 30	12.30	2.23E-10	567
	Medial frontal gyrus	R	6	6, 14, 44	11.15	1.15E-09	567
	Middle temporal gyrus	R	21	52, −8, -12	−11.80	4.49E-10	513
	Medial frontal gyrus	L	10	−6, 56, 6	−11.43	7.64E-10	405
	Anterior cingulate	R	24	6, 25, 22	11.90	3.92E-10	378
	Cuneus	R	19	30, −73, 28	−10.74	2.15E-09	378
	Paracentral lobule	R	6	6, −33, 60	−13.62	3.86E-11	324
	Precuneus	R	31	25, −67, 20	−12.91	9.72E-11	243
	Middle frontal gyrus	R	8	25, 17, 46	−11.13	1.19E-09	243
	Cingulate gyrus	R	23	6, −16, 30	11.10	1.25E-09	216
	Cingulate gyrus	R	24	6, 11, 28	9.89	8.15E-09	216
	Cingulate gyrus	L	24	−3, 0, 38	10.35	3.94E-09	216

(Continued)

Table 1 | Continued

Task	Area	Left/Right hemisphere	Brodmann areas	Talairach space, x,y,z	*T*–value	*p*–value	Volume (mm^3)
	Parahippocampal gyrus	R	34	28, −11, −15	−11.96	3.60E-10	189
	Middle frontal gyrus	L	8	−31, 20, 38	−11.38	8.30E-10	189
	Postcentral gyrus	R	3	22, −24, 49	−10.99	1.47E-09	162
	Declive	R	/	17, −67, −15	10.20	4.97E-09	135
	Precentral gyrus	R	4	14, −24, 68	−11.34	8.71E-10	135
	Putamen	L	/	−25, 8, −7	16.29	1.68E-12	108
	Caudate	R	/	8, 6, 12	10.29	4.32E-09	108

Displayed are voxels of maximal significance. If the activated area crosses the midline, only the side of the highest value is displayed. The coordinates are in the Talairach space. T and p value is on the voxel-level.

observed in the follow-up resting-state scan for the comparisons of ST36 with the two control points, but in different regions of right precuneus. These results suggest differential processing of acupuncture point stimulation compared to stimulation of non-acupuncture control points, including a potential mechanism of pain modulation due to a complex somatosensory stimulation.

To answer our focused research question we applied a rigorous study design. The subjects were blinded regarding the character of the different point locations and the researchers were blinded during the pre-processing of the data and during the first steps of data interpretation. To prevent systematic errors, different randomization procedures were used. The order of point locations was randomized for both experiments, and the interstimulus intervals were randomized during the fMRI experiment. The washout period of acupuncture stimulation is still unknown. By randomizing the order of point locations all three interventions should be comparably affected by possible carry-over effects. A broad range of somatosensory effects were assessed using EEG, BOLD, and resting-state fcMRI data analysis. Thus, we evaluated event-related changes as well as longer lasting brain activity changes (connectivity and EEG rhythm). Event-related designs can robustly image brain response to discrete, short duration acupuncture stimuli (Napadow et al., 2012) which correspond well with the clinical application of acupuncture stimulation.

Manual acupuncture was chosen because it is more relevant for the clinical setting. But this might also be a cause of systematic error, because acupuncturists obviously could not be blinded in our study. Therefore, we evaluated the needle sensations as reported by the subjects. In part, needle sensations were different between the stimulated points, but we found that sensation was not correlated with brain activity changes. All subjects received the stimulation on all three point locations, therefore the groups we compared were based only on different point locations not on different subjects. We used intra-individual comparisons because the variance of physiological parameters between subjects is typically more pronounced than intra-subject differences caused by an intervention like a somatosensory stimulation on three different points. Because of intra-individual comparisons our data was not independent, though this was taken into account during our statistical analysis. Moreover, age and gender were included into the statistical models as covariates, since these factors might influence the outcome when evaluating the effects of acupuncture. In general, with the subtractive design used in our study, possible interferences between acupuncture effects and the somatotopic organization of evoked brain responses cannot be fully disentangled. This question could be addressed with a 2×2 factorial design with two pairs of acupuncture point and control point in different dermatomes, though involving additional experimental effort.

The results of the needle sensation for the two experiments were not comparable. In the EEG experiment the MASS index for ST36 stimulation was similar to CP1 and different from CP2. However, in the fMRI experiment the MASS index for ST36 stimulation was significantly different from the two control points. Several conditions might explain the differences. The position of participants in the two experiments were different. In the EEG experiment, participants were in a sitting position while in a supine position in the fMRI experiment, where the subjects might feel more relaxed than in a sitting position. Moreover, muscle tension on the leg where the needling stimulation was applied can be different in these two positions, and thus influence the sensation processing. In addition, a finer needle (different material and size) had to be used in the fMRI experiment because of the magnetic field of the scanner. Due to the repeated intermittent stimulation in the event-related design of the fMRI experiment, the stimulation protocol might have been more intense than in the EEG experiment.

Many studies show that various forms of somatosensory stimulation (from light touch to painful stimuli) cause transient desynchronization (suppression) of the somatosensory (mu) background rhythm (Neuper et al., 2006; Ploner et al., 2006b; Stancak, 2006). In our study, we observed increased mu rhythm following needle stimulation. Until now, to our best knowledge, such an after-effect of a peripheral somatosensory stimulation has not been described in the literature. A recent EEG study indicated that acupuncture stimulation on acupuncture point LI4 seemed to lead to specific changes in alpha EEG-frequency (Streitberger et al., 2008). However, the authors compared manual penetrating acupuncture with non-penetrating needle stimulation on the same point, i.e., they compared different kinds of stimulation rather than different points. Similar effects of long lasting increased background rhythm have been described for non-invasive brain stimulation protocols such as TDCS/TACS (transcranial direct/alternating

Table 2 | BOLD changes: a comparison of the three points showing all significant contrasts ($P < 0.05$, corrected).

	Area	Left/Right hemisphere	Brodmann areas	Talairach space, x,y,z	*T*-value	*p*–value	Volume (mm^3)
ST36-CP1	Insula	R	44	47, 8, 14	9.42	1.79E-08	7020
	SII	L	43	−53, −16, 20	8.68	6.33E-08	6777
	SII	R	40	58, −21, 25	7.64	4.26E-07	3294
	Angular gyrus	L	19	−36, −73, 33	−7.59	4.76E-07	2322
	Insula	L	13	−34, 0, −2	8.70	6.12E-08	2214
	Medial frontal gyrus	R	10	6, 50, 9	−7.67	4.02E-07	1755
	Medial frontal gyrus	L	9	−6, 50, 20	−7.10	1.23E-06	1701
	Precuneus	R	7	8, −53, 44	−8.26	1.34E-07	1404
	Angular gyrus	R	39	47, −64, 33	−6.42	4.77E-06	1350
	Insula	L	13	−34, −3, 12	7.12	1.18E-06	1323
	Posterior cingulate	R	23	11, −50, 25	−6.44	4.57E-06	1269
	Middle temporal gyrus	L	19	−39, −59, 12	7.06	1.32E-06	1026
ST36-CP2	Insula	R	13	36, 0, 1	11.15	1.16E-09	11232
	Middle temporal gyrus	R	37	47, −53, −4	9.78	9.84E-09	7641
	Cuneus	L	18	−3, −93, 12	−9.68	1.16E-08	5616
	SII	R	40	61, −30, 25	9.27	2.31E-08	5022
	Superior frontal gyrus	L	10	−22, 50, 25	−7.96	2.35E-07	4536
	Superior temporal gyrus	L	22	−48, -13, 1	−9.01	3.60E-08	3699
	Precuneus	R	7	8, −56, 44	−8.23	1.42E-07	2646
	Middle temporal gyrus	L	37	−42, −56, 1	9.08	3.16E-08	2565
	Middle temporal gyrus	L	21	−39, 3, -28	−7.42	6.49E-07	2025
	Inferior Parietal Lobule	L	40	−56, −30, 38	7.72	3.70E-07	1998
	Cerebellar Tonsil	L	/	−42, −64, −28	−6.85	2.00E-06	1944
	Inferior semi-lunar lobule	R	/	11, −64, −38	8.77	5.46E-08	1431
	Precentral gyrus	L	6	−48, −11, 30	−6.62	3.20E-06	1404
	Middle temporal gyrus	R	21	61, −27, -10	−6.95	1.63E-06	1377
	Precuneus	L	7	−3, −59, 46	−6.47	4.36E-06	1296
	Inferior frontal gyrus	L	9	−50, 8, 33	9.70	1.11E-08	1269
	Superior frontal gyrus	R	10	11, 62, 22	−6.85	2.02E-06	1242
	Culmen	R	/	17, −30, −18	8.92	4.20E-08	1188
	Posterior cingulate	L	29	−8, −41, 12	−8.67	6.54E-08	1134
	Medial frontal gyrus	L	32	−11, 39, 14	−7.25	9.17E-07	972
	Cerebellar Tonsil	L	/	−6, −50, -44	−6.59	3.41E-06	837
	Declive	R	/	28, −76, −20	−5.81	1.71E-05	837
	Insula	L	13	−39, 3, 1	6.89	1.85E-06	837
	Precentral gyrus	L	9	−39, 20, 36	−6.48	4.28E-06	810
CP1-CP2	Middle temporal gyrus	R	37	44, −47, −2	8.74	5.70E-08	3861
	Superior temporal gyrus	L	22	−48, −21, 1	−6.88	1.90E-06	1917
	Inferior frontal gyrus	L	47	−31, 20, −2	−7.41	6.60E-07	1890
	Superior frontal gyrus	L	6	−14, 17, 52	−7.29	8.41E-07	1539
	Middle temporal gyrus	L	37	−48, −53, −2	9.16	2.76E-08	1485
	Parahippocampal gyrus	R	36	39, −21, −15	8.37	1.11E-07	1323
	Tuber	L	/	−42, −67, −25	−7.66	4.12E-07	1134
	Parahippocampal gyrus	R	36	36, −33, −10	6.79	2.27E-06	918
ST36-CP1 and ST36-CP2	Insula	R	13	/	positive	/	5346
	SII	R	42	/	positive	/	2214
	Precuneus / PCC	R	7	/	negative	/	1134
ST36-CP2 and CP1-CP2	Middle temporal gyrus	R	37	/	positive	/	2916
	Superior temporal gyrus	L	21	/	negative	/	810

Displayed are voxels of maximal significance. If the activated area crosses the midline, only the side of the highest value is displayed. The coordinates are in the Talairach space. T and p value is on the voxel-level. The results of the conjunction analysis are also listed. "Positive" means ST36 presented higher activity than two control points, and vice versa.

Table 3 | Brain regions which were detected on the group level in the somatosensory network analysis from all resting-state sessions ($P < 0.05$, corrected).

Resting-state	Area	Left/Right hemisphere	Brodmann areas	Talairach space, x,y,z	*T*-value	*p*-value	Volume (mm^3)
RS_ST36	SII	L	40	−50, −19, 22	66.37	7.68E-24	66285
	SII	R	40	58, −19, 25	28.07	8.12E-17	43983
	Inferior semi-lunar lobule	L	/	−17, −62, −41	24.14	1.33E-15	10854
	Medial frontal gyrus/SMA	R	6	11, −5, 62	17.59	4.23E-13	7425
	Culmen	R	/	14, −47, −12	16.94	8.31E-13	5211
	Middle temporal gyrus	L	37	−48, −64, 9	15.56	3.75E-12	4158
	Middle temporal gyrus	R	37	52, −59, 6	17.26	5.93E-13	2538
	Precuneus	L	39	−39, −67, 36	−14.47	1.35E-11	1998
	Precuneus	L	31	−14, −44, 33	−12.90	9.94E-11	1107
	Cingulate gyrus	R	31	11, −21, 41	12.54	1.61E-10	1107
	Precuneus	R	7	14, −47, 57	13.11	7.47E-11	1080
	Inferior Parietal Lobule	R	40	44, −59, 38	−14.94	7.69E-12	1026
	Culmen	L	/	−17, −50, −18	11.93	3.72E-10	648
	Superior frontal gyrus	L	9	−14, 45, 36	−11.76	4.79E-10	432
	Fusiform gyrus	L	37	−42, −44, -12	11.39	8.19E-10	297
	Parahippocampal gyrus	L	19	−34, −59, −4	10.10	5.87E-09	243
	Middle frontal gyrus	L	6	−20, 22, 54	−11.11	1.23E-09	243
	Middle frontal gyrus	R	6	19, −16, 60	14.61	1.14E-11	243
	Anterior cingulate	R	32	6, 36, 25	−10.89	1.71E-09	216
	Fusiform gyrus	L	20	−39, −21, −23	11.49	6.99E-10	162
	Middle temporal gyrus	R	39	41, −62, 17	9.90	8.10E-09	162
	Postcentral gyrus	R	2	28, −36, 60	10.55	2.86E-09	162
	Declive	L	/	−22, −59, −15	9.99	6.97E-09	135
	Precentral gyrus	L	6	−14, −21, 68	13.06	8.02E-11	135
	Fusiform gyrus	R	37	41, −41, −12	10.22	4.82E-09	108
	Postcentral gyrus	R	3	44, −24, 54	11.69	5.24E-10	108
	Postcentral gyrus	L	3	−42, −27, 54	11.42	7.74E-10	108
RS_CP1	SII	L	43	−50, −19, 20	83.81	9.26E-26	71010
	SII	R	43	50, −16, 14	28.31	6.94E-17	47142
	Medial frontal gyrus / SMA	R	32	6, 6, 44	29.27	3.74E-17	9153
	Inferior semi-lunar lobule	L	/	−14, -62, −44	18.80	1.28E-13	3672
	Inferior semi-lunar lobule	R	/	11, −64, −44	14.60	1.15E-11	2970
	Precuneus	L	19	−31, −73, 38	−16.54	1.28E-12	2484
	Inferior Parietal Lobule	R	40	41, −59, 41	−11.78	4.66E-10	2376
	Culmen	R	/	19, −53, −18	14.49	1.32E-11	1944
	Middle temporal gyrus	L	39	−45, −53, 6	13.05	8.06E-11	1944
	Culmen	L	/	−17, −56, −18	14.46	1.37E-11	1836
	Middle temporal gyrus	R	19	50, −53, 4	12.99	8.80E-11	1782
	Postcentral gyrus	R	3	19, −36, 60	18.09	2.57E-13	1674
	Cingulate gyrus	R	31	14, −24, 41	12.75	1.21E-10	999
	Middle frontal gyrus	R	8	39, 25, 38	−13.82	3.02E-11	972
	Culmen	L	/	−22, −44, −23	12.08	3.04E-10	324
	Parahippocampal gyrus	R	27	30, −30, −7	−13.15	7.13E-11	270
	Middle frontal gyrus	R	46	47, 31, 17	−10.71	2.25E-09	216
	Middle frontal gyrus	L	6	−31, 17, 54	−14.02	2.34E-11	189
	Precuneus	R	19	33, −73, 33	−10.46	3.32E-09	162
	Postcentral gyrus	L	3	−42, −27, 54	15.10	6.37E-12	162
	Inferior frontal gyrus	R	47	28, 28, −2	11.21	1.06E-09	135
	Middle frontal gyrus	R	11	25, 48, −10	13.20	6.65E-11	108
	Middle temporal gyrus	L	39	−56, −56, 9	10.50	3.14E-09	108
	Precuneus	L	31	−6, −59, 30	−9.79	9.73E-09	108
	Superior frontal gyrus	R	8	17, 22, 46	−9.76	1.01E-08	108
	Postcentral gyrus	R	3	28, −33, 57	11.33	8.85E-10	108

(Continued)

Table 3 | Continued

Resting-state	Area	Left/Right hemisphere	Brodmann areas	Talairach space, x,y,z	*T*-value	*p*-value	Volume (mm^3)
RS_CP2	SII	L	43	−50, −19, 20	79.22	2.69E-25	56430
	SII	R	43	58, −19, 22	35.20	1.19E-18	47061
	SMA	L	24	−3, 3, 41	24.16	1.31E-15	11718
	SMA	R	24	6, 6, 44	22.23	6.05E-15	5940
	Inferior semi-lunar lobule	R	/	14, −64, −44	17.17	6.54E-13	3078
	Middle temporal gyrus	L	39	−45, −53, 9	14.47	1.35E-11	2079
	Fusiform gyrus	L	37	−39, −47, −15	22.08	6.84E-15	1971
	Fusiform gyrus	R	20	41, −38, −12	16.87	8.99E-13	1593
	Cerebellar Tonsil	L	/	−25, −53, −46	14.16	1.97E-11	1431
	Parahippocampal gyrus	R	34	19, 0, −12	20.29	3.20E-14	756
	Postcentral gyrus	R	40	22, −38, 57	11.41	7.88E-10	756
	Cingulate gyrus	R	31	11, −21, 41	14.04	2.29E-11	540
	Inferior semi-lunar lobule	L	/	−11, −64, −44	15.10	6.37E-12	432
	Paracentral Lobule	L	31	−8, −27, 44	14.41	1.46E-11	405
	Middle occipital gyrus	R	37	47, −64, −7	11.02	1.40E-09	324
	Middle temporal gyrus	L	20	−31, 0, −33	10.74	2.14E-09	243
	Parahippocampal gyrus	L	36	−39, −24, −15	12.39	1.98E-10	189
	Culmen	R	/	33, −38, −25	10.67	2.40E-09	162
	Middle frontal gyrus	L	10	−31, 39, 14	10.72	2.21E-09	135
	Caudate	R	/	14, 11, 17	−11.89	3.97E-10	135
	Superior frontal gyrus	L	6	−17, −3, 68	10.80	1.98E-09	135
	Fusiform gyrus	L	37	−36, −59, −12	10.10	5.83E-09	108
RS_B	SII	L	40	−50, −19, 22	52.90	5.59E-22	61398
	SII	R	40	44, −19, 22	22.59	4.49E-15	59967
	Cerebellar Tonsil	R	/	14, −59, −41	19.38	7.38E-14	4752
	Inferior semi-lunar lobule	L	/	−17, −62, −38	13.82	3.01E-11	2673
	Culmen	L	/	−28, −47, −23	13.74	3.34E-11	2079
	Declive	R	/	19, −62, −12	13.86	2.87E-11	1485
	Middle temporal gyrus	L	39	−50, −67, 9	10.89	1.72E-09	1323
	Middle temporal gyrus	R	37	52, −59, 1	12.30	2.22E-10	1242
	Paracentral Lobule	L	5	−6, −33, 57	14.58	1.18E-11	702
	Angular gyrus	L	39	−39, −62, 33	−10.96	1.55E-09	594
	Cerebellar Tonsil	L	/	−28, −44, −41	11.29	9.41E-10	432
	Cingulate gyrus	R	31	17, −41, 33	−11.05	1.34E-09	432
	Middle frontal gyrus	R	8	36, 17, 44	−10.61	2.62E-09	324
	Inferior frontal gyrus	L	10	−31, 36, 14	10.16	5.32E-09	297
	Precuneus	L	31	−11, −53, 30	−10.27	4.50E-09	297
	Precentral gyrus	R	4	33, −16, 52	11.75	4.86E-10	297
	Subcallosal gyrus	R	34	14, 6, −12	11.44	7.60E-10	270
	Putamen	R	/	25, 11, 6	11.95	3.63E-10	216
	Postcentral gyrus	L	4	−17, −33, 62	11.91	3.83E-10	216
	Postcentral gyrus	L	2	−22, −36, 65	15.53	3.91E-12	216
	Cingulate gyrus	L	31	−3, −30, 36	−11.65	5.54E-10	189
	Culmen	R	/	14, −44, −15	11.08	1.28E-09	162
	Putamen	L	/	−22, 11, 4	10.41	3.58E-09	162
	Supramarginal gyrus	R	39	39, −53, 28	−9.84	8.93E-09	162
	Cingulate gyrus	R	31	3, −33, 36	−10.63	2.55E-09	135
	Postcentral gyrus	L	4	−36, −27, 57	10.11	5.75E-09	135
	Middle temporal gyrus	L	22	−36, -53, 9	10.59	2.69E-09	108
	Claustrum	L	13	−25, 22, 9	11.09	1.27E-09	108
	Superior frontal gyrus	R	9	30, 34, 30	9.81	9.36E-09	108
	Postcentral gyrus	R	4	14, −41, 65	11.04	1.37E-09	108
	Precentral gyrus	L	4	−22, −24, 65	10.82	1.90E-09	108

Displayed are voxels of maximal significance. If the activated area crosses the midline, only the side of the highest value is displayed. The coordinates are in the Talairach space. T and p value is on the voxel-level.

Table 4 | Brain regions which were detected on the group level in the somatosensory network analysis for the comparison of the post-stimulation resting-state sessions vs. the first resting-state session (baseline), and for the comparison of the three post-stimulation sessions with each other ($P < 0.05$, corrected).

Resting-state	Area	Left/Right hemisphere	Brodmann areas	Talairach space, x,y,z	*T*-value	*p*-value	Volume (mm^3)
RS_ST36- RS_B	Anterior cingulate	R	32	6, 34, 22	−7.73	3.59E-07	1728
	Precuneus	R	31	22, −56, 28	7.12	1.17E-06	1377
	Superior frontal gyrus	R	6	8, −16, 65	−7.35	7.48E-07	1215
	Culmen	R	/	28, −47, −18	5.82	1.70E-05	1053
	Parahippocampal gyrus	L	19	−31, −47, −4	6.84	2.06E-06	864
	Fusiform gyrus	L	19	−28, −59, −7	6.72	2.59E-06	783
RS_CP1- RS_B	Medial frontal gyrus	R	6	3, −24, 65	−7.12	1.16E-06	2025
	Culmen	L	/	0, −38, −10	−8.11	1.79E-07	999
	Parahippocampal gyrus	L	19	−31, −62, -7	6.59	3.40E-06	837
	Paracentral Lobule	L	6	−6, −30, 54	−8.11	1.77E-07	783
RS_CP2- RS_B	Parahippocampal gyrus	L	36	−31, −33, −15	6.85	2.01E-06	1053
RS_ST36- RS_CP1	Precuneus/Cuneus	R	7	28, −67, 33	6.51	4.03E-06	2835
	Middle temporal gyrus	R	21	58, −47, 9	7.93	2.50E-07	1674
	Parahippocampal gyrus	R	36	36, −33, −10	7.61	4.54E-07	1242
RS_ST36- RS_CP2	Medial frontal gyrus	L	9	−11, 39, 22	−8.90	4.30E-08	1890
	Inferior frontal gyrus	L	47	−25, 17, −12	−7.58	4.81E-07	1566
	Culmen	R	/	11, −59, −10	6.42	4.82E-06	1053
	Superior temporal gyrus	L	38	−36, 14, −25	−7.01	1.46E-06	891
	Precuneus/Cuneus	R	18	14, −79, 20	6.27	6.51E-06	837
RS_CP1- RS_CP2	Parahippocampal gyrus	R	27	30, −30, −7	−7.79	3.21E-07	2295
	Precuneus	L	19	−34, −73, 38	−8.45	9.57E-08	1161
	Superior temporal gyrus	L	39	−53, −56, 20	−6.03	1.07E-05	918

Displayed are voxels of maximal significance. If the activated area crosses the midline, only the side of the highest value is displayed. The coordinates are in the Talairach space. T and p value is on the voxel-level.

current stimulation) or TMS (transcranial magnetic stimulation) (Wagner et al., 2007).

The BOLD activation pattern and connectivity changes we found in our fMRI analysis correspond well with previous findings showing that acupuncture stimulation modulates activity and connectivity of somatosensory as well as pain-related areas (especially insula cortex and S2). Recent neuroimaging studies that compared the stimulation of acupuncture points to control points revealed strengthened BOLD activation in somatosensory areas, the cingulum, the basal ganglia, the brainstem, the cerebellum, as well as the insula cortex. Besides these increases in BOLD activation, these studies also found pronounced acupuncture related deactivation of BOLD signaling in the amygdala, the hippocampus, and brain areas well described as hubs of the brain's default mode network (Dhond et al., 2007; Huang et al., 2012). These observations are in good agreement with the present findings since we also found acupuncture related deactivation in default mode network associated areas and higher BOLD activation in S2 and insula, which are well described as dominant hubs of the central nervous pain network (also known as pain matrix Apkarian et al., 2005; May, 2007). Furthermore, for ST36 as compared to the control points, we found a significantly deactivated right precuneus during stimulation. Although no voxels survived the conjunction analysis for the connectivity comparison of acupuncture point vs. control points, both comparisons (RS_ST36-RS_CP1 and RS_ST36-RS_CP2) showed increased connectivity between right precuneus and S2 in the follow-up resting-state scan. Whereas S2 and insula are assumed to contribute to the experience of pain (Craig, 2009), the precuneus seems to be involved in the assessment and integration of pain (Goffaux et al., 2014). Acupuncture related strengthened functional connectivity between S2 and precuneus might represent a possible mechanism that explains the pain relieving effectiveness of acupuncture, especially in chronic pain (Berman et al., 2010; Vickers et al., 2012). Additionally, our finding of an increased mu rhythm following stimulation of ST36 may represent another potential mechanisms of pain modulation, since an increased mu rhythm was previously shown to be associated with a pronounced cortical inhibition (Klimesch et al., 2007; Jensen and Mazaheri, 2010) and a reduced cortical excitability to painful stimulation (Ploner et al., 2006a). Further studies combining acupuncture with multimodal brain imaging are necessary

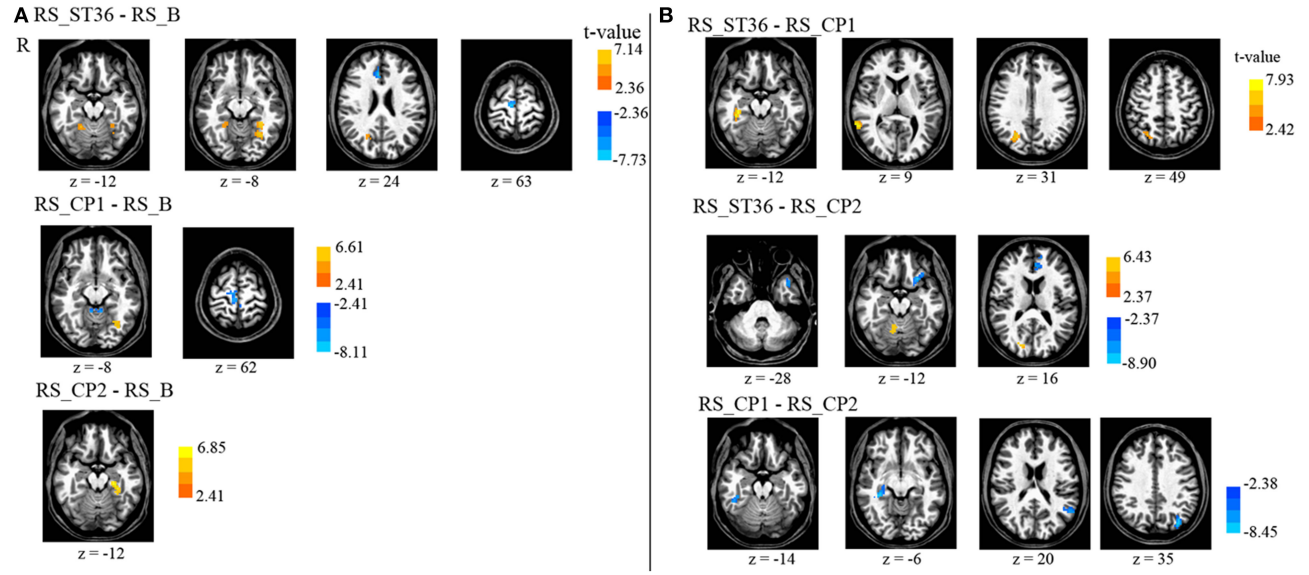

FIGURE 4 | Comparison of the seed-based somatosensory resting-state connectivity between all resting-state sessions ($P < 0.05$, corrected). (A) The comparison of post-stimulation resting-state scans with the baseline scan. **(B)** The comparison of the post-stimulation resting-state scans with each other. There is no cluster surviving the conjunction analyses across the first and second row (acupuncture vs. control points) as well as across the second and the third row (dermatome L5 vs. L2). R means right hemisphere. Talairach z coordinates are displayed. positive values: red, negative: blue.

to test these hypotheses in patients suffering from chronic pain.

Furthermore, we found a pronounced activation at right middle temporal gyrus and deactivation at left superior temporal gyrus during needle stimulation, which was also found by other studies that investigate acupuncture (Zhang et al., 2012; Kim et al., 2013). However, we found these effects only for the comparison between the different dermatomes (L2 and L5) when stimulating dermatome L5 (ST36 or CP1). These effects might hint toward a different sensitivity of the two different regions used for the needle stimulation, but still remain elusive.

In conclusion, our findings suggest that stimulation at acupuncture points may modulate somatosensory and saliency processing regions more readily than stimulation at non-acupuncture point locations. In addition, our results hint toward potential mechanisms of pain modulation due to acupuncture stimulation. Furthermore, our results might have an impact on experiments using conventional somatosensory stimulation protocols. For example, electrical stimulation applied to the median nerve or the finger might produce different imaging results when the stimulation electrodes are located near an acupuncture point. Further experiments using electrical acupuncture and EEG will assess if direct stimulation of acupuncture points also affects established EEG markers, such as evoked potentials or evoked and induced rhythmic activity.

FUNDING

This study had no additional funding. Wenjing Huang received a scholarship from the Carstens Foundation. Vitaly Napadow was supported by NCCAM, National Institutes of Health [R01-AT004714, R01-AT005280, P01-AT006663, R21-DK097499, R01-AT007550].

AUTHOR CONTRIBUTIONS

Conceived and designed the experiments: TN, WH, DP, CMW, AV, VN, FL. Performed the trial: TN, WH, DP. Analyzed the data: TN, XL, SR. Discussed the data: TN, WH, DP, XL, CMW, AV, VN, BP, SR, FL. Wrote the first draft of the paper: TN, DP, WH. Revised the paper and approved the final version: TN, WH, DP, CMW, AV, VN, SR, BP, FL.

ACKNOWLEDGMENTS

We thank Sylvia Stasch and Annett Wiedemann for their support. We also thank the reviewers' generous suggestions.

SUPPLEMENTARY MATERIAL

The Supplementary Material for this article can be found online at: http://www.frontiersin.org/journal/10.3389/fnhum.2015.00074/abstract

REFERENCES

Apkarian, A. V., Bushnell, M. C., Treede, R. D., and Zubieta, J. K. (2005). Human brain mechanisms of pain perception and regulation in health and disease. *Eur. J. Pain* 9, 463–484. doi: 10.1016/j.ejpain.2004.11.001

Bäcker, M., Hammes, M., Sander, D., Funke, D., Deppe, M., Tolle, T. R., et al. (2004). Changes of cerebrovascular response to visual stimulation in migraineurs after repetitive sessions of somatosensory stimulation (acupuncture): a pilot study. *Headache* 44, 95–101. doi: 10.1111/j.1526-4610.2004.04017.x

Bandettini, P. A., Wong, E. C., Hinks, R. S., Tikofsky, R. S., and Hyde, J. S. (1992). Time course EPI of human brain function during task activation. *Magn. Reson. Med.* 25, 390–397.

Behzadi, Y., Restom, K., Liau, J., and Liu, T. T. (2007). A component based noise correction method (CompCor) for BOLD and perfusion based fMRI. *Neuroimage* 37, 90–101. doi: 10.1016/j.neuroimage.2007.04.042

Berman, B. M., Langevin, H. M., Witt, C. M., and Dubner, R. (2010). Acupuncture for chronic low back pain. *New Engl. J. Med.* 363, 454–461. doi: 10.1056/NEJMct0806114

Brinkhaus, B., Becker-Witt, C., Jena, S., Linde, K., Streng, A., Wagenpfeil, S., et al. (2003). Acupuncture Randomized Trials (ART) in patients with chronic low back pain and osteoarthritis of the knee - design and protocols. *Forsch. Komplementarmed. Klass. Naturheilkd.* 10, 185–191. doi: 10.1159/000073474

Cox, R. W. (1996). AFNI: software for analysis and visualization of functional magnetic resonance neuroimages. *Comput. Biomed. Res.* 29, 162–173.

Craig, A. D. (2009). How do you feel–now? The anterior insula and human awareness. *Nat. Rev. Neurosci.* 10, 59–70. doi: 10.1038/nrn2555

Dhond, R. P., Kettner, N., and Napadow, V. (2007). Neuroimaging acupuncture effects in the human brain. *J. Altern. Complement. Med.* 13, 603–616. doi: 10.1089/acm.2007.7040

Dhond, R. P., Yeh, C., Park, K., Kettner, N., and Napadow, V. (2008). Acupuncture modulates resting state connectivity in default and sensorimotor brain networks. *Pain* 136, 407–418. doi: 10.1016/j.pain.2008.01.011

Diener, H. C., Kronfeld, K., Boewing, G., Lungenhausen, M., Maier, C., Molsberger, A., et al. (2006). Efficacy of acupuncture for the prophylaxis of migraine: a multicentre randomised controlled clinical trial. *Lancet Neurol.* 5, 310–316. doi: 10.1016/S1474-4422(06)70382-9

Drake, R., Vogl, A. W., and Mitchell, A. W. (2009). *Gray's Anatomy For Students.* London: Elsevier Health Sciences.

Fox, M. D., Snyder, A. Z., Vincent, J. L., Corbetta, M., Van Essen, D. C., and Raichle, M. E. (2005). The human brain is intrinsically organized into dynamic, anticorrelated functional networks. *Proc. Natl. Acad. Sci. U.S.A.* 102, 9673–9678. doi: 10.1073/pnas.0504136102

Frahm, J., Bruhn, H., Merboldt, K. D., and Hanicke, W. (1992). Dynamic MR imaging of human brain oxygenation during rest and photic stimulation. *J. Magn. Reson. Imaging* 2, 501–505.

Gastaut, H. (1952). Électrocorticographique de la Réactivité des Rhythmes Rolandiques. *Rev. Neurol. Paris* 87, 176–182.

Goffaux, P., Girard-Tremblay, L., Marchand, S., Daigle, K., and Whittingstall, K. (2014). Individual differences in pain sensitivity vary as a function of precuneus reactivity. *Brain Topogr.* 27, 366–374. doi: 10.1007/s10548-013-0291-0

Greicius, M. D., Flores, B. H., Menon, V., Glover, G. H., Solvason, H. B., Kenna, H., et al. (2007). Resting-state functional connectivity in major depression: abnormally increased contributions from subgenual cingulate cortex and thalamus. *Biol. Psychiatry* 62, 429–437. doi: 10.1016/j.biopsych.2006.09.020

Hori, E., Takamoto, K., Urakawa, S., Ono, T., and Nishijo, H. (2010). Effects of acupuncture on the brain hemodynamics. *Auton. Neurosci.* 157, 74–80. doi: 10.1016/j.autneu.2010.06.007

Huang, W., Pach, D., Napadow, V., Park, K., Long, X., Neumann, J., et al. (2012). Characterizing acupuncture stimuli using brain imaging with FMRI–a systematic review and meta-analysis of the literature. *PLoS ONE* 7:e32960. doi: 10.1371/journal.pone.0032960

Hui, K. K., Liu, J., Makris, N., Gollub, R. L., Chen, A. J., Moore, C. I., et al. (2000). Acupuncture modulates the limbic system and subcortical gray structures of the human brain: evidence from fMRI studies in normal subjects. *Hum. Brain Mapp.* 9, 13–25. doi: 10.1002/(SICI)1097-0193(2000)9:1%3C13::AID-HBM2%3E3.0.CO;2-F

Jensen, O., and Mazaheri, A. (2010). Shaping functional architecture by oscillatory alpha activity: gating by inhibition. *Front. Hum. Neurosci.* 4:186. doi: 10.3389/fnhum.2010.00186

Kim, N. H., Cho, S. Y., Jahng, G. H., Ryu, C. W., Park, S. U., Ko, C. N., et al. (2013). Differential localization of pain-related and pain-unrelated neural responses for acupuncture at BL60 using BOLD fMRI. *Evid. Based Complement. Alternat. Med.* 2013:804696. doi: 10.1155/2013/804696

Kleinhenz, J., Streitberger, K., Windeler, J., Gussbacher, A., Mavridis, G., and Martin, E. (1999). Randomised clinical trial comparing the effects of acupuncture and a newly designed placebo needle in rotator cuff tendinitis. *Pain* 83, 235–241.

Klimesch, W., Sauseng, P., and Hanslmayr, S. (2007). EEG alpha oscillations: the inhibition-timing hypothesis. *Brain Res. Rev.* 53, 63–88. doi: 10.1016/j.brainresrev.2006.06.003

Kong, J., Gollub, R., Huang, T., Polich, G., Napadow, V., Hui, K., et al. (2007). Acupuncture de qi, from qualitative history to quantitative measurement. *J. Altern. Complement. Med.* 13, 1059–1070. doi: 10.1089/acm.2007.0524

Kuhlman, W. N. (1978). Functional topography of the human mu rhythm. *Electroencephalogr. Clin. Neurophysiol.* 44, 83–93.

Kurth, R., Villringer, K., Curio, G., Wolf, K. J., Krause, T., Repenthin, J., et al. (2000). fMRI shows multiple somatotopic digit representations in human primary somatosensory cortex. *Neuroreport* 11, 1487–1491. doi: 10.1097/00001756-200005150-00025

Kwong, K. K., Belliveau, J. W., Chesler, D. A., Goldberg, I. E., Weisskoff, R. M., Poncelet, B. P., et al. (1992). Dynamic magnetic resonance imaging of human brain activity during primary sensory stimulation. *Proc. Natl. Acad. Sci. U.S.A.* 89, 5675–5679.

Linde, K., Streng, A., Hoppe, A., Brinkhaus, B., Becker-Witt, C., Hammes, M., et al. (2006). Treatment in a randomized multicenter trial of acupuncture for migraine (ART Migraine). *Forsch. Komplementärmed* 13, 101–108. doi: 10.1159/000091999

Ma, T. T., Yu, S. Y., Li, Y., Liang, F. R., Tian, X. P., Zheng, H., et al. (2012). Randomised clinical trial: an assessment of acupuncture on specific meridian or specific acupoint vs. sham acupuncture for treating functional dyspepsia. *Aliment. Pharmacol. Ther.* 35, 552–561. doi: 10.1111/j.1365-2036.2011.04979.x

May, A. (2007). Neuroimaging: visualising the brain in pain. *Neurol. Sci.* 28(Suppl. 2), S101–S107. doi: 10.1007/s10072-007-0760-x

Melchart, D., Streng, A., Hoppe, A., Brinkhaus, B., Witt, C., Wagenpfeil, S., et al. (2005). Acupuncture in patients with tension-type headache: randomised controlled trial. *BMJ* 331, 376–382. doi: 10.1136/bmj.38512.405440.8F

Napadow, V., Dhond, R., Park, K., Kim, J., Makris, N., Kwong, K. K., et al. (2009). Time-variant fMRI activity in the brainstem and higher structures in response to acupuncture. *Neuroimage* 47, 289–301. doi: 10.1016/j.neuroimage.2009.03.060

Napadow, V., Lee, J., Kim, J., Cina, S., Maeda, Y., Barbieri, R., et al. (2012). Brain correlates of phasic autonomic response to acupuncture stimulation: an event-related fMRI study. *Hum. Brain Mapp.* 34, 2592–2606. doi: 10.1002/hbm.22091

Neuper, C., Wortz, M., and Pfurtscheller, G. (2006). ERD/ERS patterns reflecting sensorimotor activation and deactivation. *Prog. Brain Res.* 159, 211–222. doi: 10.1016/S0079-6123(06)59014-4

Ogawa, S., Tank, D. W., Menon, R., Ellermann, J. M., Kim, S. G., Merkle, H., et al. (1992). Intrinsic signal changes accompanying sensory stimulation: functional brain mapping with magnetic resonance imaging. *Proc. Natl. Acad. Sci. U.S.A.* 89, 5951–5955.

Oldfield, R. C. (1971). The assessment and analysis of handedness: the Edinburgh inventory. *Neuropsychologia* 9, 97–113.

Ploner, M., Gross, J., Timmermann, L., Pollok, B., and Schnitzler, A. (2006a). Oscillatory activity reflects the excitability of the human somatosensory system. *Neuroimage* 32, 1231–1236. doi: 10.1016/j.neuroimage.2006.06.004

Ploner, M., Gross, J., Timmermann, L., Pollok, B., and Schnitzler, A. (2006b). Pain suppresses spontaneous brain rhythms. *Cereb. Cortex* 16, 537–540. doi: 10.1093/cercor/bhj001

Ritter, P., Moosmann, M., and Villringer, A. (2009). Rolandic alpha and beta EEG rhythms' strengths are inversely related to fMRI-BOLD signal in primary somatosensory and motor cortex. *Hum. Brain Mapp.* 30, 1168–1187. doi: 10.1002/hbm.20585

Ruben, J., Schwiemann, J., Deuchert, M., Meyer, R., Krause, T., Curio, G., et al. (2001). Somatotopic organization of human secondary somatosensory cortex. *Cereb. Cortex* 11, 463–473. doi: 10.1093/cercor/11.5.463

Salmelin, R., and Hari, R. (1994). Spatiotemporal characteristics of sensorimotor neuromagnetic rhythms related to thumb movement. *Neuroscience* 60, 537–550. doi: 10.1016/0306-4522(94)90263-1

Sanchez-Araujo, M. (1998). Does the choice of placebo determine the results of clinical studies on acupuncture? *Forsch. Komplementarmed.* 5, 8–11.

Stancak, A. (2006). Cortical oscillatory changes occurring during somatosensory and thermal stimulation. *Prog. Brain Res.* 159, 237–252. doi: 10.1016/S0079-6123(06)59016-8

Streitberger, K., Steppan, J., Maier, C., Hill, H., Backs, J., and Plaschke, K. (2008). Effects of verum acupuncture compared to placebo acupuncture on quantitative EEG and heart rate variability in healthy volunteers. *J. Altern. Complement. Med.* 14, 505–513. doi: 10.1089/acm.2007.0552

Vickers, A. J., Cronin, A. M., Maschino, A. C., Lewith, G., Macpherson, H., Foster, N. E., et al. (2012). Acupuncture for chronic pain: individual patient data meta-analysis. *Arch. Int. Med.* 1–10. doi: 10.1001/archinternmed.2012.3654

Wagner, T., Valero-Cabre, A., and Pascual-Leone, A. (2007). Noninvasive human brain stimulation. *Annu. Rev. Biomed. Eng.* 9, 527–565. doi: 10.1146/annurev.bioeng.9.061206.133100

Who Regional Office for the Western Pacific. (2008). *WHO Standard Acupuncture Point Locations in the Western Pacific Region.* Manila: World Health Organization.

Yan, Z. (2006). *Anatomy of Acupuncture Points and Clinical Applications.* Shanghai: Publishing House of Shanghai University of TCM.

Yang, X., Li, Y., Tian, X., and Liang, F. (2009). Locations and evaluations of non-acupuncture points in acupuncture studys from China and Abroad. *J. Tradit. Chin. Med.* 50, 748–750.

Zhang, Y., Glielmi, C. B., Jiang, Y., Wang, J., Wang, X., Fang, J., et al. (2012). Simultaneous CBF and BOLD mapping of high frequency acupuncture induced brain activity. *Neurosci. Lett.* 530, 12–17. doi: 10.1016/j.neulet.2012.09.050

Conflict of Interest Statement: The authors declare that the research was conducted in the absence of any commercial or financial relationships that could be construed as a potential conflict of interest.

Received: 25 July 2014; accepted: 29 January 2015; published online: 13 February 2015.
Citation: Nierhaus T, Pach D, Huang W, Long X, Napadow V, Roll S, Liang F, Pleger B, Villringer A and Witt CM (2015) Differential cerebral response to somatosensory stimulation of an acupuncture point vs. two non-acupuncture points measured with EEG and fMRI. Front. Hum. Neurosci. ***9****:74. doi: 10.3389/fnhum.2015.00074*
This article was submitted to the journal Frontiers in Human Neuroscience.

Publication 3: Long X*, Huang W*, Napadow V, Liang F, Pleger B, Villringer A, Witt CM, Nierhaus T, Pach D. Sustained effects of acupuncture stimulation investigated with centrality mapping analysis. *Frontiers in human neuroscience.* 2016;10:510. (*equal contribution)

frontiers in Human Neuroscience

ORIGINAL RESEARCH
published: 18 October 2016
doi: 10.3389/fnhum.2016.00510

Sustained Effects of Acupuncture Stimulation Investigated with Centrality Mapping Analysis

Xiangyu Long[1†], Wenjing Huang[2,3†], Vitaly Napadow[4,5], Fanrong Liang[3], Burkhard Pleger[1], Arno Villringer[1,6], Claudia M. Witt[2,7], Till Nierhaus[1,6,8†] and Daniel Pach[2*†]*

[1] Department of Neurology, Max Planck Institute for Human Cognitive and Brain Sciences, Leipzig, Germany, [2] Institute for Social Medicine, Epidemiology, and Health Economics, Charité – Universitätsmedizin Berlin, Berlin, Germany, [3] Acupuncture and Tuina School, The 3rd Teaching Hospital, Chengdu University of Traditional Chinese Medicine, Chengdu, China, [4] Athinoula A. Martinos Center for Biomedical Imaging, Department of Radiology, Massachusetts General Hospital, Charlestown, MA, USA, [5] Department of Radiology, Logan University, Chesterfield, MO, USA, [6] The Mind-Brain Institute at Berlin School of Mind and Brain, Charité and Humboldt-Universität, Berlin, Germany, [7] Institute for Complementary and Integrative Medicine, University of Zurich and University Hospital Zurich, Zurich, Switzerland, [8] Neurocomputation and Neuroimaging Unit, Department of Education and Psychology, Freie Universität Berlin, Berlin, Germany

OPEN ACCESS

Edited by:
Srikantan S. Nagarajan, University of California, San Francisco, USA

Reviewed by:
Arun Bokde, Trinity College, Dublin, Ireland
Xin Di, New Jersey Institute of Technology, USA

***Correspondence:**
Daniel Pach
daniel.pach@charite.de
Till Nierhaus
till.nierhaus@fu-berlin.de

[†] These authors have contributed equally to this work.

Received: *02 June 2016*
Accepted: *27 September 2016*
Published: *18 October 2016*

Citation:
Long X, Huang W, Napadow V, Liang F, Pleger B, Villringer A, Witt CM, Nierhaus T and Pach D (2016) Sustained Effects of Acupuncture Stimulation Investigated with Centrality Mapping Analysis. Front. Hum. Neurosci. 10:510. doi: 10.3389/fnhum.2016.00510

Acupuncture can have instant and sustained effects, however, its mechanisms of action are still unclear. Here, we investigated the sustained effect of acupuncture by evaluating centrality changes in resting-state functional magnetic resonance imaging after manually stimulating the acupuncture point ST36 at the lower leg or two control point locations (CP1 same dermatome, CP2 different dermatome). Data from a previously published experiment evaluating instant BOLD effects and S2-seed-based resting state connectivity was re-analyzed using eigenvector centrality mapping and degree centrality mapping. These data-driven methods might add new insights into sustained acupuncture effects on both global and local inter-region connectivity (centrality) by evaluating the summary of connections of every voxel. We found higher centrality in parahippocampal gyrus and middle temporal gyrus after ST36 stimulation in comparison to the two control points. These regions are positively correlated to major hubs of the default mode network, which might be the primary network affected by chronic pain. The stronger integration of both regions within the whole-brain connectome after stimulation of ST36 might be a potential contributor to pain modulation by acupuncture. These findings highlight centrality mapping as a valuable analysis for future imaging studies investigating clinically relevant outcomes associated with physiological response to acupuncture stimulation. Clinical trial registration: NCT01079689, ClinicalTrials.gov.

Keywords: resting-state fMRI, acupuncture, functional connectivity, centrality, pain

INTRODUCTION

The time-variant characteristic of acupuncture includes instant effects as well as sustained effects (Li et al., 2007), which may contribute both to a successful treatment. Clinical reports (Vickers, 2004; Melchart et al., 2005; Li et al., 2012; Ma et al., 2012) and systematic reviews (White et al., 2007; Linde et al., 2009) have provided evidence that the acupuncture effect can last far beyond

its application. Also, studies using animal models found that there are sustained effects which might accumulate at a certain intensity of stimulation (Han, 1994; Liang et al., 2001; Huang, 2006). Over the last decade, an increasing number of studies on acupuncture using functional magnetic resonance imaging (fMRI) has explored instant effects with blood oxygenation level-dependent (BOLD) signal changes and sustained effects with resting-state network modulations (Qin et al., 2006, 2008; Dhond et al., 2007, 2008; Bai et al., 2009; Feng et al., 2011; Huang et al., 2012; Zhong et al., 2012; Jiang et al., 2013; You et al., 2013; Nierhaus et al., 2015). Common approaches for the analysis of resting-state fMRI data are seed-based correlation analysis and spatial independent component analysis (ICA). Dhond et al. (2008) used ICA on resting-state data and reported that the acupuncture point stimulation increased functional connectivity of the default mode network (DMN) to pain, affective and memory related regions, and also increased sensorimotor network (SMN) connectivity to pain-related brain regions. Qin et al. (2008) used seed-based correlation analysis to identify the amygdala-related network both after real and penetrating sham acupuncture. However, both methods are limited by *a priori* definitions of a "seed" or a "component of interest" for the analysis, thus, interesting associations may have been overlooked.

Recently, the functional connectome of the human brain has attracted increasing interest and graph theory based investigation of "network hubs" or functional structure property has been successfully implemented in several neuroimaging studies (Lohmann et al., 2010; Taubert et al., 2011). However, to our knowledge only a few studies have used this approach to explore the modulation of the entire brain's functional connectome after acupuncture stimulation (Liu et al., 2010, 2011). Centrality mapping is a graph theory based connectivity analysis, which can be used to characterize one aspect of the whole-brain functional connectome. Independent of assumptions, every voxel is considered as a "seed" (node) and its connectivity to all other voxels is estimated. Based on this, a centrality value is determined that describes the impact of each voxel within the whole brain network. Thus, centrality mapping is a data driven approach that summarizes the connectome information for each voxel (Zuo et al., 2012).

We previously investigated instant acupuncture effects based on BOLD data derived from an event-related needle stimulation, as well as sustained effects using seed-based resting state connectivity (Nierhaus et al., 2015). Cerebral responses were evaluated after standardized needle stimulation on three different point locations on the right leg: one acupuncture point ST36 and two control points which are not acupuncture points. One of the control points was nearby ST36 in the same dermatome L5 (CP1), while the other was in a different dermatome L2 (CP2). Compared to control point stimulation, we found more pronounced activations in insula and secondary somatosensory cortex (S2), as well as a deactivation in precuneus during stimulation of ST36. In addition, S2 seed-based functional connectivity analysis showed increased connectivity of S2 to right precuneus after stimulation of ST36. These regions are well known pain-related areas and hint to a potential mechanism of pain modulation due to ST36 acupuncture stimulation (Nierhaus et al., 2015). However, the seed-based approach describes only the connectivity of one pre-defined region.

For this study, we re-analyzed the resting-state data with two centrality mapping analyses: degree centrality mapping (DCM) and eigenvector centrality mapping (ECM). While DCM is simply the sum of connectivity strength between all pairs of nodes (voxels), ECM uses the first eigenvector of the correlation matrix as the weight to summarize the connections of every voxel. Hence, DCM can be defined as the number of links which a node has, while ECM measures the influence of a node within a network [favors nodes that are connected to nodes that are themselves central within the network (Lohmann et al., 2010)]. A well-known example of an ECM application is Google's PageRank algorithm. Thus, DCM measures more local centrality and ECM measures more global centrality (Zuo et al., 2012). Both DCM and ECM have been implemented in previous fMRI studies and significant as well as meaningful differences between different brain states or participants have been reported (Buckner et al., 2009; Lohmann et al., 2010; Fransson et al., 2011; Taubert et al., 2011). Based on our prior results, we wanted to evaluate whether these two centrality approaches also show differences when comparing needle stimulation at an acupuncture point with stimulation at two non-acupuncture control points.

MATERIALS AND METHODS

Subjects

Twenty-two healthy subjects (11 male, mean age 26 years, range 21–32 years, right-handed) participated in the fMRI measurement as described in Nierhaus et al. (2015). Participants had no medical knowledge about acupuncture and all except one had never been treated with acupuncture before the study. The original study consisted of an EEG and an fMRI experiment. Eight subjects participated in both EEG and fMRI, thus were not completely naïve to acupuncture when performing the fMRI measurement. Participants were informed about the needle stimulation as follows: "...one acupuncture needle will be inserted in the muscle at three different points at the upper and lower leg...." All participants were right-handed and gave written informed consent to participate in the experiment according to the declaration of Helsinki. The ethics committee of Leipzig University approved the study (Nr. 214-09-28092009) and we registered the study at ClinicalTrials.gov (NCT01079689). Prior to participation, all subjects underwent a comprehensive neurological examination and confirmed they were not taking any acute or chronic medication. One female subject was excluded from the measurements because of vegetative side effects (severe sweating) during the stimulation on the acupuncture point.

Experimental Procedure

Subjects were scanned and received the needle stimulation at the three points within one session. The acupuncture point was ST36 (Zusanli). Control point 1 (CP1) was in the same dermatome L5 as ST36, and control point 2 (CP2) was in the (different)

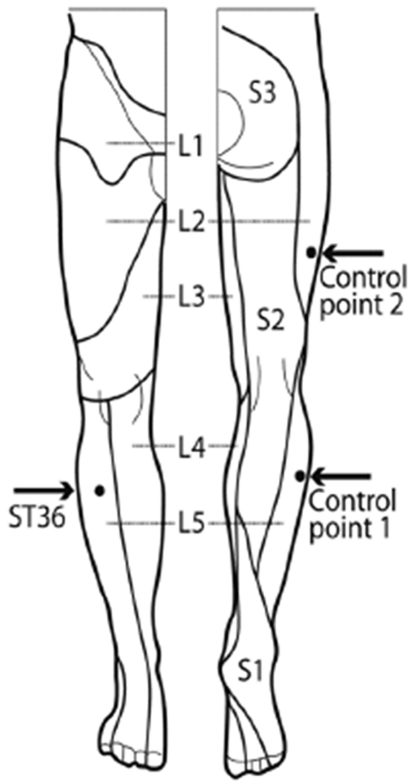

FIGURE 1 | Locations of acupuncture point ST36 and the control points on the right leg [view from the front and from the back, figure adapted (Drake et al., 2009)]. ST36 is located on the anterior aspect of the right leg, on the line connecting ST35 with ST41, 3 B-cun inferior to ST35. The location of ST36 belongs to the dermatome L5. Control point 1 (CP1) is located lateral to ST36, at the middle line between Bladder meridian and Gallbladder meridian, in the same dermatome L5. Control point 2 (CP2) is located 2 B-cun dorsally of GB31, the location of CP2 belongs to the dermatome L2 (Nierhaus et al., 2015).

dermatome L2 (**Figure 1**). The locations for the control points were carefully chosen after literature screening and a consensus process between one of the authors (FL) and a second expert of the Chengdu University of TCM (Prof Li Ying). The rational of the point selection can be found in previous publications (Nierhaus et al., 2015, 2016; Wong, 2016).

The experimental paradigm is shown in **Figure 2**. One resting-state scan was performed at the beginning as the baseline scan (RS_B), then three scans with needle stimulation of one point in an event-related design, each followed by a 6 min' corresponding resting state scan (i.e., RS_ST36, RS_CP1, and RS_CP2). During scanning, subjects were told to remain in the supine position with open eyes and concentrate on the sensation caused by the needle stimulation. During the resting-state, participants were requested to keep calm and stay still with eyes open.

The penetrating needle stimulation was performed by an acupuncture physician with sterile, single use, individually wrapped needles (0.20 mm × 30 mm; titanium, DongBang, Acupuncture, Inc., Boryeong, Korea). The needle was first inserted 1–2 cm deep into the skin depending on the size of the muscle vertically on the right leg. Then the needle was manually manipulated according to the event-related design starting immediately after insertion. Auditory cues signaled the timing of the stimulation events to the acupuncturist via headphones. Each event consisted of 3 s stimulation from needle rotating 60–90/rpm and lift-thrusting 0.3–0.5 cm. The length of the inter-stimulus interval was randomized from 13 to 21 s. The needle was taken out after the 6 min event-related needle manipulation. Identical penetrating needle stimulation was performed on the three different point locations (**Figure 2**). The order of point locations was randomized.

Data Acquisition

Data was acquired using a 3T Siemens Verio MRI System (Siemens Medical, Erlangen, Germany) equipped for echo planar imaging with a 12-channel head coil. fMRI images were acquired using an EPI sequence (30 axial slices, in-plane resolution is 3 mm × 3 mm, slice thickness = 4 mm, flip angle = 90°, gap = 1 mm, repetition time = 2000 ms, echo time = 30 ms). A structural image was also acquired for each participant, using a T1-weighted MPRAGE sequence (repetition time = 1200 ms, echo time = 5.65 ms, and flip angle = 19°, with elliptical sampling of *k* space, giving a voxel size of 1 mm × 1 mm × 1 mm). The

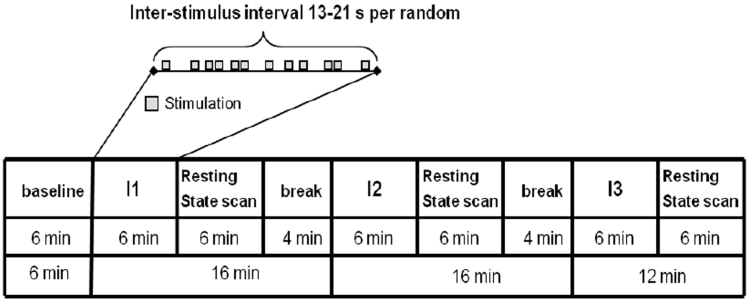

FIGURE 2 | The paradigm of the experiment included needle interventions and resting-state scans. The upper part represents the needle stimulation sequence. The lower part represents the whole run of the experiment. Four resting-state scans including one baseline resting-state scan and three scans after needle stimulation were performed. For the Interventions I1/I2/I3 the sequence of the stimulated points (ST36/CP1/CP2) was randomized across participants (Nierhaus et al., 2015).

subjects' heads were immobilized by cushioned supports and they wore earplugs to attenuate MRI gradient noise throughout the experiment.

Resting-State fMRI Data Analysis

The first ten volumes of each resting-state scan (RS_B, RS_ST36, RS_CP1, and RS_CP2) were removed to account for adaptation of the participant to scanner noise and environment. Slice timing, head motion correction and spatial normalization to MNI152 space were performed by SPM8[1]. T1 images were segmented into gray matter, whiter matter and cerebral spinal fluid (CSF). For spatial normalization, the gray matter image was co-registered to the MNI152 template and a transformation matrix was created. The functional images were co-registered to the gray matter image, and then the transformation matrix was used for spatial normalization to the MNI152 space with the voxel size 3 mm × 3 mm × 3 mm. The differences of head motion across resting-state scans were examined by comparing the averaged frame-wise displacement (mean FD) using BRAMILA tools (Power et al., 2012)[2]. The toolbox REST[3] was used for temporal band-pass filtering (0.01–0.08 Hz) and removal of linear trends (Fox et al., 2009). The global mean signal was not regressed out since this step might affect the correlation between time courses (Buckner et al., 2009; Lohmann et al., 2010; Fransson et al., 2011; Taubert et al., 2011). DPABI toolbox (toolbox for Data Processing & Analysis of Brain Imaging[4]) was used to apply the CompCor method (Behzadi et al., 2007). This method applies the combined CSF/white matter mask on the resting-state data and performs a principal component analysis to extract associated variance. The first five principal components from the CompCor analysis and six head motion parameters from the motion correction were used as nuisance signals to regress out associated variance. No spatial smoothing was applied before the centrality analysis, as this could generate artificially high correlation coefficients (Zuo et al., 2012). A gray matter mask [around 39429 voxels, more details in Nierhaus et al. (2015)] derived from the segmented T1 images was used for the centrality analysis. For each individual resting-state scan, the eigenvector centrality map and degree centrality map was generated by fastECM, which provides a more efficient way to perform the centrality analysis without calculating the voxel-wise correlation matrix (Wink et al., 2012). Z-standard transform (i.e., for each voxel, subtract the mean value of the whole brain then divide by the standard deviation of the whole brain) and 6 mm FWHM smoothing were performed on the individual DCM and ECM maps (Zuo et al., 2012; Yan et al., 2013). A within subjects ANOVA on the ECM/DCM maps of all four resting-state scans as well as age and gender as covariates were performed. The comparisons to baseline (RS_ST36-RS_B, RS_CP1-RS_B, and RS_CP2-RS_B, see Supplementary Material), the inter-points comparisons (RS_ST36-RS_CP1, RS_ST36-RS_CP2, and RS_CP1-RS_CP2), and the conjunction maps were generated. Conjunction of "RS_ST36-RS_CP1 and RS_ST36-RS_CP2" was calculated to compare the acupuncture point and the control points, while conjunction of "RS_ST36-RS_CP2 and RS_CP1-RS_CP2" was calculated to compare the different dermatomes (L5 vs. L2). All statistical maps (i.e., T-map) were corrected for multiple comparison to the alpha-level $p_{corr} < 0.05$ using AlphaSim in AFNI [Version 16.2.12, (Cox, 1996)] as follows: (1) The smoothing parameters were estimated using the 3dFWHMx function on the 6 mm (FWHM) smoothed, pre-processed fMRI time courses and averaged across all participants' resting-state sessions; (2) These smoothing parameters, the voxel-level p-value ($p_{vox} < 0.01$), and the gray matter mask (39429 voxels) were used as the input for the 3dClustSim function, resulting in a cluster size of 2052 mm^3 to reach significance ($p_{corr} < 0.05$); (3) The combination of voxel-level p-value (<0.01) and cluster size (2052 mm^3) was then applied to threshold each statistical map. Regions which were detected in the conjunction analysis were selected as ROI. The average and standard error of mean (SEM) of the z-value within each ROI were calculated for each resting-state scan and both centrality approaches.

Dice's coefficient (DC, from 0 to 100%, with 100% meaning that two maps are completely overlapping with one another) was employed to estimate the overlap ratio between the corrected statistical maps of post-stimulation centrality of the two different centrality analyses (ECM vs. DCM) (Dice, 1945).

RESULTS

Head Motion

There was no significant difference in head motion (mean FD) across all three post-stimulation resting-state scans ($p = 0.7495$, one-way ANOVA). There was no significant difference between scans: RS_ST36 vs. RS_CP1, $p = 0.2610$; RS_ST36 vs. RS_CP2, $p = 0.5931$; RS_CP1 vs. RS_CP2, $p = 0.2429$.

Post-effects of Needle Stimulation of all Three Points against each Other

The comparison between ST36 and CP1 revealed higher centrality for ST36 in the right parahippocampal gyrus, bilateral posterior cingulate cortex/precuneus, lower centrality for ST36 in the left dorsolateral prefrontal cortex by both ECM and DCM analyses (**Table 1**, **Figure 3**). Lower centrality for ST36 in the right middle frontal cortex was only detected by DCM, and higher centrality in right middle temporal gyrus only by ECM.

Compared to CP2, ST36 showed higher centrality in the right parahippocampal gyrus, right sensorimotor cortex and right middle temporal gyrus, and lower centrality in cerebellum by ECM and DCM. Lower centrality for ST36 in the right inferior frontal gyrus and higher centrality for ST36 in the left sensorimotor cortex was only seen in ECM (**Table 1**, **Figure 3**).

There was no significant result in the comparison between CP1 and CP2 for both ECM and DCM analysis.

[1] www.fil.ion.ucl.ac.uk/spm/

[2] http://becs.aalto.fi/~eglerean/bramila.html

[3] www.restfmri.net

[4] http://rfmri.org/dpabi

TABLE 1 | Post-stimulation centrality changes of all three points against each other ($P < 0.05$, corrected) and the results of the conjunction analysis.

	Area	Left/ Right	BA	*x*, *y*, *z*	*T*-value	*p*-value	Volume (mm^3)
DCM							
RS_ST36-RS_CP1	Parahippocampal gyrus	R	30	28, −53, 1	4,35	4,25E-04	7344
	Posterior cingulate/Precuneus	L	31	−17, −64, 25	4,30	4,78E-04	4536
	Dorsolateral prefrontal cortex	R	6	39, 8, 41	−3,65	2,04E-03	2160
		L	10	−42, 45, 12	−3,87	1,24E-03	2133
RS_ST36- RS_CP2	Parahippocampal gyrus/Middle temporal gyrus	R	19	25, −44, −4	4,70	1,97E-04	5940
	Pre/Postcentral gyrus (M1/S1)	R	6	39, −11, 41	3,93	1,09E-03	2835
	Declive	R	/	19, −79, −20	−3,59	2,31E-03	2133
Conjunction	Parahippocampal gyrus	R	19	/	/	/	1026
ECM							
RS_ST36-RS_CP1	Parahippocampal gyrus	R	30	28, −53, 1	4,42	3,65E-04	11097
	Posterior cingulate/Precuneus	L	31	−17, −64, 25	4,19	6,09E-04	5670
	Dorsolateral prefrontal cortex	L	10	−42, 45, 12	−3,76	1,58E-03	2322
RS_ST36- RS_CP2	Parahippocampal gyrus/Middle temporal gyrus	R	19	25, −44, −4	5,12	7,78E-05	7317
	Declive	R	/	19, −79, −20	−3,92	1,11E-03	4077
	Pre/Postcentral gyrus (M1/S1)	R	6	39, −11, 41	4,12	7,10E-04	3537
		L	4	−34, −13, 46	3,99	9,58E-04	2970
	Orbital frontal cortex	R	45	47, 36, 1	−3,29	4,53E-03	2214
Conjunction	Parahippocampal gyrus	R	19	/	/	/	1296
	Middle temporal gyrus	R	37	/	/	/	1161

x, y, z is in Talairach space. Displayed are voxels of maximal significance. If the activated area crosses the midline, only the side of the highest value is displayed. T- and p-value is on the voxel-level. No significant result was found in the comparison between CP1 and CP2 for both ECM and DCM analysis.

Conjunction Analysis

In order to identify brain areas which were specifically modulated due to the acupuncture point and dermatome effect, respectively, we performed two conjunction analyses. The comparison of acupuncture point vs. control points (conjunction of RS_ST36-RS_CP1 and RS_ST36-RS_CP2) showed common positive differences (higher centrality for ST36) in parahippocampal gyrus by both ECM and DCM. Another common region with positive differences was found in middle temporal gyrus, but only by ECM (**Figure 3**). Comparing the effects after stimulation in two different dermatomes L5 and L2 (conjunction of RS_ST36-RS_CP2 and RS_CP1-RS_CP2) revealed no overlapping regions with common differences in centrality.

The mean values for the ROIs selected from the conjunction analysis are shown in **Figure 3**. PHG showed significantly higher centrality for RS_ST36, in contrast to lower centrality for the other three resting-state scans (baseline and the two control points) in both, ECM and DCM. The cluster in middle temporal gyrus (only for ECM) also showed higher centrality for RS_ST36.

Dice Coefficient Analysis

The overlap of two different methods was also calculated (**Table 2**). DCM and ECM showed an overlap of 76.62 and 69.80% for the point comparisons RS_ST36-RS_CP1 and RS_ST36-RS_CP2, respectively. The overlap for the baseline comparisons is shown in the Supplementary Material.

DISCUSSION

We applied centrality mapping analysis to previously published data from an acupuncture neuroimaging study (Nierhaus et al., 2015). Employing different types of analyses, we evaluated instant and sustained acupuncture effects after event-related needle stimulation on one acupuncture point (ST36) in comparison to needle stimulation of two control points (non-acupuncture points, CP1 in the same dermatome, CP2 in a different dermatome). While in our previous analysis, we had evaluated instant BOLD effects and S2-seed-based resting state connectivity (Nierhaus et al., 2015), here, we used ECM and DCM to add new insights in the sustained acupuncture effect on both global and local connectivity (centrality) within the whole-brain.

To identify centrality differences between stimulation at ST36 and both control points, we performed a conjunction analysis of the point comparisons between ST36-CP1 and ST36-CP2, and we furthermore performed a conjunction analysis of the point comparisons between CP2-CP1 and CP2-ST36. If the main differential effects of the three stimulation sites are due to the different dermatomes then one would expect a strong discriminating effect of CP2 when comparing it to the two other sites. If the main differential effects, however, are due to stimulating the acupuncture point, one would expect the strongest discriminating effect when comparing ST36 to the other two stimulation sites. Our results demonstrate that the latter was the case: The conjunction ST36-CP1/ST36-CP2 showed overlapping clusters of increased centrality for ST36 in

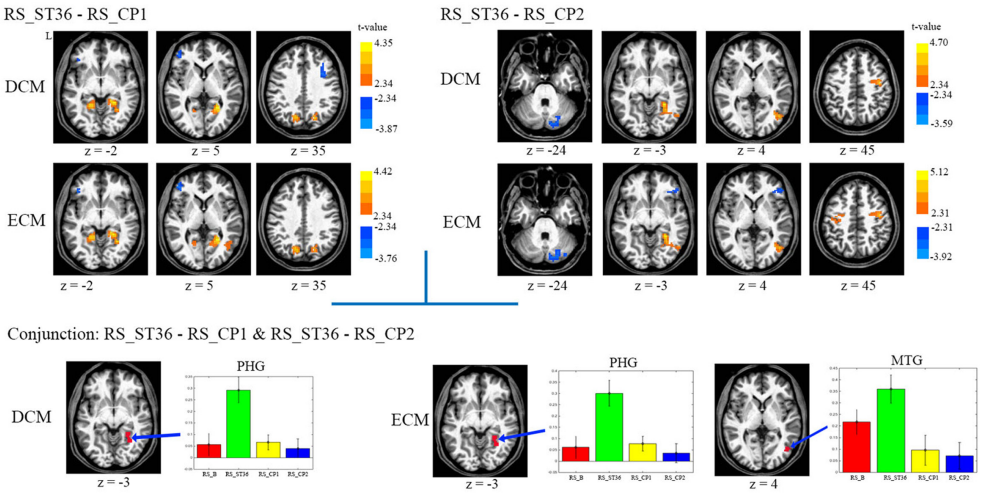

FIGURE 3 | The centrality changes of the post-stimulation of all three points against each other. L means the left hemisphere. The warm color means increased centrality and the cold color means decreased centrality. All images were in the Talairach space. $P < 0.05$, corrected. The average centrality value (mean ± SEM) of the related centrality measures from each resting-state scan within the selected ROIs which were detected in the conjunction analysis were displayed. No significant result was found in the comparison between CP1 and CP2 for both ECM and DCM analysis. Abbreviations: PHG, parahippocampus gyrus; MTG, middle temporal gyrus.

right parahippocampal gyrus, by both DCM and ECM. This conjunction analysis also showed a common cluster of increased centrality for ST36 in right middle temporal gyrus, but only in the ECM analysis. We performed no conjunction for the dermatome comparison (CP2 vs. ST36 and CP2 vs. CP1), because already the control point comparison (CP1 vs. CP2) showed no significant clusters. Thus, in accordance with our previous analysis (Nierhaus et al., 2015), these results suggest differential processing of acupuncture point stimulation compared to stimulation of non-acupuncture control points, now from the perspective of the whole-brain network. Parahippocampal gyrus and middle temporal gyrus might be important hubs affected by stimulation of an acupuncture point and these results provide further hints toward potential mechanisms of pain modulation by acupuncture stimulation.

Previous studies already indicated that parahippocampal gyrus might contribute to the effect of acupuncture of an acupuncture point (Huang et al., 2012; Chae et al., 2013). The BOLD signal in parahippocampal gyrus was found mainly deactivated during acupuncture stimulation in several previous neuroimaging studies (Wu et al., 1999, 2002; Hui et al., 2005; Napadow et al., 2005; Yan et al., 2005; Wang et al., 2007; Fang et al., 2009), and also in our previous analysis for all three points during stimulation (Nierhaus et al., 2015). Deactivation in parahippocampal gyrus was found to be related to acupuncture sensation, such as pressure, numbness, heaviness, and fullness (Wang et al., 2013). According to Jiang et al. (2014) the level of cerebral blood flow in parahippocampal gyrus is negatively correlated to analgesia after transcutaneous electric stimulation of an acupuncture point, suggesting acupuncture might inhibit pain by inhibiting the pain signal in the parahippocampal gyrus at a later stage. Moreover, recent research found that parahippocampal gyrus is related to the experience of chronic pain and anxiety, and structural changes in parahippocampal gyrus were found in chronic pain patients (Smallwood et al., 2013). When accompanying anxiety increases, the pain worsens, resulting in activation in parahippocampal gyrus (Ploghaus et al., 2001). In a study by Vachon-Presseau et al. (2013) chronic pain was associated with maladaptive stress and was reflected in hippocampal structural differences.

TABLE 2 | Dice coefficient analysis: Overlap ratio (percentage) of ECM and DCM results.

	All	Positive	Negative
RS_ST36-RS_CP1	76.72	80.87	58.78
RS_ST36-RS_CP2	69.80	76.94	50.64

Positive/negative means the positive/negative differences in the statistical maps.

Beside its participation in cognitive processes such as language and multimodal semantic processing (Tranel et al., 1997; Chao et al., 1999; Cabeza and Nyberg, 2000; Visser et al., 2012). Middle temporal gyrus has previously been shown to be related to pain and effects of acupuncture. Recent studies found significantly reduced gray matter volumes in middle temporal gyrus in chronic pain patients, e.g., lower back pain (Luchtmann et al., 2014), cluster headache (Absinta et al., 2012), migraine (Rocca et al., 2006), and cerebral post stroke pain (Krause et al., 2016). However, the role of middle temporal gyrus involved in chronic pain processing is still unclear (Krause et al., 2016). According to a study by Yan et al. (2005) the BOLD signal in middle temporal gyrus increased when acupuncture points were stimulated. Also in our previous analyses middle temporal gyrus was activated during stimulation, but for ST36 and CP1 in the same dermatome, whereas deactivated for CP2 in a more proximal different dermatome.

Moreover, both parahippocampal gyrus and middle temporal gyrus can be linked to the DMN (Greicius et al., 2003; Laird et al., 2009; Ward et al., 2014) (see also supplemental analysis). The DMN might be the primary network affected by chronic pain (Farmer et al., 2012; Baliki et al., 2014). Dhond et al. (2008) showed increased DMN connectivity with limbic antinociceptive (anterior cingulated cortex, periaqueductal gray), affective (amygdala, anterior cingulated cortex), and memory (hippocampal formation, middle temporal gyrus) related brain regions following acupuncture, but not sham. The DMN was deactivated during acupuncture stimulation (Bai et al., 2009; Napadow et al., 2013), but not when acupuncture was associated with sharp pain (Hui et al., 2009). For chronic pain conditions, such as chronic lower back pain and migraine, the pain relief was correlated with DMN alteration after acupuncture treatments (Li et al., 2014; Zhao et al., 2014). Also DMN modulation was found after acupuncture stimulation in mental disorders, e.g., major depressive disorder (Deng et al., 2016) and Alzheimer's disease (Liang et al., 2014). In another study parahippocampal gyrus was shown to be a connecting hub between the DMN and the temporal lobe memory system (Ward et al., 2014). Several studies show that the DMN activity/connectivity is related to memory-based processing (Buckner et al., 2008; Vatansever et al., 2015), and is modulated in the presence of pain, especially chronic pain (Baliki et al., 2014).

Together with our previous results (Nierhaus et al., 2015), our data point to a possible mechanism that explains the pain relieving effectiveness of acupuncture, especially in chronic pain: we found acupuncture related (i) activation of S2 and insula, which are assumed to contribute to the experience of pain (Craig, 2009), (ii) strengthened functional connectivity between S2 and precuneus which seems to be involved in the assessment and integration of pain (Goffaux et al., 2014), and (iii) increased whole brain functional connectivity in parahippocampal gyrus and middle temporal gyrus, which are both involved in DMN activity and might modulate the memory for pain.

Possible limitations of our study should be discussed: Regarding the experimental setup, we tried to come as close as possible to a double-blind study (Nierhaus et al., 2015) but of course the person applying the acupuncture stimulation knew about the "meaning" of the different points. Regarding data analysis, although the centrality mapping could give new insights into imaging data it can be limited by its voxel-wise temporal correlation analysis which may produce spurious correlations between voxels. For instance, a spurious correlation may be introduced between regions if this correlation is modulated by other regions. To avoid this, partial correlation analysis might be included into centrality mapping methods in future studies (Smith et al., 2011). Moreover, centrality mapping allows the characterization of only one aspect of the whole-brain functional connectome, i.e., the summary of connections of every voxel. For the broader picture, other graph theory based methods should be used in future research. Possible 'carry-over effects' between the different interventions might be an additional limitation. However, by randomizing the order of point locations all three interventions should be comparably affected by this phenomenon in our study. To avoid carry-over effects, the different interventions might be separated over a longer period of time, e.g., 24 h or even more. But the allocation of the different interventions to separate days would require a more complex experimental setup. Moreover, the duration of the sustained effect of acupuncture is not clear and our 6-min resting-state measurements might cover only its initial phase. Longer measurement periods would be necessary to cover long-term effects and to analyse the variation of functional connectivity in time.

To our knowledge, this is the first study applying ECM for the investigation of the sustained effect of acupuncture stimulation. Employing ECM and DCM, we investigated global and local functional connectivity of the acupuncture effect and compared both methods. As shown by a high Dice coefficient (around 75%) most of the results were similar between the ECM and the DCM analysis for all three stimulation points, maybe because the whole brain centrality intensity calculated by these two approaches are both highly positively correlated (Zuo et al., 2012). However, we found also differences when using the two approaches, e.g., the right frontal cortex was detected by DCM but not by ECM in the comparison between RS_ST36 and RS_CP1. Both methods' sensitivity seems to be different and the sensitivity might depend on the role of the respective brain areas within the whole-brain connectome (Gottlich et al., 2014). Previous studies (Liu et al., 2010, 2011; Ren et al., 2010; Fang et al., 2012) had applied graph theory analysis to investigate the post-needling resting state in healthy subjects. Ren et al. (2010) observed distinct signal changes in different brain regions within a group of ROIs between manual manipulations on three different acupuncture points by graph theory analysis. For the acupuncture point GB37 (located on the leg) they found PCC to show a larger degree of connectivity following stimulation. Liu et al. (2010, 2011) also used graph theory to investigate the whole-brain functional connectivity between identical manual stimulation on ST36 and one nearby control point. Significant degree differences were found in limbic areas, thalamus, brain stem, prefrontal cortices, temporal cortices, and cerebellum. Fang et al. (2012) measured local and distant degree centrality changes after electro-acupuncture stimulation on two acupuncture points separately, and found that ST36 led to stronger degree centrality changes than CV4 in the limbic-paralimbic-neocortical network. The analysis methods used in these studies are similar to DCM in our current study, however, the t-maps of them were all uncorrected. In our study, we additionally used ECM analysis, and all the t-maps were statistically corrected. Our findings correspond well with the significant differences between ST36 and control points that were already described by Liu et al. (2010, 2011) and Fang et al. (2012).

CONCLUSION

According to our data-driven methods, centrality changes in parahippocampal gyrus and middle temporal gyrus hint to possible specific differences of the sustained effect between the acupuncture point ST36 and two control points. The stronger

integration of parahippocampal gyrus and middle temporal gyrus within the whole-brain network after stimulation of an acupuncture point might be a potential contributor to pain modulation. We think both centrality mapping analysis ECM and DCM could be valuable data-driven tools with add-on value for future imaging studies investigating the effect of acupuncture.

AUTHOR CONTRIBUTIONS

Conceived and designed the experiments: TN, WH, DP, CW, AV, VN, and FL. Performed the trial: TN, WH, and DP. Analyzed the data: XL. Discussed the data: TN, WH, DP, XL, CW, AV, VN, BP, and FL. Wrote the first draft of the paper: XL, WH, TN, and DP. Revised the paper and approved the final version: TN, WH, DP, XL, CW, AV, VN, BP, and FL.

FUNDING

This study had no additional funding. WH received a scholarship from the Carstens Foundation. VN was supported by NCCAM, National Institutes of Health [R01-AT004714, R01-AT005280, P01-AT006663, R21-DK097499, and R01-AT007550].

ACKNOWLEDGMENT

We thank Annett Wiedemann and Prof. Li Ying for the support.

SUPPLEMENTARY MATERIAL

The Supplementary Material for this article can be found online at: http://journal.frontiersin.org/article/10.3389/fnhum.2016.00510

REFERENCES

Absinta, M., Rocca, M. A., Colombo, B., Falini, A., Comi, G., and Filippi, M. (2012). Selective decreased grey matter volume of the pain-matrix network in cluster headache. *Cephalalgia* 32, 109–115. doi: 10.1177/0333102411431334

Bai, L., Qin, W., Tian, J., Dong, M., Pan, X., Chen, P., et al. (2009). Acupuncture modulates spontaneous activities in the anticorrelated resting brain networks. *Brain Res.* 1279, 37–49. doi: 10.1016/j.brainres.2009.04.056

Baliki, M. N., Mansour, A. R., Baria, A. T., and Apkarian, A. V. (2014). Functional reorganization of the default mode network across chronic pain conditions. *PLoS ONE* 9:e106133. doi: 10.1371/journal.pone.0106133

Behzadi, Y., Restom, K., Liau, J., and Liu, T. T. (2007). A component based noise correction method (CompCor) for BOLD and perfusion based fMRI. *Neuroimage* 37, 90–101. doi: 10.1016/j.neuroimage.2007.04.042

Buckner, R. L., Andrews-Hanna, J. R., and Schacter, D. L. (2008). The brain's default network: anatomy, function, and relevance to disease. *Ann. N. Y. Acad. Sci.* 1124, 1–38. doi: 10.1196/annals.1440.011

Buckner, R. L., Sepulcre, J., Talukdar, T., Krienen, F. M., Liu, H., Hedden, T., et al. (2009). Cortical hubs revealed by intrinsic functional connectivity: mapping, assessment of stability, and relation to Alzheimer's disease. *J. Neurosci.* 29, 1860–1873. doi: 10.1523/JNEUROSCI.5062-08.2009

Cabeza, R., and Nyberg, L. (2000). Imaging cognition II: an empirical review of 275 PET and fMRI studies. *J. Cogn. Neurosci.* 12, 1–47. doi: 10.1162/08989290051137585

Chae, Y., Chang, D. S., Lee, S. H., Jung, W. M., Lee, I. S., Jackson, S., et al. (2013). Inserting needles into the body: a meta-analysis of brain activity associated with acupuncture needle stimulation. *J. Pain* 14, 215–222. doi: 10.1016/j.jpain.2012.11.011

Chao, L. L., Haxby, J. V., and Martin, A. (1999). Attribute-based neural substrates in temporal cortex for perceiving and knowing about objects. *Nat. Neurosci.* 2, 913–919. doi: 10.1038/13217

Cox, R. W. (1996). AFNI: software for analysis and visualization of functional magnetic resonance neuroimages. *Comput. Biomed. Res.* 29, 162–173. doi: 10.1006/cbmr.1996.0014

Craig, A. D. (2009). How do you feel–now? The anterior insula and human awareness. *Nat. Rev. Neurosci.* 10, 59–70. doi: 10.1038/nrn2555

Deng, D., Liao, H., Duan, G., Liu, Y., He, Q., Liu, H., et al. (2016). Modulation of the default mode network in first-episode, drug-naive major depressive disorder via acupuncture at Baihui (GV20) acupoint. *Front. Hum. Neurosci.* 10:230. doi: 10.3389/fnhum.2016.00230

Dhond, R. P., Kettner, N., and Napadow, V. (2007). Neuroimaging acupuncture effects in the human brain. *J. Altern. Complement. Med.* 13, 603–616. doi: 10.1089/acm.2007.7040

Dhond, R. P., Yeh, C., Park, K., Kettner, N., and Napadow, V. (2008). Acupuncture modulates resting state connectivity in default and sensorimotor brain networks. *Pain* 136, 407–418. doi: 10.1016/j.pain.2008.01.011

Dice, L. R. (1945). Measures of the amount of ecologic association between species. *Ecology* 26, 297–302. doi: 10.2307/1932409

Drake, R., Vogl, A. W., and Mitchell, A. W. M. (2009). *Gray's Anatomy for Students*. London: Elsevier Health Sciences.

Fang, J., Jin, Z., Wang, Y., Li, K., Kong, J., Nixon, E. E., et al. (2009). The salient characteristics of the central effects of acupuncture needling: limbic-paralimbic-neocortical network modulation. *Hum. Brain Mapp.* 30, 1196–1206. doi: 10.1002/hbm.20583

Fang, J. L., Wang, X. L., Wang, Y., Hong, Y., Liu, H. S., Liu, J., et al. (2012). [Comparison of brain effects of electroacupuncture at Zusanli (ST 36) and Guanyuan (CV 4) shown by fMRI in 21 healthy volunteers]. *Zhen Ci Yan Jiu* 37, 46–52.

Farmer, M. A., Baliki, M. N., and Apkarian, A. V. (2012). A dynamic network perspective of chronic pain. *Neurosci. Lett.* 520, 197–203. doi: 10.1016/j.neulet.2012.05.001

Feng, Y., Bai, L., Ren, Y., Wang, H., Liu, Z., Zhang, W., et al. (2011). Investigation of the large-scale functional brain networks modulated by acupuncture. *Magn. Reson. Imaging* 29, 958–965. doi: 10.1016/j.mri.2011.04.009

Fox, M. D., Zhang, D., Snyder, A. Z., and Raichle, M. E. (2009). The global signal and observed anticorrelated resting state brain networks. *J. Neurophysiol.* 101, 3270–3283. doi: 10.1152/jn.90777.2008

Fransson, P., Aden, U., Blennow, M., and Lagercrantz, H. (2011). The functional architecture of the infant brain as revealed by resting-state fMRI. *Cereb. Cortex* 21, 145–154. doi: 10.1093/cercor/bhq071

Goffaux, P., Girard-Tremblay, L., Marchand, S., Daigle, K., and Whittingstall, K. (2014). Individual differences in pain sensitivity vary as a function of precuneus reactivity. *Brain Topogr.* 27, 366–374. doi: 10.1007/s10548-013-0291-0

Gottlich, M., Kramer, U. M., Kordon, A., Hohagen, F., and Zurowski, B. (2014). Decreased limbic and increased fronto-parietal connectivity in unmedicated patients with obsessive-compulsive disorder. *Hum. Brain Mapp.* 35, 5617–5632. doi: 10.1002/hbm.22574

Greicius, M. D., Krasnow, B., Reiss, A. L., and Menon, V. (2003). Functional connectivity in the resting brain: a network analysis of the default mode hypothesis. *Proc. Natl. Acad. Sci. U.S.A.* 100, 253–258. doi: 10.1073/pnas.0135058100

Han, J. (1994). Some factors affecting acupuncture-indeced analgesia. *Acupunct. Res.* 1–3.

Huang, S. (2006). The aftereffect, tolerence and frequecy in acupuncture analgesia. *Chin. J. Pain Med.* 12, 360–362.

Huang, W., Pach, D., Napadow, V., Park, K., Long, X., Neumann, J., et al. (2012). Characterizing acupuncture stimuli using brain imaging with FMRI - a

systematic review and meta-analysis of the literature. *PLoS ONE* 7:e32960. doi: 10.1371/journal.pone.0032960

Hui, K. K., Liu, J., Marina, O., Napadow, V., Haselgrove, C., Kwong, K. K., et al. (2005). The integrated response of the human cerebro-cerebellar and limbic systems to acupuncture stimulation at ST 36 as evidenced by fMRI. *Neuroimage* 27, 479–496. doi: 10.1016/j.neuroimage.2005.04.037

Hui, K. K., Marina, O., Claunch, J. D., Nixon, E. E., Fang, J., Liu, J., et al. (2009). Acupuncture mobilizes the brain's default mode and its anti-correlated network in healthy subjects. *Brain Res.* 1287, 84–103. doi: 10.1016/j.brainres.2009.06.061

Jiang, Y., Liu, J., Liu, J., Han, J., Wang, X., and Cui, C. (2014). Cerebral blood flow-based evidence for mechanisms of low- versus high-frequency transcutaneous electric acupoint stimulation analgesia: a perfusion fMRI study in humans. *Neuroscience* 268, 180–193. doi: 10.1016/j.neuroscience.2014.03.019

Jiang, Y., Wang, H., Liu, Z., Dong, Y., Xiang, X., Bai, L., et al. (2013). Manipulation of and sustained effects on the human brain induced by different modalities of acupuncture: an FMRI study. *PLoS ONE* 8:e66815. doi: 10.1371/journal.pone.0066815

Krause, T., Asseyer, S., Taskin, B., Floel, A., Witte, A. V., Mueller, K., et al. (2016). The cortical signature of central poststroke pain: gray matter decreases in somatosensory, insular, and prefrontal cortices. *Cereb. Cortex* 26, 80–88. doi: 10.1093/cercor/bhu177

Laird, A. R., Eickhoff, S. B., Li, K., Robin, D. A., Glahn, D. C., and Fox, P. T. (2009). Investigating the functional heterogeneity of the default mode network using coordinate-based meta-analytic modeling. *J. Neurosci.* 29, 14496–14505. doi: 10.1523/JNEUROSCI.4004-09.2009

Li, J., Zhang, J. H., Yi, T., Tang, W. J., Wang, S. W., and Dong, J. C. (2014). Acupuncture treatment of chronic low back pain reverses an abnormal brain default mode network in correlation with clinical pain relief. *Acupunct. Med.* 32, 102–108. doi: 10.1136/acupmed-2013-010423

Li, Y., Zheng, H., Witt, C. M., Roll, S., Yu, S. G., Yan, J., et al. (2012). Acupuncture for migraine prophylaxis: a randomized controlled trial. *CMAJ* 184, 401–410. doi: 10.1503/cmaj.110551

Li, Z., Fang, J., Yi, S., and Guo, Y. (2007). *Experimental Acupuncture*. Beijing: China Press of Traditional Chinese Medicine.

Liang, F., Luo, R., Liu, Y., and Zhao, J. (2001). Experimental research of the relationship between analgesia aftereffect by electro-acupuncture and contents of 5-HT, NE, DA in inflamed area. *Chin. J. Basic Med. Tradit. Chin. Med.* 7, 52–55.

Liang, P., Wang, Z., Qian, T., and Li, K. (2014). Acupuncture stimulation of Taichong (Liv3) and Hegu (LI4) modulates the default mode network activity in alzheimer's disease. *Am. J. Alzheimers Dis. Other Demen.* 29, 739–748. doi: 10.1177/1533317514536600

Linde, K., Allais, G., Brinkhaus, B., Manheimer, E., Vickers, A., and White, A. R. (2009). Acupuncture for migraine prophylaxis. *Cochrane Database Syst. Rev.* 1:CD001218.

Liu, J., Qin, W., Guo, Q., Sun, J., Yuan, K., Dong, M., et al. (2011). Divergent neural processes specific to the acute and sustained phases of verum and SHAM acupuncture. *J. Magn. Reson. Imaging* 33, 33–40. doi: 10.1002/jmri.22393

Liu, J., Qin, W., Guo, Q., Sun, J., Yuan, K., Liu, P., et al. (2010). Distinct brain networks for time-varied characteristics of acupuncture. *Neurosci. Lett.* 468, 353–358. doi: 10.1016/j.neulet.2009.11.031

Lohmann, G., Margulies, D. S., Horstmann, A., Pleger, B., Lepsien, J., Goldhahn, D., et al. (2010). Eigenvector centrality mapping for analyzing connectivity patterns in fMRI data of the human brain. *PLoS ONE* 5:e10232. doi: 10.1371/journal.pone.0010232

Luchtmann, M., Steinecke, Y., Baecke, S., Lutzkendorf, R., Bernarding, J., Kohl, J., et al. (2014). Structural brain alterations in patients with lumbar disc herniation: a preliminary study. *PLoS ONE* 9:e90816. doi: 10.1371/journal.pone.0090816

Ma, T. T., Yu, S. Y., Li, Y., Liang, F. R., Tian, X. P., Zheng, H., et al. (2012). Randomised clinical trial: an assessment of acupuncture on specific meridian or specific acupoint vs. sham acupuncture for treating functional dyspepsia. *Aliment. Pharmacol. Ther.* 35, 552–561. doi: 10.1111/j.1365-2036.2011.04979.x

Melchart, D., Streng, A., Hoppe, A., Brinkhaus, B., Witt, C., Wagenpfeil, S., et al. (2005). Acupuncture in patients with tension-type headache: randomised controlled trial. *BMJ* 331, 376–382. doi: 10.1136/bmj.38512.405440.8F

Napadow, V., Lee, J., Kim, J., Cina, S., Maeda, Y., Barbieri, R., et al. (2013). Brain correlates of phasic autonomic response to acupuncture stimulation: an event-related fMRI study. *Hum. Brain Mapp.* 34, 2592–2606. doi: 10.1002/hbm.22091

Napadow, V., Makris, N., Liu, J., Kettner, N. W., Kwong, K. K., and Hui, K. K. (2005). Effects of electroacupuncture versus manual acupuncture on the human brain as measured by fMRI. *Hum. Brain Mapp.* 24, 193–205. doi: 10.1002/hbm.20081

Nierhaus, T., Pach, D., Huang, W., Long, X., Napadow, V., Roll, S., et al. (2015). Differential cerebral response to somatosensory stimulation of an acupuncture point versus two non-acupuncture points measured with EEG and fMRI. *Front. Hum. Neurosci.* 9:74. doi: 10.3389/fnhum.2015.00074

Nierhaus, T., Pach, D., Huang, W., Long, X., Napadow, V., Roll, S., et al. (2016). Difficulties choosing control points in acupuncture research. response: commentary: differential cerebral response, measured with both an EEG and fMRI, to somatosensory stimulation of a single acupuncture point vs. two non-acupuncture points. *Front. Hum. Neurosci.* 10:404. doi: 10.3389/fnhum.2016.00404

Ploghaus, A., Narain, C., Beckmann, C. F., Clare, S., Bantick, S., Wise, R., et al. (2001). Exacerbation of pain by anxiety is associated with activity in a hippocampal network. *J. Neurosci.* 21, 9896–9903.

Power, J. D., Barnes, K. A., Snyder, A. Z., Schlaggar, B. L., and Petersen, S. E. (2012). Spurious but systematic correlations in functional connectivity MRI networks arise from subject motion. *Neuroimage* 59, 2142–2154. doi: 10.1016/j.neuroimage.2011.10.018

Qin, W., Tian, J., Bai, L., Pan, X., Yang, L., Chen, P., et al. (2008). FMRI connectivity analysis of acupuncture effects on an amygdala-associated brain network. *Mol. Pain* 4:55. doi: 10.1186/1744-8069-4-55

Qin, W., Tian, J., Pan, X., Yang, L., and Zhen, Z. (2006). The correlated network of acupuncture effect: a functional connectivity study. *Conf. Proc. IEEE Eng. Med. Biol. Soc.* 1, 480–483.

Ren, Y., Bai, L., Feng, Y., Tian, J., and Li, K. (2010). Investigation of acupoint specificity by functional connectivity analysis based on graph theory. *Neurosci. Lett.* 482, 95–100. doi: 10.1016/j.neulet.2010.06.091

Rocca, M. A., Ceccarelli, A., Falini, A., Colombo, B., Tortorella, P., Bernasconi, L., et al. (2006). Brain gray matter changes in migraine patients with T2-visible lesions: a 3-T MRI study. *Stroke* 37, 1765–1770. doi: 10.1161/01.STR.0000226589.00599.4d

Smallwood, R. F., Laird, A. R., Ramage, A. E., Parkinson, A. L., Lewis, J., Clauw, D. J., et al. (2013). Structural brain anomalies and chronic pain: a quantitative meta-analysis of gray matter volume. *J. Pain* 14, 663–675. doi: 10.1016/j.jpain.2013.03.001

Smith, S. M., Miller, K. L., Salimi-Khorshidi, G., Webster, M., Beckmann, C. F., Nichols, T. E., et al. (2011). Network modelling methods for FMRI. *Neuroimage* 54, 875–891. doi: 10.1016/j.neuroimage.2010.08.063

Taubert, M., Lohmann, G., Margulies, D. S., Villringer, A., and Ragert, P. (2011). Long-term effects of motor training on resting-state networks and underlying brain structure. *Neuroimage* 57, 1492–1498. doi: 10.1016/j.neuroimage.2011.05.078

Tranel, D., Damasio, H., and Damasio, A. R. (1997). A neural basis for the retrieval of conceptual knowledge. *Neuropsychologia* 35, 1319–1327. doi: 10.1016/S0028-3932(97)00085-7

Vachon-Presseau, E., Roy, M., Martel, M. O., Caron, E., Marin, M. F., Chen, J., et al. (2013). The stress model of chronic pain: evidence from basal cortisol and hippocampal structure and function in humans. *Brain* 136, 815–827. doi: 10.1093/brain/aws371

Vatansever, D., Menon, D. K., Manktelow, A. E., Sahakian, B. J., and Stamatakis, E. A. (2015). Default mode dynamics for global functional integration. *J. Neurosci.* 35, 15254–15262. doi: 10.1523/JNEUROSCI.2135-15.2015

Vickers, A. J. (2004). Statistical reanalysis of four recent randomized trials of acupuncture for pain using analysis of covariance. *Clin. J. Pain* 20, 319–323. doi: 10.1097/00002508-200409000-00006

Visser, M., Jefferies, E., Embleton, K. V., and Lambon Ralph, M. A. (2012). Both the middle temporal gyrus and the ventral anterior temporal area are crucial for multimodal semantic processing: distortion-corrected fMRI evidence for a double gradient of information convergence in the temporal lobes. *J. Cogn. Neurosci.* 24, 1766–1778. doi: 10.1162/jocn_a_00244

Wang, W., Liu, L., Zhi, X., Huang, J. B., Liu, D. X., Wang, H., et al. (2007). Study on the regulatory effect of electro-acupuncture on hegu point (LI4) in cerebral response with functional magnetic resonance imaging. *Chin. J. Integr. Med.* 13, 10–16. doi: 10.1007/s11655-007-0010-3

Wang, X., Chan, S. T., Fang, J., Nixon, E. E., Liu, J., Kwong, K. K., et al. (2013). Neural encoding of acupuncture needling sensations: evidence from a FMRI study. *Evid. Based Complement. Alternat. Med.* 2013:483105.

Ward, A. M., Schultz, A. P., Huijbers, W., Van Dijk, K. R., Hedden, T., and Sperling, R. A. (2014). The parahippocampal gyrus links the default-mode cortical network with the medial temporal lobe memory system. *Hum. Brain Mapp.* 35, 1061–1073. doi: 10.1002/hbm.22234

White, A., Foster, N. E., Cummings, M., and Barlas, P. (2007). Acupuncture treatment for chronic knee pain: a systematic review. *Rheumatology (Oxford)* 46, 384–390. doi: 10.1093/rheumatology/kel413

Wink, A. M., De Munck, J. C., Van Der Werf, Y. D., Van Den Heuvel, O. A., and Barkhof, F. (2012). Fast eigenvector centrality mapping of voxel-wise connectivity in functional magnetic resonance imaging: implementation, validation, and interpretation. *Brain Connect.* 2, 265–274. doi: 10.1089/brain.2012.0087

Wong, Y. M. (2016). Commentary: differential cerebral response, measured with both an EEG and fMRI, to somatosensory stimulation of a single acupuncture point vs. two non-acupuncture points. *Front. Hum. Neurosci.* 10:63. doi: 10.3389/fnhum.2016.00063

Wu, M. T., Hsieh, J. C., Xiong, J., Yang, C. F., Pan, H. B., Chen, Y. C., et al. (1999). Central nervous pathway for acupuncture stimulation: localization of processing with functional MR imaging of the brain–preliminary experience. *Radiology* 212, 133–141. doi: 10.1148/radiology.212.1.r99jl04133

Wu, M. T., Sheen, J. M., Chuang, K. H., Yang, P., Chin, S. L., Tsai, C. Y., et al. (2002). Neuronal specificity of acupuncture response: a fMRI study with electroacupuncture. *Neuroimage* 16, 1028–1037. doi: 10.1006/nimg.2002.1145

Yan, B., Li, K., Xu, J., Wang, W., Liu, H., Shan, B., et al. (2005). Acupoint-specific fMRI patterns in human brain. *Neurosci. Lett.* 383, 236–240. doi: 10.1016/j.neulet.2005.04.021

Yan, C. G., Cheung, B., Kelly, C., Colcombe, S., Craddock, R. C., Di Martino, A., et al. (2013). A comprehensive assessment of regional variation in the impact of head micromovements on functional connectomics. *Neuroimage* 76C, 183–201. doi: 10.1016/j.neuroimage.2013.03.004

You, Y., Bai, L., Dai, R., Cheng, H., Liu, Z., Wei, W., et al. (2013). Altered hub configurations within default mode network following acupuncture at ST36: a multimodal investigation combining fMRI and MEG. *PLoS ONE* 8:e64509. doi: 10.1371/journal.pone.0064509

Zhao, L., Liu, J., Zhang, F., Dong, X., Peng, Y., Qin, W., et al. (2014). Effects of long-term acupuncture treatment on resting-state brain activity in migraine patients: a randomized controlled trial on active acupoints and inactive acupoints. *PLoS ONE* 9:e99538. doi: 10.1371/journal.pone.0099538

Zhong, C., Bai, L., Dai, R., Xue, T., Wang, H., Feng, Y., et al. (2012). Modulatory effects of acupuncture on resting-state networks: a functional MRI study combining independent component analysis and multivariate Granger causality analysis. *J. Magn. Reson. Imaging* 35, 572–581. doi: 10.1002/jmri.22887

Zuo, X. N., Ehmke, R., Mennes, M., Imperati, D., Castellanos, F. X., Sporns, O., et al. (2012). Network centrality in the human functional connectome. *Cereb. Cortex* 22, 1862–1875. doi: 10.1093/cercor/bhr269

Conflict of Interest Statement: The authors declare that the research was conducted in the absence of any commercial or financial relationships that could be construed as a potential conflict of interest.

Curriculum vitae

My curriculum vitae does not appear in the electronic version of my paper for reasons of data protection.

Complete list of publications

1. Nierhaus T, Pach D, Huang W, Long X, Napadow V, Roll S, Liang F, Pleger B, Villringer A, Witt CM. Difficulties Choosing Control Points in Acupuncture Research. Response: Commentary: Differential Cerebral Response, Measured with Both an EEG and fMRI, to Somatosensory Stimulation of a Single Acupuncture Point vs. Two Non-Acupuncture Points. *Frontiers in human neuroscience.* 2016;10:404.
2. Long X*, Huang W*, Napadow V, Liang F, Pleger B, Villringer A, Witt CM, Nierhaus T, Pach D. Sustained Effects of Acupuncture Stimulation Investigated with Centrality Mapping Analysis. *Frontiers in human neuroscience.* 2016;10:510. (*equal contribution)
3. Zheng Q, Zheng H, Lu L, Leng J, Zhou S, Zheng H, Huang W, Liu Z, Zhu B, Li Y. Acupuncture for functional constipation: protocol of an individual patient data meta-analysis. *BMJ Open.* 2015;5(5):e007137.
4. Tang LW, Zheng H, Chen L, Zhou SY, Huang WJ, Li Y, Wu X. Gray Matter Volumes in Patients with Chronic Fatigue Syndrome. *Evidence-Based Complementary and Alternative Medicine.* 2015.
5. Nierhaus T*, Pach D*, Huang W*, Long X, Napadow V, Roll S, Liang F, Pleger B, Villringer A, Witt CM. Differential cerebral response to somatosensory stimulation of an acupuncture point vs. two non-acupuncture points measured with EEG and fMRI. *Frontiers in human neuroscience.* 2015;9:74. (*equal contribution)
6. Zheng H, Huang W, Li J, Zheng Q, Li Y, Chang X, Sun G, Liang F. Association of pre- and post-treatment expectations with improvements after acupuncture in patients with migraine. *Acupuncture in medicine : journal of the British Medical Acupuncture Society.* 2014.
7. Zhou S, Zeng F, Liu J, Zheng H, Huang W, Liu T, Chen D, Qin W, Gong Q, Tian J, Li Y. Influence of acupuncture stimulation on cerebral network in functional diarrhea. *Evidence-based complementary and alternative medicine : eCAM.* 2013;2013:975769.
8. Blodt S, Schutzler L, Huang W, Pach D, Brinkhaus B, Hummelsberger J, Kirschbaum B, Kuhlmann K, Lao L, Liang F, Mietzner A, Mittring N, Muller S, Paul A, Pimpao-Niederle C, Roll S, Wu H, Zhu J, Witt C. Effectiveness of additional self-care acupressure for women with menstrual pain compared to usual care alone: using stakeholder engagement to design a pragmatic randomized trial and study protocol. *Trials.* 2013;14(1):99.
9. Witt CM, Huang WJ, Lao L, Bm B. Which research is needed to support clinical decision-making on integrative medicine?-Can comparative effectiveness research close the gap? *Chinese journal of integrative medicine.* 2012;18(10):723-729.
10. Li Y, Zheng H, Witt CM, Roll S, Yu SG, Yan J, Sun GJ, Zhao L, Huang WJ, Chang XR, Zhang HX, Wang DJ, Lan L, Zou R, Liang FR. Acupuncture for migraine prophylaxis: a randomized controlled trial. *CMAJ : Canadian Medical Association journal = journal de l'Association medicale canadienne.* 2012;184(4):401-410.

11. Huang W, Pach D, Napadow V, Park K, Long X, Neumann J, Maeda Y, Nierhaus T, Liang F, Witt CM. Characterizing acupuncture stimuli using brain imaging with FMRI--a systematic review and meta-analysis of the literature. *PloS one.* 2012;7(4):e32960.
12. Witt CM, Liang F, Huang W, Zeng F, Willich SN. First Sino-German International Symposium on acupuncture and moxibustion. *European Journal of Integrative Medicine.* 2010;2(1):33-36.
13. Streitberger K, Shi J, Pfab F, Huang W, Witt CM, Duan Y, Willich SN. Acupuncture assisted anesthesia for nasal surgery as an example for integrative medicine in China. *European Journal of Integrative Medicine.* 2010;2(1):37-39.

Acknowledgements

I would like to express my sincere thanks to my supervisor Prof. Dr. med. Claudia M. Witt for providing me with the opportunity to start and finish my doctoral research in her group, giving me outstanding guidance, kind encouragement and generous support and dedication to the completion of the work.

I would also like to express my gratitude to Prof. Dr. Arno Villringer who supported in carrying out the neuroimaging experiments at the Max-Planck-Institute for Human Cognitive and Brain Sciences Leipzig, and for the valuable advice and fruitful discussion on the study.

I'm very grateful to Dr. Vitaly Napadow from Harvard Medical School for the professional advice and helpful guidance at every step of the study. I'd like to thank Prof. Dr. Burkhard Pleger for the support during the experiments and revision on the publications. Many thanks to PD. Dr. Jane Neumann who gave me valuable guidance on the meta-analysis.

Deep thanks to Dr. Daniel Pach for the kind help and valuable support during the whole process of my doctoral study, and also to Dr. Till Nierhaus and Dr. Xiangyu Long for the extremely good teamwork, scientific advice and reliable support.

Special thanks to Prof. Liang Fanrong and Prof. Li Ying from the Chengdu University of TCM for the support for the study.

Last but not least, I want to thank my family for their selfless love and support at all time during my doctoral study. Also, I would like to express my sincere appreciation to all the people who supported me and contributed to the completion of the thesis.